

**Cardiometabolic and Neuroimaging
correlates of cognitive function in
Polycystic Ovary Syndrome**

Maneesh Vasanth Udiawar

MBBS, MRCP (UK)

Centre for Endocrine and Diabetes Sciences, Institute of
Molecular and Experimental Medicine,
School of Medicine, Cardiff University

A thesis submitted to Cardiff University in candidature for the
degree of Doctor of Medicine (MD)

2017

DECLARATION

This work has not been submitted in substance for any other degree or award at this or any other university or place of learning, nor is being submitted concurrently in candidature for any degree or other award.

Signed (candidate) Date

STATEMENT 1

This thesis is being submitted in partial fulfillment of the requirements for the degree of(insert MCh, MD, MPhil, PhD etc, as appropriate)

Signed (candidate) Date

STATEMENT 2

This thesis is the result of my own independent work/investigation, except where otherwise stated. Other sources are acknowledged by explicit references. The views expressed are my own.

Signed (candidate) Date

STATEMENT 3

I hereby give consent for my thesis, if accepted, to be available online in the University's Open Access repository and for inter-library loan, and for the title and summary to be made available to outside organisations.

Signed (candidate) Date

STATEMENT 4: PREVIOUSLY APPROVED BAR ON ACCESS

I hereby give consent for my thesis, if accepted, to be available online in the University's Open Access repository and for inter-library loans **after expiry of a bar on access previously approved by the Academic Standards & Quality Committee.**

Signed

CONTENTS

Contents	i
Summary	vi
Acknowledgements	viii
Publications and Presentations	ix
Abbreviations	x
List of Figures	xiii
List of Tables	xv

CHAPTER 1 Cognitive Impairment

1.1	Introduction	1
1.2	Cardiometabolic risk factors	1
1.2.1	Hypercholesterolaemia	1
1.2.2	Diabetes Mellitus	3
1.2.3	Obesity and Body Mass Index	4
1.2.4	Hypertension	5
1.2.5	Smoking	6
1.3	Polycystic Ovary Syndrome	7
1.3.1	Introduction	7
1.3.2	Historical Overview and Diagnosis	7
1.3.3	Limitations of Research	9
1.3.4	Pathogenesis	10
1.3.4.1	Abnormalities in hypothalamic pituitary function	11

1.3.4.2	Androgen production by the ovaries	12
1.3.4.3	Insulin secretion and action	12
1.3.4.4	Prenatal Androgen Exposure	14
1.3.4.5	Low birth weight and premature pubarche	14
1.3.4.6	Genetic Factors	15
1.3.5	Prevalence	16
1.3.6	Clinical Features	15
1.3.6.1	Reproductive	17
1.3.6.2	Dermatological	17
1.3.6.3	Metabolic	17
1.3.7	Morbidity associated with PCOS	18
1.3.7.1	Cardiovascular Disease	18
1.3.7.2	Type 2 Diabetes Mellitus	20
1.3.7.3	Non Alcoholic Fatty Liver Disease (NAFLD) and Non Alcoholic Steatohepatitis	21
1.3.7.4	Obesity	22
1.3.7.5	Depression	23
1.3.7.6	Sleep Disordered Breathing/ Obstructive Sleep Apnoea	24
1.3.7.7	Cognitive Function	25
1.4	Magnetic Resonance Imaging	26
1.4.1	Introduction	26
1.4.2	Principles of MRI	26
1.4.3	Diffusion Tensor Imaging	26
1.4.4	Diffusion Metrics	31

1.4.5	White Matter Tractography	33
1.4.6	Tract Based Spatial Statistics	35
1.4.7	Thesis Aims	36
CHAPTER 3	Methods	
2.1	Outline of study	38
2.1.1	Study Approval	38
2.1.2	Recruitment	38
2.1.3	Inclusion and Exclusion criteria of Study Participants	38
2.1.4	Consent	39
2.1.5	Protocol	39
2.2	Clinical Assessment	40
2.2.1	History and Examination	40
2.2.2	Blood Pressure Measurement	40
2.3	Biochemical and Metabolic measurements	40
2.3.1	Sample collection and storage	40
2.3.2	Assays	41
2.3.3	Estimation of Insulin sensitivity and Insulin resistance	41
2.4	Body composition measurements	42
2.4.1	Anthropometric measurements	42
2.4.2	Computed Tomography	43
2.5	Cognitive function tests	44
2.5.1	Assessment of premorbid IQ	45
2.5.2	Assessment of Intelligence and Executive function	45

2.5.2.1	Digit Span Task	45
2.5.2.2	Digit Symbol Substitution Test	46
2.5.2.3	Verbal Trails Test	46
2.5.2.4	Verbal Fluency Test	47
2.5.2.5	Stroop Colour Word Test	47
2.5.2.6	Free and Cued Selective Reminding Test	48
2.5.2.7	The Rey–Osterrieth Complex Figure Test	49
2.5.2.8	Wechsler abbreviated scale of Intelligence	49
2.5.2.9	Beck’s Depression Inventory	50
2.6	MRI data acquisition	50
2.6.1	Materials	50
2.6.2	Methods	51
2.6.3	White matter tractography and tract specific measures	53
2.6.4	Tract Based Spatial Statistics	58
2.7	Statistical analysis	65
2.8	Power calculations	65
 CHAPTER 4 Results		
3.1	Introduction	67
3.2	Aims	67
3.2.1	Study recruitment	68
3.2.2	Demographic data	68
3.3	Biochemical Characteristics of the Study Population	70
3.3.1	Glucose Tolerance status	70

3.4	Cognitive Function Tests	72
3.4.1	Results	72
3.5	Discussion	74

CHAPTER 5 White Matter Tractography and Tract Based Spatial Statistics

4.1	Introduction	78
4.2	Aims	78
4.3	White Matter Tractography	79
4.4	Tract Based Spatial Statistics	81
4.4.1	Results	82
4.4.1.1	Diffusion metrics and white matter microstructure	82
4.4.1.2	Insulin resistance and white matter microstructure	84
4.4.1.3	Androgens and white matter microstructure	86
4.4.1.4	Metabolic status and white matter microstructure	86
4.5	Discussion	87

CHAPTER 5 Discussion

References	98
-------------------	-----------

SUMMARY

Background: Polycystic ovary syndrome (PCOS) is a disorder characterized by insulin resistance and hyperandrogenism, which leads to an increased risk of type 2 diabetes in later life. Androgens and insulin signalling affect brain function but little is known about brain structure and function in younger adults with PCOS.

Aims and Methods: To establish whether young women with PCOS display altered white matter microstructure and cognitive function. Eighteen individuals with PCOS (age, 31 ± 6 y; body mass index [BMI] 30 ± 6 kg/m²) and 18 control subjects (age, 31 ± 7 y; BMI, 29 ± 6 kg/m²), matched for age, IQ, and BMI, underwent anthropometric and metabolic evaluation, diffusion tensor MRI, a technique especially sensitive to brain white matter structure, and cognitive assessment. Cognitive scores and white matter diffusion metrics were compared between groups. White matter microstructure was evaluated across the whole white matter skeleton using tract-based spatial statistics. Associations with metabolic indices were also evaluated.

Results: PCOS was associated with a widespread reduction in axial diffusivity (diffusion along the main axis of white matter fibres) and increased tissue volume fraction (the proportion of volume filled by white or grey matter rather than cerebrospinal fluid) in the corpus callosum. Cognitive performance was reduced compared with controls (first principal component, $t = 2.9$, $P = .007$), reflecting subtle decrements across a broad range of cognitive tests, despite similar education and premorbid intelligence. In PCOS, there was a reversal of the relationship seen in controls between brain microstructure and both androgens and insulin resistance.

Conclusion: White matter microstructure is altered, and cognitive performance is compromised, in young adults with PCOS. These alterations in brain structure and function are independent of age, education and BMI. If reversible, these changes represent a potential target for treatment.

Acknowledgements

Firstly, I would like to thank my supervisors Dr Aled Rees and Dr Mike O’Sullivan for their guidance and support provided throughout this study.

I would also like to thank the people who assisted in this project;

1. Dr Kate Craig and team for allowing access to the Clinical Research Facility.
2. Dr Helen Blundell for the capture and interpretation of the abdominal CT scans.
3. John Evans and Peter Hobden who carried out the Magnetic resonance imaging at Cardiff University Brain Research and Imaging Centre.
4. Dr Claudia-Metzler Baddeley for providing me training in carrying out the cognitive function tests and assisting me with analysing the MRI data in relation to Diffusion tensor imaging.
5. Dr Rok Berlot for performing Tract based spatial statistics and analysing the results.

Without the patients and volunteers who willingly gave up their time to participate in this study, this research would not have been possible and I am very grateful to them all.

This thesis is dedicated to my two lovely darling children Lathika and Aaditya who were born during the period that I undertook this research project and made it a very challenging yet rewarding period of my career.

PUBLICATIONS AND PRESENTATIONS

Publication Arising from this Research

Rees DA, Udiawar M, Berlot R, Jones DK, O'Sullivan MJ. White Matter Microstructure and Cognitive Function in Young Women with Polycystic Ovary Syndrome. *Journal of Clinical Endocrinology and Metabolism*, 2016. 101(1): 314-23.

Presentations to Learned Societies

Udiawar M, Berlot R, Rees DA, O'Sullivan MJ. Reduced cognitive performance and altered white matter microstructure in young insulin-resistant women with Polycystic Ovary Syndrome. (Oral) British Endocrine Society, Liverpool March 2014.

Udiawar M, Berlot R, Rees DA, O'Sullivan MJ. Reduced cognitive performance and altered white matter microstructure in young insulin-resistant women with Polycystic Ovary Syndrome. (Oral) Welsh Endocrine and Diabetes Society Meeting, May 2013.

ABBREVIATIONS

17 β	17 β -hydroxysteroid dehydrogenase
ADC	Apparent Diffusion Coefficient
AE-PCOS	Androgen Excess and PCOS Society
ARIC	Atherosclerosis Risk in Communities
ASRM	American Society of Reproductive Medicine
ASSET	Array Spatial Sensitivity Encoding Technique
AUC	Area Under Curve
AD	Axial Diffusivity
BDI	Beck's Depression Inventory
BMI	Body Mass Index
CU	Cardiff University
CUBRIC	Cardiff University Brain Research Imaging Centre
DENND1A	DENN/MADD domain containing 1A
DICOM	Digital Imaging and Communications in Medicine
DST	Digit Symbol Substitution Test
DTI	Diffusion tensor Imaging
DWI	Diffusion Weighted Imaging
EPI	Echo Planar Imaging
ESHRE	European Society for Human Reproduction
FA	Fractional Anisotropy
FCSRT	Free and Cued Selective Reminding Test
FLAIR	Fluid Attenuated Inversion Recovery Scans
FMRIB	Functional MRI of the Brain
FPI	Fasting Plasma Insulin

FSH	Follicle Stimulating Hormone
FSL	FMRIB Software Library
FTO	Fat mass and Obesity associated
GDM	Gestational Diabetes Mellitus
GLUT-4	Glucose Transporter 4
GnRH	Gonadotrophin-Releasing Hormone
GWAS	Genome Wide Association Study
IGT	Impaired Glucose Tolerance
IL-6	Interleukin 6
IR	Insulin Resistance
IRS	Insulin Receptor Substrate
LH	Luteinising Hormone
LHCGR	Luteinising Hormone/Chorio-gonadotrophin Receptor
MAPK	Mitogen Activated Protein Kinase
MD	Mean Diffusivity
miRNA	micro RNA
MMSE	Mini-Mental State Exam
NAFLD	Non Alcoholic Fatty Liver Disease
NART-R	National Adult Reading Test Revised
NASH	Non Alcoholic Steatohepatitis
NIH	National Institutes of Health
NIFTI	Neuroimaging Informatics Technology Initiative
OGTT	Oral Glucose Tolerance Test
OSA	Obstructive Sleep apnoea
PHC	Parahippocampal Cingulum

PIQ	Performance Intelligence Quotient
PVE	Partial Volume Effects
QUICKI	Quantitative Insulin sensitivity Check Index
RD	Radial Diffusivity
ROCF	Rey-Osterrieth Complex Figure Test
ROI	Region of Interest
SDB	Sleep Disordered Breathing
SHBG	Sex Hormone Binding Globulin
TBSS	Tract Based Spatial Statistics
TFCE	Threshold-Free Cluster Enhancement
THADA	Thyroid adenoma-associated protein
UF	Uncinate Fasciculus
UHW	University Hospital of Wales
VIQ	Verbal Intelligence Quotient
VLDL	Very Low Density Lipoprotein
WAIS	Wechsler Adult Intelligence Scale
WASI	Wechsler Abbreviated Scale of Intelligence

LIST OF FIGURES

Figure No.	Title	Page No.
1.1	Causative risk factors linked to development of cognitive Impairment	2
1.2	Pathophysiology of Polycystic Ovary Syndrome	11
1.3	Isotropic and anisotropic diffusion	28
1.4	Axial tractographic image demonstrating white matter tracts in the brain	28
1.5	Schematic representation of fibre tracts	30
1.6	Diffusion Ellipsoid characterised by eigenvectors	30
1.7	Schematic diagram showing a basic algorithm for tract reconstruction	33
1.8	Image generated from whole brain diffusion tensor tractography	35
2.1	Cross sectional CT scan image	44
2.2	Digit symbol substitution Test	46
2.3	Schematic diagram showing region of interest operations	54
2.4	Tractography using region of interest (ROI waypoints) for the fornix (A), uncinate fasciculus (B) and the parahippocampal cingulum (C)	58
2.5	Voxel-wise non linear registration to prealign all subject's FA	60
2.6	Mean FA image with no smoothing	62
2.7	Examples of fibre bundles; a thick sheet as it's skeleton (A) and a 'tube' as it's skeleton (B)	62

2.8	A. Original mean FA image with final skeleton and ROI used for sub-image	63
	B. Skeletonisation using FA centre of gravity to find tract Perpendiculars	63
2.9	A. Example of white matter skeleton which is shown in green	63
	B. Projection of data on to white matter skeleton	63
4.1	Example of reconstruction of the fornix registered on native space of one participant	78
4.2	Example of reconstruction of the uncinated fasciculus registered on native space of one participant	78
4.3	Example of reconstruction of the parahippocampal cingulum Registered on native space of one participant	79
4.4	A. Mean white matter skeleton voxels showing significant lower value of AD and higher value of tissue volume fraction in PCOS compared with healthy volunteers	82
	B. Group differences based on TBSS	82
4.5	Contrasting associations between white matter microstructure and insulin resistance in PCOS and healthy volunteers	84
4.6	Correlation of testosterone level with microstructural measures in PCOS	85

LIST OF TABLES

Table No.	Title	Page No
1.1	Diagnosis of Polycystic Ovary Syndrome	9
3.1	PCOS (subphenotypes as per Rotterdam criteria)	69
3.2	General characteristics of the study population	69
3.3	Biochemical characteristics of the study population	70
3.4	Outcome of screening tests for diabetes and dysglycaemia In PCOS	71
3.5	Performance on individual cognitive function tests	73
4.1	Group differences in fractional anisotropy (FA), mean Diffusivity (MD) and axial diffusivity (AD)	80
APPENDIX 1	Principal Component Analysis (Cognitive Function Tests)	95

CHAPTER 1 COGNITIVE IMPAIRMENT

1.1 Introduction

Dementia affects around 7% of the general population over 65 years, and 30% of people over 80 years. The prevalence of dementia is expected to double over the next 30 years, making disorders of cognition a priority for healthcare and social-care services. The two most common forms of dementia are Alzheimer's disease (AD) and vascular dementia, accounting for over 75% of all dementia cases. Although they have been regarded as two separate entities for decades, it is now well known that both these conditions show mixed pathology suggesting a continuum in underlying pathologies ranging from pure vascular dementia to pure Alzheimer's disease.

There is growing interest in strategies to modify the environment in midlife to increase the probability of maintaining cognitive health in late life. Several potentially modifiable risk factors have been studied in relation to cognitive impairment and dementia in late life.

1.2 Cardiometabolic Risk Factors

1.2.1 Hypercholesterolaemia

Several studies have showed an association between raised cholesterol levels and dementia [1, 2], AD [3] and vascular dementia [4, 5]. Whitmer et al. conducted a retrospective cohort study of 9000 participants who underwent health evaluations over a period of 9 years with ages between 40 to 44. Approximately 700 participants had dementia (8%) with high cholesterol being associated with a 20% to 40% increase in risk of dementia (HR 1.42 95% CI 1.22 to 1.66 for high cholesterol) [6].

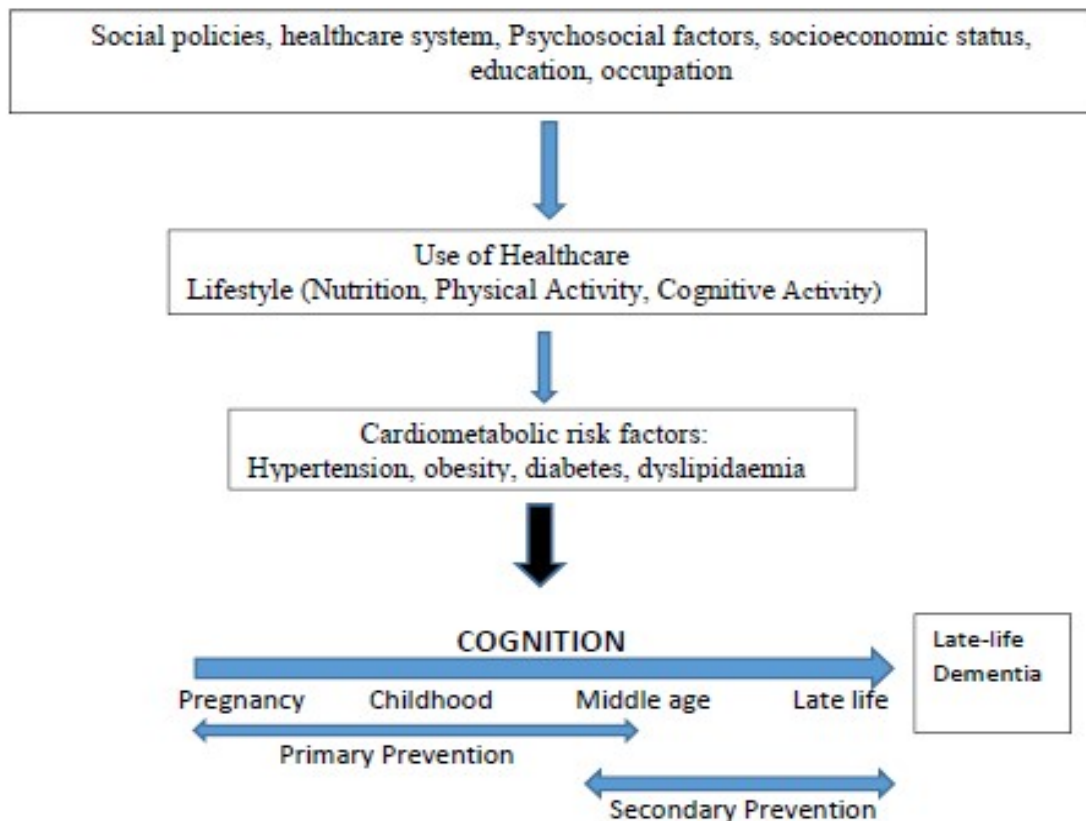


Fig 1.1 Causative risk factors linked to the development of cognitive impairment. Modifiable risk factors can be addressed from as early as in utero to early middle age to prevent the onset of cognitive decline.

The Atherosclerosis Risk in Communities (ARIC) study was a prospective study looking at 11,000 participants aged between 46 to 70 [1]. The risk of dementia with hypercholesterolaemia was modest (HR 1.7 in age < 55, 0.9 > 70) compared to other traditional risk factors such as diabetes (HR 3.4 in < 55, 2.0 in ≥70) and smoking (4.8 in < 55, 0.5 in ≥70). Some studies such as the Framingham study have failed to show a similar association [7]. Some have even shown a lower risk of dementia with high cholesterol levels [8]. These discrepancies may be related to study methodology, the definition of dementia used and the groups of subjects studied including the timing of the diagnosis of hypercholesterolaemia (midlife versus late life). Some longitudinal

studies have shown that the relationship may be bidirectional with high midlife serum total cholesterol (TC) associated with a high risk for subsequent dementia, and decreasing serum TC after mid life representing a risk marker for late-life cognitive impairment [2].

1.2.2 Diabetes Mellitus

Diabetes is associated with an increased risk of cognitive decline and dementia [9-11]. The presence of diabetes confers a 20% to 40% increase in risk of dementia (HR 1.46, 95% CI 1.19 to 1.79)[6]. A systematic review of 14 studies found that diabetes is associated with a 50 to 100 percent increase in risk of AD and of dementia overall, and a 100 to 150 percent increased risk of vascular dementia [12]. Diabetes is more commonly associated with cerebrovascular disease [13, 14] but one study has shown an association with hippocampal atrophy which is more commonly associated with Alzheimer's disease [15]. Higher glucose levels have also been associated with risk of cognitive impairment and dementia in nondiabetic individuals, implicating a possible role of insulin resistance as the causative aetiology [16, 17]. A cross sectional study showed that chronically higher blood glucose levels were associated with worsening scores in delayed recall, learning ability and memory consolidation [17]. The Targeting INflammation Using SALsalate in CardioVascular Disease (TINSAL-CVD) trial showed significant decrements in cognitive function test scores for every 1% increase in Hba1C in a mixed cohort of male individuals on a background of metabolic syndrome and coronary artery disease with normoglycaemia, impaired fasting glucose and type 2 diabetes [18].

1.2.3 Obesity and Body Mass Index (BMI)

Over the past decade, obesity has been increasingly recognised as a potential risk factor for cognitive decline particularly in older individuals. In cross-sectional studies, elevated body mass index as well as the metabolic syndrome, have been associated with deficits in memory, executive function, processing speed, semantic fluency, and overall cognitive function [19, 20]. Most of these studies found that mid-life obesity increases the risk of dementia later in life. In a 27-year follow up study of 10,276 participants, obesity was associated with an increased risk of dementia, HR=1.74 (95% CI 1.34-2.26), as was being overweight, HR=1.35 (95% CI 1.14-1.60) [21]. This relationship was maintained even after controlling for hyperlipidaemia and diabetes. Increased BMI has also been linked to lower baseline cognitive function and increased five year cognitive decline in a population based study of 2223 healthy non-demented individuals aged 32 to 62 years after adjustment for age, sex, educational level, blood pressure, diabetes and other psychosocial covariables [22]. Data from longitudinal studies have shown that an elevated BMI is an independent risk factor for accelerated brain atrophy and increased risk of cognitive decline [23, 24]. More recent studies suggest that the hormonal changes associated with obesity may mediate changes in cognitive function, of which insulin resistance is considered particularly relevant because of the link between metabolic syndrome and cognitive dysfunction [25, 26]. Cognitive domains affected include executive function [19], verbal fluency [27] and working memory [28]. Bove *et al.* [29] studied the effects of obesity on cognitive function in 49 young healthy lean and overweight women aged 20 – 45 years and found a significant negative association between visceral adiposity and performance in the domain of verbal learning and memory, after controlling for age and education. Additionally the degree

of insulin resistance was negatively associated with executive function domain. No association was noted between hormonal factors and cognitive function. These findings suggest a possible association between obesity and cognitive function in healthy young women of reproductive age group. The mechanism of cognitive dysfunction in young adults is not clear but important mediators such as insulin resistance may play a role through modulation of hippocampal synaptic plasticity [30], neuroinflammation and subsequent protein deposition [31] and may have gender specific effects due to interactions with gonadal steroids [32].

1.2.4 Hypertension

High blood pressure raises the risks of vascular dementia and cognitive dysfunction in older adults, by acting on the cerebral vasculature and directly on the brain itself. The relationship between hypertension and dementia risk is not entirely clear but epidemiologic and treatment studies support this hypothesis [1, 6]. Data from the Framingham Heart Study indicates that attention and memory measures are inversely related to blood pressure levels and duration of hypertension[33]. The Honolulu Asia Aging Study found that every 10 mm Hg increase in systolic blood pressure was associated with a 9% increased risk for poor cognitive function [34]. Although most studies have studied middle aged or elderly subjects there is evidence to suggest that young adults may also be susceptible to the deleterious effects of hypertension on cognition. In a 20-year longitudinal study of 529 adults comprising two age groups (18 to 46 and 47 to 83 years), higher levels of baseline systolic, diastolic, and mean blood pressure in both younger and older age groups were significantly associated with decline in one neuropsychological measure of cognitive ability, the visualisation/fluid abilities composite score [35].

The pathophysiologic mechanisms linking hypertension and cognitive dysfunction may be direct or indirect. Long standing hypertension may indirectly increase the risk of atherosclerosis, stroke, or cerebral infarction, which in turn may cause cognitive decline [36]. Hypertension may have a direct effect on brain volume: a small study by Strassburger et al. reported that patients with hypertension (age 56 to 84) had smaller volumes of thalamic nuclei, larger volumes of cerebrospinal fluid in the cerebellum and temporal lobes and performed worse on language and memory tests. This suggests that the occipital and temporal regions appear more vulnerable to brain atrophy due to the interactive effects of age and hypertension [37]. Progressive changes in cerebral blood flow in hypertensive individuals were observed compared to controls by Positron emission tomography (PET) scans and this correlated with the duration of hypertension [38]. Blood pressure lowering treatments have been associated with improved cognitive outcomes measured by MMSE [39-41] .

1.2.5 Smoking

Data regarding the impact of smoking on the risk of dementia are conflicting. Population-based evidence of an effect of smoking on cognitive function has been inconclusive, with most longitudinal studies reporting weak or no associations [42]. Several prospective studies have suggested that smoking in middle aged and elderly people is associated with an increased risk of dementia [1, 6, 43]. A meta-analysis of 19 studies with at least 12 months of follow-up concluded that elderly smokers have increased risk of AD, vascular dementia and any dementia, with relative risks of 1.27 (95% CI 1.02-1.60) to 1.79 (95% CI 1.43-2.23) [44]. Current smoking was also associated with greater yearly declines in Mini-Mental State examination scores.

Possible mechanisms include cerebral hypoxia resulting in free radical injury and microvascular disease [45].

1.3 Polycystic Ovary Syndrome

1.3.1 Introduction

Polycystic ovary syndrome (PCOS) is one of the most common endocrine disorders seen in premenopausal women, and is characterised by hyperandrogenism and chronic anovulation. The high prevalence of obesity and insulin resistance in these patients predisposes them to an increased risk of type 2 diabetes mellitus. An unfavourable metabolic profile persists after menopausal transition as a result of increased androgen levels and decreased oestrogen levels with further exacerbation of insulin resistance, chronic inflammation and adiposity. The estimated prevalence is between 5-10% in women of reproductive age although it may be as high as 15-20% depending on the diagnostic criteria used.

1.3.2 Historical Overview and Diagnosis

The first documented account of PCOS dates back to the period of Hippocrates (460-377 BC) who noted “But those women whose menstruation is less than three days or is meagre, are robust, with a healthy complexion and a masculine appearance; yet they are not concerned about bearing children nor do they become pregnant ”[46]. However applying a diagnosis retrospectively must be undertaken with caution.

The modern description of PCOS can be traced back to 1935 when Stein and Leventhal reported a case series of seven women aged between 20 and 33 years with infertility, amenorrhoea and bilateral polycystic ovaries at laparotomy. Four of the women were

noted to have hirsutism, one woman had acne and three were obese. This is thought to be the first definitive description of the syndrome, which thus bore the name ‘Stein-Leventhal syndrome’ until the middle of the twentieth century when it became known as PCOS. Since its original definition in 1935, the definition of PCOS has undergone several revisions. At the National Institutes of Health (NIH) consensus conference held in 1990, PCOS was defined as chronic anovulation with clinical and/or biochemical hyperandrogenism, with exclusion of other mimicking aetiologies, such as thyroid or adrenal dysfunction [47]. In 2003, the Rotterdam European Society for Human Reproduction/American Society of Reproductive Medicine (ESHRE/ASRM)-sponsored PCOS consensus workshop group proposed that the diagnosis include two of the following three criteria: oligo- and/or anovulation, clinical and/or biochemical hyperandrogenism, and polycystic ovaries on ultrasound; other aetiologies must be excluded. (Please see Table 2.1) The Rotterdam criteria extended the diagnosis of PCOS to women with oligo-ovulation and polycystic ovaries (non hyperandrogenic) as well as to women with hyperandrogenism and polycystic ovaries (ovulatory) neither of which would have met the narrower NIH criteria for PCOS. These broader criterion have also led to the argument that the expanded Rotterdam definition can result in an overdiagnosis or misdiagnosis of PCOS, and the different phenotypes may not have similar risks of long term metabolic complications. The diagnostic criteria were updated in 2006 by the Androgen Excess and PCOS society (AE-PCOS). Outlined in Table 1.1 are the main consensus groups and the definitions of PCOS that were agreed upon. The Rotterdam criteria include a broader spectrum of PCOS than the NIH and AE-PCOS society criteria, as hyperandrogenism does not need to be present for the diagnosis. In December 2013, the Endocrine Society endorsed the Rotterdam criteria for the diagnosis of PCOS in pre-menopausal women [48].

Table 1.1 Diagnosis of Polycystic Ovary Syndrome

Consensus Group	Year	Criteria
National Institute of Health (NIH) Bethesda, USA [47]	1990	Chronic anovulation and Clinical and/or biochemical signs of hyperandrogenism and Exclusion of other aetiologies*
European Society for Human Reproduction and Embryology and the American Society for Reproductive Medicine Rotterdam [49]	2003	Oligo- and/or anovulation and/or Clinical and/or biochemical signs of hyperandrogenism and/or Polycystic Ovaries and Exclusion of other aetiologies* (2 or more of the first three criteria must be present and the exclusion of other aetiologies)
The Androgen Excess and PCOS Society (AE-PCOS)[50]	2006	Hyperandrogenism (clinical and /or biochemical) and Ovarian dysfunction (oligo-anovulation and/or polycystic ovaries) and Exclusion of other aetiologies* and **

*Congenital Adrenal Hyperplasia, Androgen secreting neoplasms, Cushing's syndrome, Thyroid dysfunction, Hyperprolactinaemia, Idiopathic Hirsutism and **Syndromes of severe insulin resistance

1.3.3 Limitations of Research

PCOS is a syndrome and not a disease entity. Its aetiology is complex, heterogeneous, and poorly understood. There are three definitions for PCOS currently in use that variably rely on androgen excess, chronic anovulation, and PCO to make the diagnosis.

Different phenotypes exist depending on the diagnostic criteria used and this may result in different risk and comorbidity profiles. The Endocrine Society guidelines state that biochemical hyperandrogenism refers to an elevated serum androgen level and includes an elevated total, bioavailable or free serum testosterone level [48]. The guideline acknowledges that there is no absolute level which is diagnostic of PCOS due to variability in testosterone levels and the poor standardisation of assays [51]. The ultrasound criteria is also a subject of debate with differences across study groups as to the number of follicles (presence of 12 or more follicles 2-9mm in diameter and /or an increased ovarian volume >10ml, without a cyst or dominant follicle) in either ovary)[52]. This has implications in interpreting published research as the diagnostic criteria used may vary from one study to another.

1.3.4 Pathogenesis

Despite the high prevalence and significant morbidity resulting from both reproductive and hyperandrogenic features and the associated cardiovascular risk, the aetiology of PCOS remains incompletely understood. As PCOS is a heterogeneous disorder, the underlying pathophysiology of this condition is yet to be determined with the aetiology likely to be multifactorial. Several theories have been explained to determine the pathogenesis of PCOS focussing on the following observed physiological abnormalities: hypersecretion of Luteinising hormone (LH), increasing ovarian androgen production and insulin resistance. Other hypotheses include prenatal androgen exposure, low birth weight and premature pubarche.

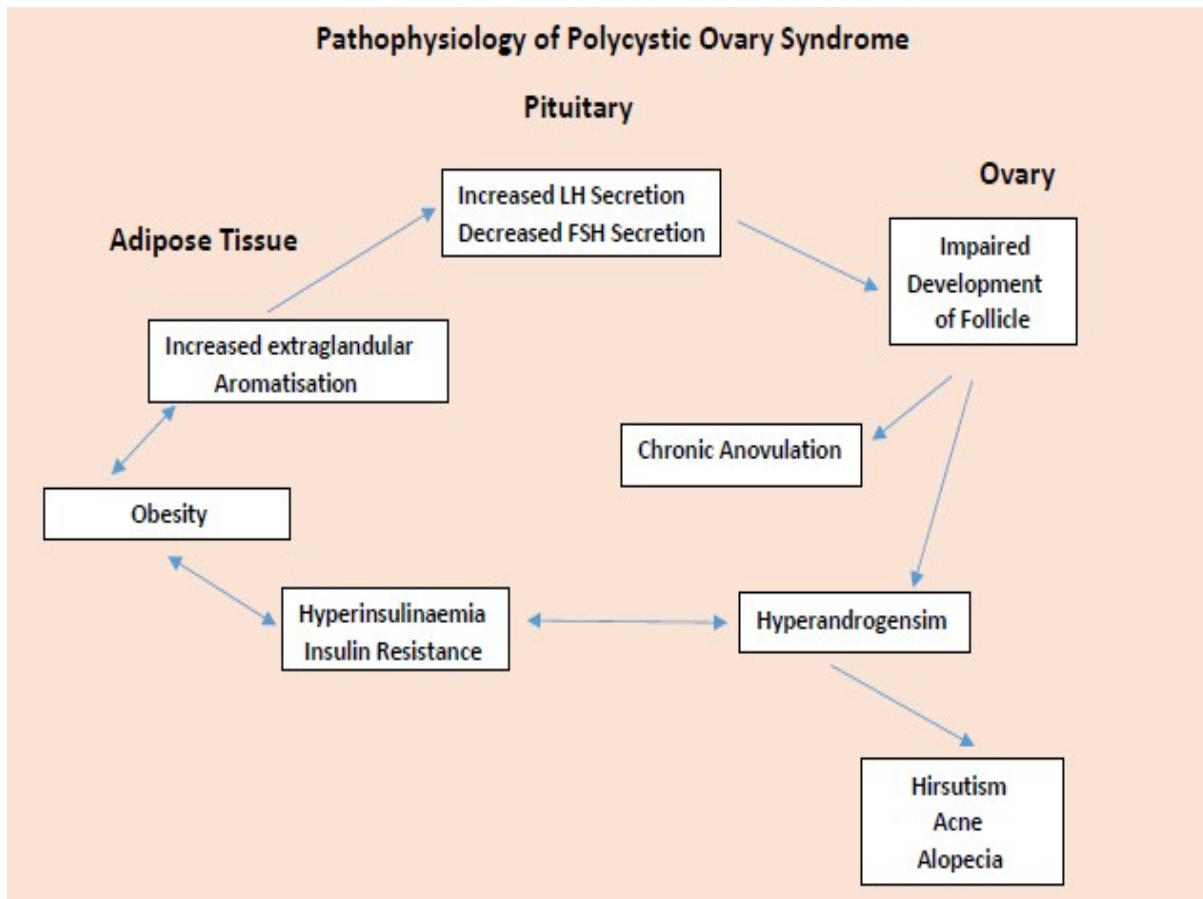


Fig 1.2 Pathophysiology of Polycystic Ovary Syndrome

1.3.4.1 Abnormalities in hypothalamic pituitary function

Increasing LH relative to follicle-stimulating hormone (FSH) was the first laboratory abnormality identified in classic PCOS. This has been attributed to an increased gonadotrophin-releasing hormone (GnRH) pulse frequency from the hypothalamus which increases production of LH relative to FSH [53, 54]. Elevated LH is thought to play a role in the pathogenesis of PCOS by increasing androgen production and secretion by ovarian theca cells [55, 56]. Patients with PCOS have an increased LH pulse frequency and amplitude [57]. Some lines of evidence argue against this hypothesis. About half of patients with PCOS, principally obese patients, do not have elevated LH levels or abnormal gonadotrophin responses to GnRH agonist testing [55, 57]. Furthermore, about half of PCOS subjects with a documented ovarian source of

hyperandrogenism were demonstrated to have normal LH levels and LH responses to a GnRH agonist test, suggesting that the ovarian dysfunction is independent of LH excess.

1.3.4.2 Androgen production by the ovaries

Hyperandrogenism is a central feature of most phenotypes of PCOS. In PCOS androgens (androstenedione and testosterone) are predominantly secreted by the ovaries and to a lesser degree the adrenals [58]. This pattern differs from that in premenopausal women where the androgen secretion are equally contributed to by the ovaries and the adrenals. Insulin resistance does not exclusively contribute to the development of PCOS [59]. In the ovary, theca cells synthesise androgens and the granulosa cells synthesise oestrogens. The theca cells are stimulated by LH to produce androstenedione mediated by cytochrome P-450c17. Androstenedione is then converted to testosterone by 17 β -hydroxysteroid dehydrogenase (17 β) or aromatised by cytochrome P-450arom to form oestrone. Oestrone is then converted to oestradiol also within the granulosa cell. FSH regulates the aromatase activity of the granulosa cells. In normal women androstenedione is preferentially converted to oestradiol.

In PCOS, LH levels are elevated so the theca cells secrete increased quantities of androstenedione. In addition, thecal cells from women with PCOS are more sensitive to LH stimulation of androgen production [60]. Androstenedione secreted into the circulation by the ovary and adrenal can be converted to the potent androgen, testosterone, by most peripheral tissues.

1.3.4.3 Insulin secretion and action

PCOS is a condition in which tissue-selective resistance to the glucose-metabolic

effects of insulin seems to be paradoxically associated with preserved ovarian sensitivity to insulin, suggesting a role for hyperinsulinemia in ovarian dysfunction [61-64]. It is well known that hyperandrogenism correlates with hyperinsulinism in PCOS. This was first described by Burghen et al. who observed that patients with PCOS showed an exaggerated insulin response to an oral glucose tolerance test [65]. Several studies support this theory of compensatory hyperinsulinaemia, 50 to 70% of women with PCOS demonstrate clinically measurable insulin resistance *in vivo* independent of the degree of obesity. Theca cell secretion of androgens is stimulated by insulin and inhibits hepatic sex hormone binding globulin which results in an increase in free androgens [66-68]. Insulin may act as a gonadotrophin to modulate ovarian steroidogenesis and the theca cells show hyper-responsiveness to the stimulatory effects of insulin on androgen secretion [69].

Although the aetiology of increased insulin resistance remains unclear, a post-binding defect in receptor signalling likely due to increased receptor and insulin receptor substrate-1 serine phosphorylation selectively affects metabolic but not mitogenic pathways in classic insulin target tissues and in the ovary [63]. Constitutive activation of serine kinases in the MAPK-ERK pathway may contribute to resistance to insulin's metabolic actions in skeletal muscle. Studies in adipose tissue have noted that, while insulin binding and the IRS/PI3-K/AKT insulin signalling pathway overall appears to be normal in PCOS, *GLUT4* expression is significantly lower in PCOS patients and in control women with insulin resistance, although no defect in insulin receptor serine phosphorylation was observed [70]. Furthermore adipose tissue in PCOS appears to have a differentially expressed miRNA profile with upregulation of miR-93 expression : the resultant dysregulation may play a role in the insulin resistance in PCOS [70].

1.3.4.4 Prenatal Androgen Exposure

Experimental evidence supports the hypothesis that the phenotypic expression of PCOS is strongly influenced by the intrauterine environment. This is based on animal models in which prenatal exposure to androgen excess leads to biochemical and clinical features of PCOS after birth [71]. Abbott and colleagues conducted experiments on rhesus monkeys demonstrating how prenatal administration of testosterone propionate recreated the PCOS phenotype in adulthood including hyperandrogenaemia, increased secretion of androgens in response to recombinant human chorionic gonadotrophin, oligo-ovulation and polyfollicular ovaries. These abnormalities were accompanied by accumulation of visceral fat, insulin resistance and impaired insulin secretion, especially in animals exposed to androgens early during gestation [72]. However these findings are yet to be confirmed in humans. A longitudinal study of 244 unselected girls recruited prenatally, failed to demonstrate an association between diagnosis of PCOS at age 15 and maternal hyperandrogenism throughout pregnancy or foetal hyperandrogenism at birth [73]. The diagnosis of PCOS in adolescents is challenging and a longer follow up and larger study group may have yielded different results. It is also possible that sampling of androgens during pregnancy missed a window of foetal or maternal androgen excess [74].

1.3.4.5 Low birth weight and premature pubarche

It is hypothesised that foetal undernutrition selects for the thrifty genotype (genes important in energy conservation)[75]. It might appear that the activation of such genes would be beneficial at times of famine but can lead to obesity and diabetes in times of plenty. Girls with low birth weight and premature pubarche, experience menarche before 12years of age and develop hyperinsulinaemic androgen excess [76]. The

treatment of these group of individuals with metformin pre and during puberty has been shown to prevent the development of features of PCOS [77].

1.3.4.6 Genetic Factors

PCOS is a genetically heterogeneous syndrome in which the genetic contributions remain incompletely described. The problems associated with genetic studies in PCOS relate to it's heterogeneity, difficulty with retrospective diagnosis in post-menopausal women, associated subfertility, an incompletely understood aetiology and gene effect size.

There is often a clustering of PCOS within families [78, 79] and studies indicate that an autosomal dominant mode of inheritance occurs for some families with this disease. Twin studies have shown a heritability of 75% for PCOS with a correlation of 0.71 between monozygotic twins and 0.38 between dizygotic twins [80]. Many published genetics studies in PCOS have been underpowered, and the results of published candidate gene studies have been disappointing.

An initial GWAS in China found association of PCOS (Rotterdam criteria) with the following three loci: 2p16.3 (luteinising hormone/choroidogonadotrophin receptor; LHCGR), 2p21 (thyroid adenoma associated protein; THADA) and 9q33.3 (DENN/MADD domain containing 1A; DENND1A). Two of these loci, THADA and DENND1A have been confirmed as risk loci in a European PCOS cohort (NIH criteria) but there was insufficient power to confirm LHCGR as a risk locus [81]. A further GWAS has identified THADA as a novel Type 2 diabetes (T2DM) gene associated with pancreatic beta cell dysfunction [82]; this might explain in part the increased risk of T2DM observed in PCOS.

An important link between PCOS and obesity was demonstrated genetically for the first time by data from a case-control study in the United Kingdom that involved 463 patients with PCOS and more than 1300 female controls [83]. This study showed an association between the FTO gene and obesity which was confirmed by meta-analysis of European and Chinese data [84, 85].

1.3.5 Prevalence

PCOS is recognised as one of the most common endocrine and metabolic disorders in pre-menopausal women. Its prevalence depends in part on the diagnostic criteria used to define the disorder [86]. In the general population to date the prevalence of PCOS has been determined primarily using the NIH 1990 criteria. As per the NIH criteria the prevalence rates of PCOS have varied between 6 to 10% across the globe [86-90]. However, an Oxford study conducted at the same time found prevalence rates of between 8% (using NIH criteria) and 26% (using polycystic ovaries on ultrasound and an additional feature of PCOS as diagnostic criteria) [88]. A number of conditions may be associated with an increased prevalence of PCOS such as oligo-ovulatory infertility [91], obesity and/or insulin resistance [92, 93], the presence of Type1 [94], Type 2 [95] or gestational diabetes mellitus [96], a history of premature adrenarche [97] and first degree relatives with PCOS [79, 98].

1.3.6 Clinical Features

PCOS is an important cause of menstrual irregularity and androgen excess in women. As it is a syndrome with multiple potential aetiologies clinical presentations can be variable with key features of oligo or anovulation and hyperandrogenism. Other

features are polycystic ovaries on pelvic ultrasonography, infertility due to oligoovulation, obesity, and insulin resistance.

1.3.6.1 Reproductive

PCOS is estimated to be the most common cause of ovulatory dysfunction, accounting for 70–90% of ovulatory disorders [99]. Prolonged periods of anovulation are likely associated with increased infertility [100]. Women with PCOS are also more likely to develop gestational diabetes in pregnancy and have a higher risk of pregnancy complications than controls [101]. Other factors associated with PCOS, such as obesity, have also been associated with subfertility and delayed conception [102].

1.3.6.2 Dermatological

Hirsutism, acne and androgenic alopecia are the common features of hyperandrogenism in PCOS. Hirsutism is present in between 65 to 75% of subjects with PCOS [103], the prevalence of acne and male pattern balding varies between 14 to 25% [104]. Androgenic alopecia has been associated with metabolic syndrome [105] and insulin resistance [106, 107].

1.3.6.3 Metabolic

Women with PCOS are commonly overweight or obese. Although the exact prevalence is not known, most investigators find that at least one-half of women with polycystic ovary syndrome are obese [108]. Insulin resistance is common in PCOS with prevalence rates reported from 44 to 70% [63] and has been shown to be independent of obesity. In addition, the prevalence of the metabolic syndrome in women with PCOS appears to be increased [109, 110]. Most studies of women with PCOS have

demonstrated low high-density lipoprotein (HDL) cholesterol and high triglyceride concentrations, consistent with their insulin resistance [111], as well as an increase in low-density lipoprotein (LDL) cholesterol [112, 113]. Women with PCOS are more likely to have an increase in small dense LDL particles (associated with increased risk of cardiovascular disease) when compared to BMI matched women and insulin resistance without PCOS [114, 115]. There is increased risk of impaired glucose tolerance (IGT) and Type 2 Diabetes [61, 116, 117], especially in women with a first degree relative with type 2 diabetes with a reported 2.6 fold increase in prevalence [116]. In one study the annual conversion rate from normal glucose tolerance to impaired glucose tolerance was 17%. Obstructive sleep apnoea (OSA) has been found to be five- to thirty-times higher in women with PCOS compared to BMI-matched controls [118]. The prevalence of non alcoholic fatty liver disease (NAFLD), including non alcoholic steatohepatitis (NASH) may be increased in women with PCOS by 2% to 70% depending on the diagnostic criteria used for PCOS, NAFLD and the presence of obesity [119-122].

1.3.7 Morbidity associated with PCOS

1.3.7.1 Cardiovascular Disease

Obesity, hypertension, dyslipidaemia and T2DM are all risk factors for cardiovascular disease (CVD). It may appear that despite the high prevalence of risk factors for CVD in women with PCOS, there are limited longitudinal studies to definitively confirm an increased risk of CVD morbidity or mortality, and those undertaken are too small or have insufficient follow-up to detect differences in event rates [123]. Nevertheless, epidemiological data consistently point to increased cardiovascular risk in women with PCOS. The nurses' health study, a prospective cohort study of 82,439 nurses with 14

years of follow-up, found a significantly increased risk of non-fatal or fatal coronary heart disease in women who had reported very irregular menstrual cycles (age-adjusted relative risk 1.67, 95% CI 1.35-2.06) which remained after adjustment for BMI and other confounding factors (multivariate risk ratio 1.53, 95% CI 1.24-1.90) [124]. Although there was no confirmed diagnosis of PCOS in these women, the commonest cause for irregular menstrual cycles is PCOS. In addition, a case-control study based on data in the Women's Health Study database found that women who developed cardiovascular events had lower SHBG and higher calculated free androgen index [125]. Furthermore an evaluation of postmenopausal women for suspected ischaemia showed that clinical features of PCOS were associated with more angiographic coronary artery disease and worsening cardiovascular event-free survival [126]. A large community-based database review showed that women with PCOS did not have an increased risk of large vessel disease but there was an increased risk of T2DM compared to age and BMI-matched controls [127]. Therefore it appears that there are conflicting evidence with respect to cardiovascular risk.

Studies exploring surrogate markers of cardiovascular disease studies have shown increased carotid artery intima-media thickness (an independent predictor of stroke and myocardial infarction) in women with PCOS compared with age-matched control women [128]. Coronary artery calcification, is more common in women with PCOS than in controls, even after adjusting for the effects of age and BMI [129, 130]. Echocardiographic changes in PCOS showed anatomic and functional differences such as increased left atrial size, increased left ventricular mass index, lower left ventricular ejection fraction [131] and diastolic dysfunction [132]. The left ventricular mass index was related to the degree of insulin resistance [131]. In addition some studies demonstrate impaired endothelial function in women with PCOS with features of

reduced brachial artery reactivity in response to hyperaemia [133, 134] and reduced vascular compliance. This has been demonstrated in women with PCOS at an early age (early 20's) and largely independent of obesity, insulin resistance, total testosterone or total cholesterol [135]. A cross sectional study conducted by our group previously showed an association of increased central arterial stiffness and diastolic dysfunction with insulin resistance and central obesity but this was not associated with any increase in young women with PCOS per se [136]. Treatment with insulin sensitising drugs or weight loss has been associated with improvement in endothelial function although the results have been variable between study groups on account of the diagnostic criteria used and the heterogeneity of the study population [137-139].

1.3.7.2 Type 2 Diabetes Mellitus

As mentioned above, there is an increased risk of developing T2DM in PCOS. Both adolescent and adult women with PCOS are at increased risk of developing Impaired Glucose Tolerance (IGT) as well as type 2 diabetes. A diagnosis of PCOS confers a 1.5 to 2 fold increased risk of developing Type 2 diabetes [127]. The prevalence of IGT and type 2 diabetes in PCOS women varies up to 35 % and 10%, respectively depending on the criteria used for the diagnosis and the age, ethnicity and BMI of the population [108, 116, 140-142] . The rate of conversion from IGT to DM2 in 2 Australian studies ranged from 2.9% per year to 8.7% per year [143, 144]. Women with PCOS are also at a higher risk of developing gestational diabetes (GDM) independent of weight. However obesity can exacerbate the onset of GDM in PCOS [140, 143]. The International Diabetes Federation recognises PCOS as a non modifiable risk factor for the development of type 2 diabetes [145].

As discussed earlier insulin resistance and beta cell dysfunction contribute to glucose intolerance which can progress to diabetes. Glucose intolerance develops when there is a defect in the secretion of insulin or on account of the pancreatic cells being unable to compensate for insulin resistance. The occurrence of hyperinsulinaemia and insulin resistance is found more frequently in women with PCOS compared with age and weight matched controls [146, 147]. Anovulatory women have a greater degree of insulin resistance than those with menstrual regularity [148, 149]. Insulin resistance has also been correlated with androgen levels in women with PCOS [150]. Insulin resistance is a precursor for type 2 diabetes and cardiovascular disease and hence these conditions occur more frequently in PCOS. Glucose intolerance is seen at an earlier age in the third to fourth decade of life [116, 140]. It has been observed that women with PCOS have increased mortality from complications of diabetes [151].

1.3.7.3 Non Alcoholic Fatty Liver Disease (NAFLD) and Non Alcoholic Steatohepatitis (NASH)

NAFLD is characterised by excessive fat accumulation in the liver (steatosis), whereas NASH defines a subgroup of NAFLD in which steatosis coexists with liver cell injury and inflammation (after exclusion of other causes of liver disease (viral, autoimmune, genetic, alcohol consumption, etc). NAFLD is now recognised as the leading cause of cryptogenic cirrhosis and encompasses a spectrum of diseases ranging from simple steatosis to nonalcoholic steatohepatitis (NASH) to cirrhosis [152, 153]. Insulin resistance is detected in up to 80% of cases of NAFLD and there is a near universal association between NAFLD and IR irrespective of obesity [154]. The first connection between NAFLD and PCOS was reported in 2005 and subsequent retrospective studies have confirmed this association [155]. The prevalence of NAFLD within the PCOS

population is now estimated to be anywhere between 15% and 55% depending on the diagnostic index used for PCOS and NAFLD (increased serum alanine aminotransferase or ultrasound) [120, 121, 156]. Risk factors pertinent to PCOS include increasing age, ethnicity, and metabolic dysfunction (obesity, hypertension, dyslipidaemia, diabetes). A systematic review determined that IR is present in 50%-80% of women with both PCOS and NAFLD [157] and multiple studies have shown that PCOS women with hepatic steatosis have elevated levels of IR compared to PCOS women without steatosis [122, 156, 158]. It is not clear how androgens influence disease progression in NAFLD but one theory suggests suppression of LDLR gene transcription resulting in the downregulation of low density lipoprotein (LDL) receptor in women with PCOS which prolongs the half-life of very low-density lipoprotein (VLDL) and LDL and thus induce lipid accumulation in the liver [154]. Thus, women with PCOS and metabolic risk factors and/or IR may be screened using serum markers of liver dysfunction. If serum markers are elevated, noninvasive quantification of fibrosis by ultrasound and liver biopsy may be considered [159].

1.3.7.4 Obesity

Many women with PCOS are overweight or obese (between 38% to 88%) [160, 161]. Increased abdominal obesity is associated with hyperandrogenaemia and increased metabolic risk [162].

The prevalence of obesity varies greatly across the world, yet the prevalence of PCOS remains relatively similar in studies in countries with different background rates of obesity (30% – 70%) [108, 163]. A modest but non-significant trend has been reported in the prevalence of PCOS with increasing obesity [93]. This may result due to the

combined effect of a genetic predisposition to obesity in the context of an obesogenic environment as a result of reduced exercise and poor diet.

Abdominal obesity may cause relative hyperandrogenaemia, characterised by reduced SHBG (Sex Hormone Binding Globulin) and increased bioavailable androgens to target tissues [164]. This may be associated with an increased rate of testosterone production and a non-SHBG-bound androgen production rate of dehydroepiandrosterone and androstenedione [165]. This might explain the increased frequency of menstrual abnormalities and chronic anovulation in adult overweight and obese women with PCOS compared to normal weight women [164]. In addition obese women with PCOS also exhibit diminished responsiveness to ovulation inducing drugs such as clomiphene citrate, gonadotrophins or pulsatile GnRH [100, 166].

Although weight gain in both normal women and those with PCOS is associated with increasing insulin resistance, most women with PCOS (between 50% and 90%, depending on the diagnostic criteria used) have insulin resistance to a significantly greater extent than in age and BMI-matched control women, with subjects with higher BMIs showing a higher degree of insulin resistance [148, 167].

The presence of obesity in PCOS increases the risk of metabolic syndrome, Impaired glucose tolerance / diabetes mellitus, dyslipidaemia and insulin resistance [116, 140, 148, 164].

1.3.7.5 Depression

An increased prevalence of depression has been consistently observed in women with PCOS in small community based and case control studies. Most of these studies are limited by sample size and in some cases lack of control subjects. In women with PCOS compared with non-BMI-matched controls, self-rated questionnaires

demonstrate an increased rate of depressive symptoms [168, 169]. In studies with direct psychiatric interviews, there was a higher lifetime incidence of a major depression episode and recurrent depression (OR, 3.8; 95% CI, 1.5– 8.7; $P= .001$) and a history of suicide attempts that was seven times higher in PCOS cases compared to controls [170]. A U.S. study reported a 50% rate of depression in women with PCOS ($n =32$). However, there were no control subjects included in the study. Using the Centre for Epidemiological Studies Depression Rating Scale, the investigators found higher scores among women with insulin resistance and in women with elevated body mass index (BMI). This is supported by another study by Holinrake *et al.* which showed that women with PCOS were at an increased risk for depressive disorders (new cases) compared with controls (21% vs. 3%; odds ratio 5.11 [95% confidence interval (CI) 1.26–20.69]; $P=.03$). This was noted to be independent of obesity or infertility: subjects with PCOS and depression had a higher BMI and insulin resistance ($P<0.02$) [171]. The relationship between androgens and mood in women is controversial. Although a few small studies suggest a correlation between depressive symptoms and serum androgens [168, 172] other studies have failed to demonstrate this association [173].

1.3.7.6 Sleep Disordered Breathing (SDB) / Obstructive Sleep Apnoea (OSA)

Women with PCOS develop OSA at rates that equal or exceed those in men. The high prevalence of OSA is thought to be a function of hyperandrogenism as well as obesity (common in PCOS), although these factors alone do not fully account for the finding [118, 174]. Insulin resistance may be a stronger risk factor than obesity or testosterone for sleep disordered breathing [118]. Women with PCOS were 30 times more likely to have SDB independent of obesity, the use of oral contraceptives seems to protect from SDB. [118]. Oestrogen suppresses IL-6 secretion, which is elevated in sleep apnoea,

potentiates the transcription of the corticotrophin-releasing hormone (CRH) gene, and stimulates the noradrenergic system in the brain by inhibiting norepinephrine clearance [175, 176].

1.3.7.7 Cognitive Function

There is no clear evidence to suggest an adverse effect of PCOS on cognitive function. There are very few studies which have investigated this, these studies have been limited by the lack of adequately matched controls as well as sample size. In a study by Barnard *et al.* who compared neuropsychological functioning in an internet-based study in 135 women with PCOS and 322 controls, women with PCOS demonstrated impaired performance in terms of speed and accuracy, on reaction time and word recognition tasks [177]. Some studies have investigated the effects of manipulation of testosterone on cognition in women with PCOS [178]. A decrease in free testosterone levels did not affect performance on tests of visuospatial ability, verbal memory, manual dexterity, or perceptual speed. However there was an improvement in measures of verbal fluency compared to their pre-treatment scores. One study evaluated working memory function with the use of functional magnetic resonance imaging before and after anti-androgenic treatment in women with PCOS [179]. This study showed an improvement in measures of executive function with anti-androgen therapy with normalisation of activation of brain centres associated with a working memory task.

1.4 MAGNETIC RESONANCE IMAGING

1.4.1 Introduction

Magnetic Resonance Imaging (MRI) is a commonly used non invasive radiological imaging technique that produces three dimensional detailed anatomical images without the use of damaging radiation. It is often used for disease detection, diagnosis, and treatment monitoring. The use of MRI scanners are dependent on use of strong magnetic fields, radio waves and field gradients to form images of the body. Due to the absence of ionising radiation in MRI as opposed to computerised tomography (CT), this has become one of the most commonly used imaging technique for the evaluation and diagnosis of medical conditions, staging and follow up of disease.

1.4.2 Principles of MRI

MRI is based on the principles of nuclear magnetic resonance of certain atomic nuclei. Protons as in a hydrogen nucleus are present in water molecules and hence in all body tissues. When a human body is placed in a strong magnetic field hydrogen nuclei behave as magnetic dipoles and partially align themselves in the direction of the magnetic field. Through manipulations of static and dynamic magnetic fields and use of radio-frequency pulses signals can be received and localised from protons anywhere in the body. These signals are then converted into digital images which characterise the signal from each 'voxel' (volume element) of the image.

1.4.3 Diffusion Tensor Imaging

The broad spectrum of magnetic resonance contrast mechanisms makes MRI one of the most powerful and flexible imaging tools for diagnosis in the central nervous system.

The advent of echo planar imaging (EPI)[180] significantly shortened magnetic resonance imaging times. EPI allows acquisition of images in 20-100 msec. This time resolution virtually eliminates motion related artefacts. Echo planar images, with resolution and contrast similar to those of conventional MR images, can be obtained by using multishot acquisitions in only a few seconds. The most prevalent clinical application of EPI is imaging of the brain (Diffusion and functional MRI).

Diffusion MRI is a magnetic resonance imaging method which allows the mapping of the diffusion process of molecules, mainly water, in biological tissues in vivo and non-invasively. Molecular diffusion in tissues is not free, but reflects interactions with many obstacles, such as macromolecules, fibres, and membranes. Water molecule diffusion patterns can therefore reveal microscopic details about normal tissue architecture and the way that it is altered in disease. For most fluids and solid homogeneous materials like gels diffusion is the same in all directions. This diffusion pattern is described as **isotropic** (Fig 1.3A) where molecular motion is random and can be characterised by a single diffusion coefficient (diffusion coefficient is equal in whatever direction it is measured in). However in biological tissues diffusion is often anisotropic and therefore multiple coefficients are required to characterise it. This property is known as **anisotropy** (Fig 1.3B); it may be used to define the direction of the axons in a particular voxel.

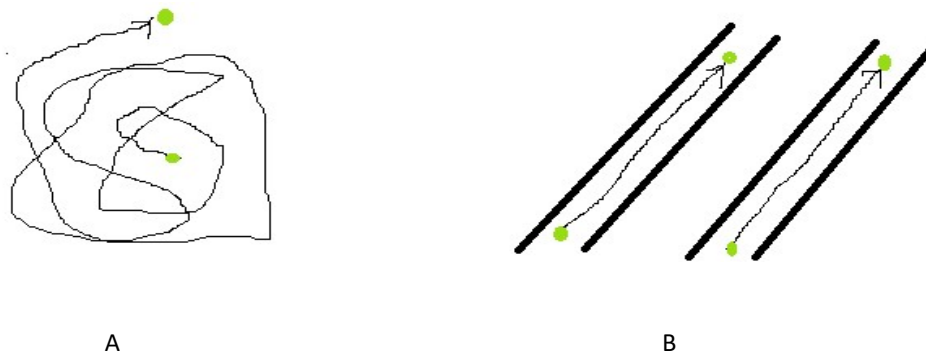


Fig 1.3 Drawings showing diffusion of water molecules

- A) Isotropic diffusion showing random diffusion of water molecules in liquids
- B) Anisotropic diffusion as seen in strongly aligned white matter fibres where random motion is constrained by physical barriers such as cell membranes

Using conventional MRI, grey matter of the brain can be easily identified. However with conventional proton magnetic resonance imaging techniques, the white matter of the brain appears homogeneous without any suggestion of the complex arrangements of fibre tracts. Hence the demonstration of anisotropic diffusion in the brain by magnetic resonance has demonstrated a means of non-invasive exploration of the structural white matter *in vivo* [181-183].

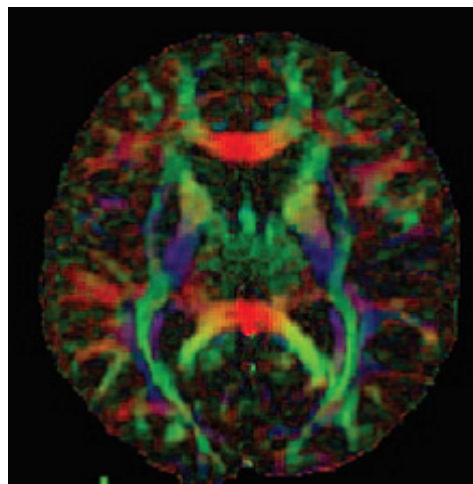


Fig 1.4 Axial tractographic image (2 dimensional image) created demonstrates white matter tracts in the brain in the left to right (red), anterior to posterior (green) and superior to inferior (blue) directions.

This orientation of fibre bundles can be visualised on 2 dimensional images by assigning a colour to each of the 3 axes, left to right (red) anteroposterior (green) and superior to inferior (blue) (Fig 1.4) [184, 185]. These colour maps are very useful for

surveying the organisation of white matter in the brain and for identifying major white matter tracts on 2 dimensional sections [185, 186].

In tissues, such as brain grey matter, where the measured apparent diffusivity is largely independent of the orientation of the tissue (i.e. isotropic), it is usually sufficient to characterize the diffusion characteristics with a single (scalar) apparent diffusion coefficient (ADC). White matter is highly anisotropic owing to parallel orientation of its nerve fibre tracts and diffusion is restricted perpendicular to the long axis of the nerve fibres [187]. As the measured diffusivity is known to depend upon the orientation of the tissue, no single ADC can characterise the orientation-dependent water mobility in these tissues. The next most complex model of diffusion that can describe anisotropic diffusion is to replace the scalar diffusion coefficient with a symmetric effective or apparent diffusion tensor of water, \underline{D} which is a mathematical tool for representing diffusion in 3D and describes the mobility of the molecules in each direction and the correlation between these directions [188]. The diffusion tensor model consists of a 3×3 matrix derived from diffusivity measurements in atleast six collinear directions [189, 190]. The tensor matrix is diagonally symmetric.

$$\underline{D} = \begin{pmatrix} D_{xx} & D_{xy} & D_{xz} \\ D_{yx} & D_{yy} & D_{yz} \\ D_{zx} & D_{zy} & D_{zz} \end{pmatrix}$$

The three diagonal elements (D_{xx} , D_{yy} , D_{zz}) represent diffusion coefficients measured along each of the principal (x , y and z) laboratory axes. The six off-diagonal terms (D_{xy} , D_{yz} , *etc*) reflect the correlation of random motions between each pair of principal directions.

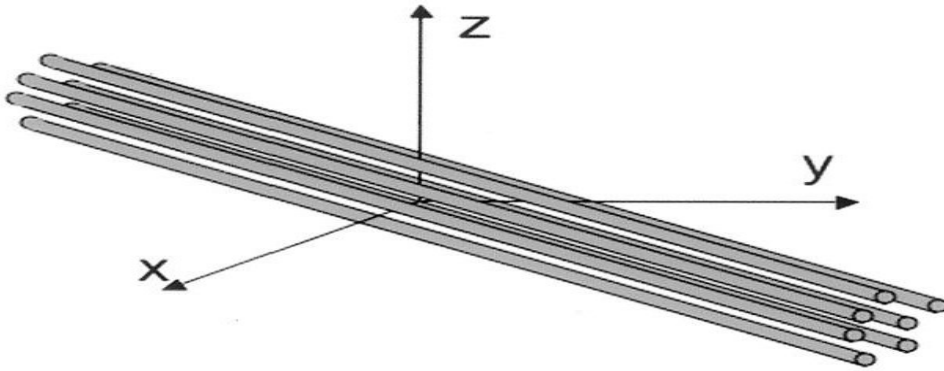


Fig 1.5 Fibre tracts have an arbitrary orientation with respect to scanner geometry (x , y , z axes) and impose directional dependence (anisotropy) on diffusion measurements.

A diffusion tensor representing these three principal axes of diffusion can be visualised as an ellipsoid whose diameter in any direction estimates the diffusion of water molecules in that direction in each voxel in the brain (fig 1.6). The ellipsoid itself has a long axis and two more small axes that describe its width and depth. All three of these are perpendicular to each other and cross at the centre point of the ellipsoid. The axes in this setting are called eigenvectors and the magnitude of their diffusion eigenvalues.

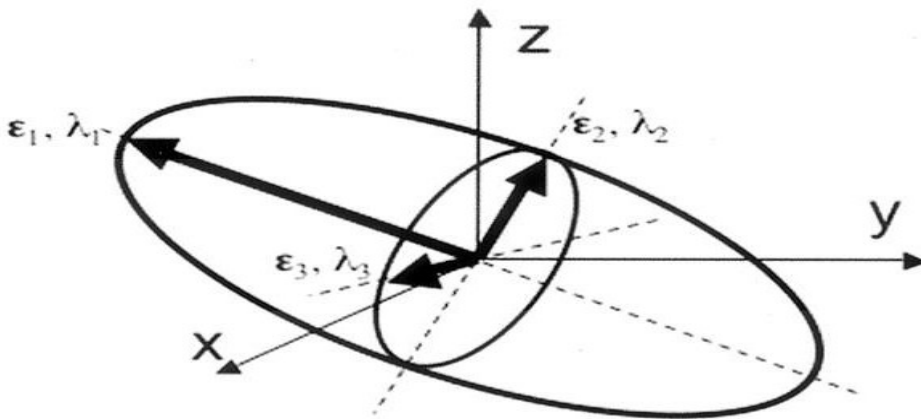


Fig 1.6 Diffusion Ellipsoid The three-dimensional diffusivity is modelled as an ellipsoid whose orientation is characterized by three eigenvectors (ϵ_1 , ϵ_2 , ϵ_3) and whose shape is characterized three eigenvalues (λ_1 , λ_2 , λ_3). The eigenvectors represent the major, medium, and minor principle axes of the ellipsoid, and the eigenvalues represent the diffusivities in these three directions, respectively.

The eigenvector corresponding to the largest eigenvalue, termed the principal eigenvector, corresponds to the main direction of diffusion of water molecules in that

voxel. By convention eigenvalues are labelled in descending order of magnitude ($\lambda_1 \geq \lambda_2 \geq \lambda_3$). Another important measure is the tensor orientation described by the major eigenvector direction. With reference to figure 1.6, when the principal eigenvalue is much larger than the second and third eigenvalues, anisotropy measures will be high, indicating a preferred direction of diffusion. This corresponds to a cigar or prolate shape of a diffusion ellipsoid. The preferred direction of diffusion is indicated by the long axis of the ellipsoid or by the primary eigenvector of the tensor. This pattern of diffusion within a voxel is found in parts of the brain with densely packed parallel fibres.

1.4.4 Diffusion Metrics

The display, meaningful measurement, and interpretation of 3D image data with a 3×3 diffusion matrix at each voxel is a challenging task. In order to simplify data the image information is distilled into simpler scalar maps. The two most common measures are the trace and anisotropy of the diffusion tensor. The trace of the tensor (Tr), or sum of the diagonal elements of D, is a measure of the magnitude of diffusion and is rotationally invariant.

$$\text{Trace of the tensor (Tr)} = \lambda_1 + \lambda_2 + \lambda_3$$

The mean diffusivity (MD) is used in many published studies and is simply the trace divided by three which is equivalent to the average of the eigenvalues.

$$\text{Mean Diffusivity (MD)} = \frac{\lambda_1 + \lambda_2 + \lambda_3}{3}$$

Another important measure of the directionality of diffusion commonly employed in diffusion MRI studies is the **fractional anisotropy** (FA) described originally by Basser

and Pierpaoli [191]. It is a scalar value that describes the degree of anisotropy of a diffusion process. FA values vary between a value of 0 indicating isotropic diffusion (cerebrospinal fluid and grey matter) to a maximum value of 1 indicating perfectly linear diffusion along the principal eigenvector (highest in major white matter tracts).

It is independent of local fibre orientation and is therefore a relatively objective and easy measure to compare across subjects. It can also be computed in each individual voxel. FA is high in white matter, especially in major tracts in which axons are packed in a coherent, parallel fashion. It is also increased by the presence of axonal membranes or myelin sheaths that hinder diffusion. Disruption of this coherent organisation or loss of axons or myelin generally leads to a decrease in FA and increase in MD. A decline in FA is often used as an index of decreasing white matter health.

The measure of diffusion along the principal axis λ_1 is called the **axial diffusivity** (AD) and is assumed to reflect the orientation of fibres in a white matter tract (measure of axonal integrity).

Radial diffusivity (RD) is a measure of diffusion perpendicular to the principal axis (This is the average of the diffusivities in the two minor axes λ_2 and λ_3).

Radial Diffusivity (RD) = $\frac{\lambda_2 + \lambda_3}{2}$

2

RD is an assessment of the degree of restriction due to membranes [192].

As mentioned earlier FA measures between a value of 0 indicating isotropic diffusion (cerebrospinal fluid and grey matter) to a maximum value of 1 indicating perfectly linear diffusion along the principal eigenvector (highest in major white matter tracts).

The use of diffusion tensor imaging (DTI) has significantly improved the imaging and interpretation of diffusion of water molecules in tissues with direct in vivo examination of aspects of tissue microstructure. The principles of diffusion anisotropy are adopted to provide excellent details of white matter microstructure and the construction of white matter tracts. (Tractography) [193].

1.4.5 White Matter Tractography

With the use of diffusion tensor fibre tracking the diffusion tensor of each voxel can be utilised to follow an axonal tract in 3D from voxel to voxel through the human brain. This follows coherent spatial patterns in the major eigenvectors of the diffusion tensor field [194, 195]. This principle is often combined with functional or anatomic information to delineate specific white matter pathways [194]. White matter patterns are estimated by starting at a specified location (also called the ‘seed’ point), estimating the direction of propagation (major eigenvector), and moving a small distance in that direction (called tract integration). The tract direction is then re-evaluated and a further step is taken until the tract is terminated.

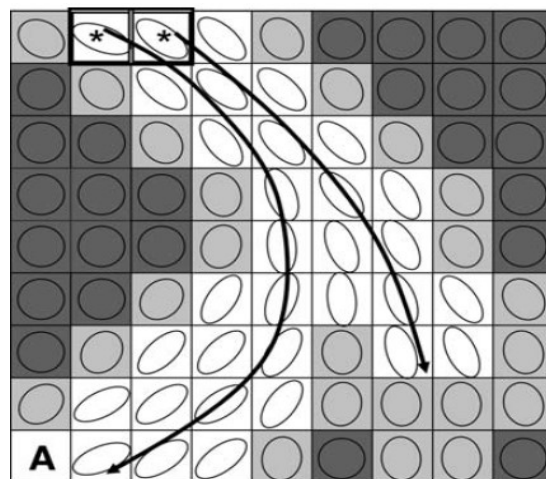


Fig 1.7 Schematic diagram showing a basic algorithm for tract reconstruction

Degree of diffusion anisotropy is indicated by gray scale (white is highest). On basis of defined thresholds, tracking (long curved arrows) is along voxels with similar measures of anisotropy and direction of principal eigenvector. Asterisks indicate starting point of tracking.

This principle is illustrated above in Fig 1.7 where average fibre orientation is estimated from diffusion anisotropy at each pixel (ellipsoids in neighbouring voxels line up), and a line is propagated from a pixel of interest (pixels with asterisks) following the fibre orientation until it reaches a brain region of low anisotropy which is depicted by the dark pixels.

There is good evidence that tracking results of prominent white matter tracts correlate well with classical definitions based on post mortem studies [196, 197]. On the other hand the technique can produce false positives and false negative results due to noise, partial volume effects, and complex fibre architectures within a pixel [198, 199]. This can be improved upon by applying anatomical constraints by employing multiple regions of interest (ROI) [197, 200]. This technique requires *a priori* knowledge about the trajectory and can be used only for well-characterised white matter tracts. Although this improves the validity of the technique it is unlikely to be fully accurate. Development of robust protocols by devising specific region of interest drawing schemes based on the anatomical features of individual tracts and using regions that are sufficiently large has improved reproducibility to a significant degree. This has developed as a valuable tool to test hypotheses whether specific white matter tracts are involved in a disease of interest.

Although tractography corresponds well to classic neuroanatomy, problems of validation remain as to the degree to which results differ from those of anatomic methods such as dissection [201]. Nevertheless this divergence would not diminish its utility as this form of 3D tractography can depict human neuroanatomy non-invasively, at the same time can detect changes to anatomy and microstructural integrity of specific white matter pathways. Microstructural abnormalities in several white matter tracts is

increasingly being recognised as a mechanism of cognitive deterioration in aging and metabolic studies [202-204].

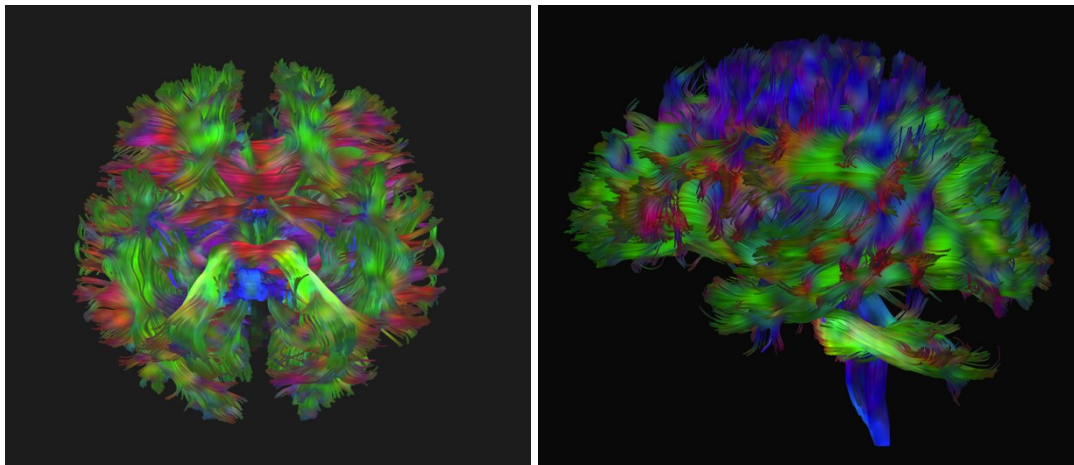


Fig 1.8 Whole brain Tractography – Axial view (Left) and sagittal view (Right) Image generated from whole brain diffusion tensor tractography using EXPLORE-DTI software. Direction of white matter fibres are illustrated : Anterior to Posterior (green), Left to Right (red) and Superior to Inferior (blue)

1.4.6 Tract Based Spatial Statistics (TBSS)

Tract-based spatial statistics (TBSS) is an automated observer-independent approach for assessing groupwise microstructural differences in the major white matter pathways of the brain [205]. It enables voxel-wise and group-wise comparison of diffusion parameters across all major white matter tracts common to subjects without the need for a prespecified region of interest.

As mentioned earlier there are several limitations to white matter tractography. This method is subjective and restricts the areas of investigation to those that are either easily identifiable or thought to be of greatest clinical significance and therefore may miss unexpected areas of injury. ROI-based analyses can be time consuming and often rely on investigator accuracy. These limitations make comparison of multiple brain regions across larger groups more difficult. In contrast, an important advantage of

TBSS is that it is free of *a priori* bias about the likely location of structural alteration in the brain. TBSS is a widely accepted approach for statistical analysis of diffusion data.

This process is done through linear and non-linear alignment, thus improving interpretability of analysis of multi-subject DTI data investigation of the brain as a whole and not specific white matter tracts. As TBSS is fully automated it is simple to apply and investigates the whole brain. TBSS is achieved first by taking the average of all the FA values of major white matter tracts as FA skeleton and then by projecting all the images of subjects to this FA skeleton. This will be explained in detail in Chapter 2.

1.4.7 Thesis Aims

PCOS is a common endocrine disorder of young women characterised by abnormalities in both reproductive and metabolic health. This is associated with an increased risk of metabolic risk factors such as type 2 diabetes, obesity and dyslipidaemia. There is evidence to suggest that these risk states may have an influence on brain structure and function. Both type 1 and type 2 diabetes are associated with altered microstructural measures derived from diffusion tensor MRI [202] [206]. Several studies have now shown associations between BMI and white matter microstructure [203, 207]. Alterations in white matter microstructure has been found to correlate with cognitive performance in type 2 diabetes [202]. It is unclear which of these factors are critical in influencing brain structure and function as these metabolic features occur in clustered syndromes rather than as isolated abnormalities. This is also true of previous cognitive studies in PCOS that might have confounded by BMI [208].

We hypothesise that young insulin resistant women with PCOS are at risk of early subtle deficits in cognition and microstructural alteration in the brain.

The aim of this study is to establish whether young women with PCOS display altered white matter microstructure and cognitive function by using advanced MRI and a series of validated measures of cognition.

CHAPTER 2: METHODS

2.1 Outline of Study

2.1.1 Study Approval

The study was approved by the Research and Development department at the University Hospital of Wales (UHW) (Ref 08/RPM/4276) and the South East Wales Research Ethics Committee (Ref 08/WSE04/53) following international guidelines on Human subjects research protection (Declaration of Helsinki). The study was sponsored by Cardiff University (CU) (Ref SPON CU 523 - 08).

2.1.2 Recruitment

Patients aged between 18 and 45 years of age were recruited from local endocrinology, dermatology and gynaecology clinics. They were provided with an information sheet giving details about the study. The initial contact was followed up with a telephone call to determine interest and confirm eligibility. Healthy volunteers aged between 18 and 45 years, were recruited from UHW and CU using intranet postings. All interested, eligible women were telephoned a week later to determine if they wished to participate or not.

2.1.3 Inclusion and Exclusion Criteria of Study Participants

Patients with a diagnosis of PCOS were recruited from the endocrine clinic at UHW. Diagnosis was according to the Rotterdam criteria [49]. Congenital adrenal hyperplasia, Cushing's syndrome, androgen-secreting tumours, hyperprolactinaemia and thyroid dysfunction were excluded by biochemical testing. Women were excluded from participation if they were pregnant, breastfeeding or if they had a history of diabetes,

hypertension or hyperlipidaemia. Potential participants who were taking anti-hypertensive agents, lipid-lowering agents, glucose lowering agents, weight reducing agents or glucocorticoids and who had used anti-androgens within 6 months were also excluded. Neurological exclusion criteria included previous or current major psychiatric illness, clinical cerebrovascular disease, previous severe head injury, current substance and alcohol abuse.

Healthy volunteers were recruited as controls with 1 to 1 matching for age and BMI. For each individual patient, a control was identified matched for age (within 2 years) and BMI (within 2kg/m²). Controls needed to have regular menstrual cycles (menses every 27-32 days). Control subjects with signs of hirsutism or with a personal history of diabetes or hypertension, or a family history of PCOS were excluded. Their health status was determined by history, physical examination and hormonal evaluation (testosterone, androstenedione, thyroid function, prolactin and 17-hydroxyprogesterone). All women were investigated during the follicular phase of their menstrual cycle.

2.1.4 Consent

All participants gave written informed consent prior to entering the study.

2.1.5 Protocol

Participants attended the Clinical Research Facility (CRF), UHW at 8 am following an overnight fast. All subjects had a pregnancy test (urine β -HCG) to confirm that they were not pregnant before a clinical assessment, venepuncture and oral glucose tolerance test were undertaken. The information acquired was recorded on case report forms.

2.2 Clinical Assessment

2.2.1 History and Examination

Details of past medical history, medication taken currently, contraceptive use, smoking history, family history and menstrual history were recorded. A routine physical examination was performed.

2.2.2 Blood Pressure Measurement

After ten minutes of rest in a seated position, three blood pressure recordings were taken from the right brachial artery using a validated semi-automated oscillometric device (Omron 7051T; Omron Corporation, Tokyo, Japan). An average of three readings taken over a 10-minute period was recorded.

2.3 Biochemical and Metabolic Measurements

2.3.1 Sample Collection and Storage

With the subject at rest, an intravenous cannula or butterfly needle was inserted into a suitable vein in the antecubital fossa or forearm and secured. Blood was collected directly via a vacutainer or via a syringe and then decanted into blood bottles. The cannula or butterfly needle was then flushed with 5 ml of normal saline. The subject then received a drink containing 113 ml of Polycal® (concentrated carbohydrate) with 187 ml of water. This provides an equivalent carbohydrate load to a standard 75g dose of anhydrous glucose. Samples were taken at 30, 60, 90 and 120 minutes and marked with the subject number and time. The first 5 ml of blood at each collection were discarded and the cannula was flushed with 5 ml of normal saline after the sampling was completed. The cannula or butterfly needle was removed after the 120 minutes

sample was taken. Samples were centrifuged at 4000 rpm for 8 minutes and stored at -30°C prior to analysis.

2.3.2 Assays

Serum total cholesterol, high density lipoprotein cholesterol (HDL) and triglycerides were assayed using an Aeroset automated analyser (Abbott Diagnostics, Berkshire,UK); LDL cholesterol (LDL) was calculated using Friedewald's formula. Insulin was measured using an immunometric assay specific for human insulin (Invitron,Monmouth, UK) and glucose was measured using the Aeroset chemistry system (Abbott Diagnostics, Berkshire, UK). High sensitivity C-reactive protein (hsCRP) was assayed by nephelometry (BN™ II system, Dade Behring, Milton Keynes, UK) and total testosterone was measured by liquid chromatography-tandem mass spectrometry (Quattro™ Premier XE triple quadrupole tandem mass spectrometer, Waters Ltd, Watford, UK). Androstenedione was measured by immunoassay [Siemens Healthcare]. The interassay coefficients of variation were all less than 9%.

2.3.3 Estimations of Insulin Sensitivity and Insulin Resistance

The hyperinsulinaemic-euglycaemic clamp is the gold standard method to measure insulin sensitivity [209]. The main advantage of this method is that whole body glucose disposal is measured directly at a defined level of hyperinsulinaemia. However, the method is labour intensive, time consuming and expensive and for these reasons was not used.

Two well described alternative methods have been established to overcome the limitations of the hyperinsulinaemic-euglycaemic clamp. These are the homeostatic model assessment (HOMA) [210] and the quantitative insulin sensitivity check index (QUICKI) [211]. HOMA-IR is a paradigm model derived from a mathematical

assessment of the interaction between β -cell function and IR and is calculated using the formula:

$$\text{HOMA-IR} = (\text{FPI} \times \text{FPG})/22.5$$

where FPI = fasting plasma insulin (mU/l) and FPG = fasting plasma glucose (mmol/l).

QUICKI uses a log transform of the insulin-glucose product and therefore correlates to HOMA-IR. These methods require a single fasting insulin and fasting glucose measurement and are therefore ideal for studies involving large numbers of subjects. HOMA-IR was used in this study for these reasons and because it correlates highly ($R_s=0.88$, $P<0.0001$) with the hyperinsulinaemic-euglycaemic clamp [210]. The above methods do not measure insulin sensitivity in a dynamic state. An OGTT assessment of glucose tolerance and insulin secretion in response to a glucose challenge was therefore also undertaken. Insulin measurements at 0, 30, 60, 90 and 120 minutes after a 75 gram glucose challenge allow calculation of area under curve (AUC) for insulin and glucose. The AUC insulin will be greater in an insulin resistant subject than a normal subject, as more insulin will be secreted in response to the glucose load. This is clinically important and has been associated with cardiovascular mortality [212]. Post-challenge insulin levels have also been shown to improve the performance of visceral fat adiposity in identifying subjects with metabolic disease [213].

2.4 Body Composition Measurements

2.4.1 Anthropometric Measurements

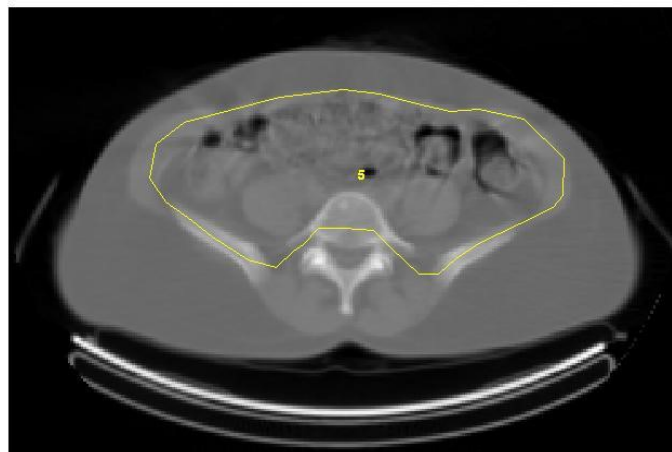
Height was measured to the nearest 0.1 centimetre (cm) using a stadiometer and recorded in metres (m). Measurements were taken with the subject's footwear removed. Their head, back, buttocks and heels were placed against the wall and they were asked

to look straight ahead. The headboard was then moved until firmly pushing on the vertex. Weight was measured to the nearest 0.5 kilogram using digital weighing scales (Omron Monitor BF500, Omron Corporation, Japan). Subjects wore light clothing and had footwear removed. Body Mass Index (BMI) was calculated as weight (kg) divided by height (m) squared. Waist circumference was measured at minimal respiration to the nearest 0.5 cm by positioning a tape parallel to the floor and immediately above the superior iliac crests. Hip circumference was measured to the nearest 0.5 cm by positioning a tape parallel to the floor and at the greatest protrusion of the buttocks.

2.4.2 Computed Tomography

Computed tomography was carried out by Dr. Helen Blundell in the Nuclear Physics department at the University hospital of Wales. With the subject in the supine position, one cross-sectional scan was obtained by CT (Hawkeye, GE Medical Systems) using standard acquisition parameters (140kV, 2.5mA, 10mm slice width, 13.6 s rotation time, 2562 pixel matrix) at the level of the fourth and fifth lumbar spines. The image was imported into MATLAB (MathsWorks) and was analysed by Dr Blundell. The image was segmented into areas of non-adipose tissue and adipose tissue using a fixed range of CT numbers (-120 to -80 to represent fat) derived from a previously published study [214]. The visceral adipose tissue area and total adipose tissue areas were calculated by segmenting an intra-peritoneal region and the whole image respectively as shown in Figure 2.1. Subcutaneous adipose tissue area was calculated by subtracting the visceral fat area from the total fat area.

Figure 2.1 Cross sectional CT scan image



Intra-peritoneal region enclosed within yellow line

Fig 2.1 A single cross sectional CT scan image obtained at level of fourth and fifth lumbar spine with visceral adipose tissue area and total adipose tissue area calculated by segmentation of intra-peritoneal region which is illustrated enclosed within the yellow line.

2.5 Cognitive Testing

A set of cognitive tests was devised based on previous literature on cognitive dysfunction in metabolic disorders [23, 215]. Test domains assessed were episodic memory, attentional and executive function. All the cognitive tests were conducted at Cardiff University Brain Research Imaging Centre (CUBRIC). Participants were subjected to the initial screening process for imaging and following successful completion performed a battery of tests lasting between one and a half to two hours for each subject. The initial process of cognitive testing for the first three participants was carried out by Dr Claudia-Metzler Baddeley, consultant neuropsychologist based at the School of Psychology, Cardiff University. Subsequent cognitive testing was carried out by myself initially under supervision of Dr Baddeley for the next three participants. I carried out independent cognitive assessments for the rest of the study.

2.5.1 Assessment of Premorbid IQ

This was estimated with the National Adult Reading Test (NART , British Edition 1982). It is a widely adopted method for estimating premorbid intelligence both for clinical and research purposes. The test requires subjects to read out loud a set of 50 words, the pronunciations of which are irregular so have to be learnt and cannot be inferred from the spellings [216]. The responses are individually scored as correct or incorrect, according to their pronunciation. This score can then be used to derive a premorbid IQ estimate. This test is a measure of early learning and peak attainment.

2.5.2 Assessment of Intelligence and Executive function

2.5.2.1 Digit Span Task

The Digit Span Task exercises short term and verbal working memory. A series of digits (e.g., '8, 2, 4') were read out to the participants at one digit per second and were told to immediately repeat them back in the same order .If they did this successfully, they were given a longer list (e.g., '9, 2, 4, 1'). Participants got 2 attempts at each span. The test begins with two to three numbers, increasing until the participant fails both trials at a given length. Recognizable patterns (for example 2, 4, 6, 8) were avoided. At the end of a sequence, the person being tested is asked to recall the items in order. The average digit span for normal adults without error is seven plus or minus two. The length of the longest list a person can remember is that person's digit span. While the participant is asked to call out the digits in the given order in the forward digit-span task, in the backward digit-span task the procedure is largely the same, except that subjects being tested are asked to recall the digits in backward order (e.g., if presented with the following string of numbers "3 7 9 1 5" the subject would be asked to recall the digits in reverse order; in this case, the correct response would be "5 1 9 7 3"). This

is a test of working memory as the participant has to hold and manipulate the digits 'online' [217].

2.5.2.2 Digit Symbol Substitution Test (DST)

Digit symbol substitution test is a neuropsychological test which measures response speed and focussed attention and is a sensitive indicator of brain damage, dementia age and depression. It consists of (e.g. nine) digit-symbol pairs followed by a list of digits. Under each digit the subject should write down the corresponding symbol as fast as possible. The number of correct symbols within the allowed time (120 sec) is measured. (Fig 2.2)

Digit	1	2	3	4	5	6	7	8	9	Score														
Symbol	—	⊥	⊐	└	└	○	∧	×	=															
Samples																								
2	1	3	7	2	4	8	2	1	3	2	1	4	2	3	5	2	3	1	4	5	6	3	1	4
⊥	—	⊐	∧	⊥	└	×																		
1	5	4	2	7	6	3	5	7	2	8	5	4	6	3	7	2	8	1	9	5	8	4	7	3
6	2	5	1	9	2	8	3	7	4	6	5	9	4	8	3	7	2	6	1	5	4	6	3	7
9	2	8	1	7	9	4	6	8	5	9	7	1	8	5	2	9	4	8	6	3	7	9	8	6

Figure 2.2 Digit symbol substitution Test

Nine digit symbol pairs followed by list of digits. The number of correct symbols obtained to each corresponding number in 120 seconds is measured.

2.5.2.3 Verbal Trails Test

Attention switching was examined with a version of the Verbal Trails Test that required alternation between letters and digits [218]. Subjects were asked to perform four tasks starting with a presentation of 50 digits in numerical sequence printed on a sheet of

paper. The amount of time required to verbally count numbers starting from 12 to 61 was measured. The second task was similar to the first task but consisted of a list of 50 letters with the subjects having to verbally start from the letter G through a sequence of 50 letters up to the letter D. The third and fourth task consisted of retrieval and recitation of letters and numbers in alternation (digit-letter switching such as “28 D 29 E 30 F31 G32 H up to 25 characters and letter-digit switching for example “R 13 S 14 T 15 U 16 V17” up to a total of 25 characters. The time taken for each of the above tasks was measured. The amount of time in seconds measured as the sum of the time taken for task one and two subtracted from the sum of the time taken for task three and four was called the Verbal trails “switching cost”. Similarly the Verbal trails “errors” was calculated as the sum of the total errors measured in the four tasks.

2.5.2.4 Verbal Fluency Test

The Verbal Fluency Test [219] consists of two tasks : category fluency (sometimes called semantic fluency) and letter fluency (sometimes called phonemic fluency). As per the standard versions of the tasks, participants were given 1 min to produce as many unique words as possible within a semantic category (category fluency) or starting with a given letter (letter fluency). The categories selected were Animals and Boy’s names and letters selected were F, A and S. The participant's score in each task is the number of unique correct words.

2.5.2.5 Stroop Colour Word Test

The suppression of response incongruent information was measured with the Stroop test. [220] The Stroop effect is a demonstration of interference in the reaction time of a task. When the name of a colour (e.g., "blue", "green", or "red") is printed in a colour not denoted by the name (e.g.,the word "red" printed in blue ink instead of red ink),

naming the colour of the word takes longer and is more prone to errors than when the colour of the ink matches the name of the colour. This test is considered to measure selective attention, cognitive flexibility and processing speed, and it is used as a tool in the evaluation of executive functions.

2.5.2.6 Free and Cued Selective Reminding Test

The 16-item version of controlled learning is called the Free and Cued Selective reminding Test (FCSRT) [221]. It has been used in several other longitudinal aging studies in North America and Europe to identify preclinical and early dementia. The test begins with a study phase in which subjects were asked to examine a card containing sixteen words (objects) for an item that goes with a unique category cue. The card was then taken away from the subject after one minute and immediate recall of the sixteen words was tested. The study phase was followed by the test phase that consisted of three recall trials, each preceded by 20 seconds of subjects counting backward to prevent recall from short-term memory. Each recall trial consisted of two parts. First, each subject had up to two minutes to freely recall as many items as possible. Next, aurally presented category cues were provided for items not retrieved by free recall. If subjects failed to retrieve the item with the category cue, they were reminded by presenting the cue and the item together. The sum of free and cued recall is total recall. The total score obtained from the three recall trials was a maximum of 48 with a maximum score of 16 points per trial.

2.5.2.7 The Rey–Osterrieth Complex Figure Test (ROCF)

The ROCF test is a neuropsychological assessment in which examinees are asked to reproduce a complicated line drawing, first by copying it freehand (recognition), and then drawing from memory (recall) [222]. It permits the evaluation of different functions, such as visuospatial abilities, memory, attention, planning, and working memory (executive functions).

The ROCF test consists of the following steps:

Copy: In the Copy condition, the subject is given a piece of paper and a pencil, and the stimulus figure is placed in front of them. They reproduce the figure to the best of their ability. The test is not timed, but the length of time needed to copy the figure is observed. Once the copy is complete, the stimulus figure and the examinee's copy are removed from view.

Immediate recall: After a short delay (2 minutes), the subject is asked to reproduce the figure from memory.

Delayed recall: After a period of 20 minutes, the subject is asked once again to reproduce the figure from memory. In this study the delayed recall component of the test was not administered.

2.5.2.8 Wechsler Abbreviated Scale of Intelligence – Second Edition (WASI-II)

WASI-II provides a brief, reliable measure of cognitive ability for use in clinical, educational, and research settings. This form has four subsets (vocabulary, similarities, Block design and matrix reasoning), two composite scores (verbal and performance) and a full scale IQ. These tests have shown to be correlated strongly with general

intellectual functioning. Specifically, the subtests of vocabulary and similarities are used to estimate verbal IQ (VIQ) which provides a measure of verbal comprehension and working memory, whereas block design and matrix reasoning are used to estimate performance IQ (PIQ) which provides a measure of perceptual organisation and processing speed. Performance on each subtest is converted to an age adjusted standardized score, from which VIQ and PIQ scores can be generated. The subtests were administered to all subjects according to standardised procedures specified in the WASI manual. Only raw scores for individual subsets were obtained.

2.5.2.9 Beck's Depression Inventory (BDI)

The BDI (BDI-II) is a 21 question multiple choice self-report inventory for measuring the severity of depression. The most current version of the questionnaire is composed of items relating to depression symptoms such as hopelessness and irritability, cognitions such as guilt or feelings of being punished, as well as physical symptoms such as fatigue, weight loss and lack of libido. When the test is scored, a value of 0 to 3 is assigned for each answer and then the total score is compared to a key to determine the depression's severity. Scores ≥ 17 indicate severe depression that needs to be treated. As depression is a common feature in patients with PCOS with incidence of up to 40% in some research studies [171, 223] this test was administered so that any contribution of depression to cognitive performance could be controlled for.

2.6 MRI data acquisition

2.6.1 Materials

MRI was done by Dr John Evans and Mr Peter Hobden, neuroscientists based at CUBRIC. MRI Scanner: General Electric HDx 3.0 T system.

- a) Gradients: Twin-speed gradient system with gradient strength = 40 mT/m and maximum slew rate = 150 T/m/s.
- b) Radio Frequency (RF) Coils: Whole-body birdcage coil used for RF transmit; eight-channel head coil (made by MRI Devices Corp.) used for RF receive.
- c) Scanner Software Capability: Software to provide diffusion tensor imaging capability.
- d) Peripherals: Adequate padding for the head (wedge cushions, etc.); hearing protection (ear plugs); a peripheral pulse-oximeter; a squeeze-bulb (for the participant to communicate to the operator)

2.6.2 Methods

The participant is warned that the diffusion tensor imaging part of the protocol is ‘louder than the other scans’ and that they ‘can expect the bed to vibrate quite a lot’. The participant is warned that ‘there will be irregularly timed knocking noises – and these will appear to move about as the scan progresses.

1. Scanning: The integrated laser alignment system is used to landmark on the nasion, and the participant slid into the magnet, taking particular care not to trap the squeeze-bulb/pulse-oximeter leads during the process. As an optional extra, the participant is provided with the option of watching a subtitled movie of their choice in the scanner via a rear projection onto a periscope mounted on the head coil.

The sequence is a twice-refocused spin-echo EPI sequence [224] with a parallel imaging (ASSET) factor of 2. Sixty axially oriented slices are prescribed to cover the entire head. The field of view is 230 mm, with an acquisition matrix of 96×96 and a slice thickness of 2.4 mm. A total of 66 images were acquired at each of 60 slice

locations. Six images are acquired with no diffusion-weighting gradients applied, and 60 diffusion-weighted images are acquired at a b-value of 1,200 s/mm². The diffusion-weighted images were acquired with encoding gradients applied along 60 non-collinear directions. The echo time is 87 milliseconds, and the sequence is triggered to the cardiac cycle via a pulse-oximeter placed on the participant's forefinger. Each image is initially stored in DICOM format. We then convert the separate DICOM images into a 4D data set (with 'time' or 'diffusion-weighted measurement' as the fourth dimension) in the NIFTI imaging format.

Fluid attenuated inversion recovery scans (FLAIR) were also obtained. The FLAIR pulse sequence is an inversion recovery technique that nulls fluids and is commonly used in brain scans to suppress cerebrospinal fluid (CSF) effects on the image so as to detect subtle changes at the periphery of the hemispheres and in the periventricular region close to CSF[225]. Acquisition time was 19 minutes. The acquired images were corrected for distortions introduced by the diffusion-weighting gradients and for between-slice motion with appropriate reorienting of the encoding vectors [226] before a model was fitted to the data to estimate the diffusion orientation in each voxel. Images were visually inspected for the presence of white matter hyperintensities. On this basis, two subjects were excluded from further analysis.

Once the 4 D (Diffusion weighted image) is obtained it is important to correct it for subject motion and eddy current induced distortions. Although the twice-refocussed spin-echo sequence will ameliorate much of the eddy currents, residual distortions are corrected by using a global affine registration software package which was done using the Explore-DTI software package [227]. Further distortions that commonly occur are partial volume effects (PVE) which can confound the results of diffusion MRI studies

because of tissue loss or atrophy. This depends on the degree of brain atrophy which affects the amount of CSF partial voluming as decreasing volume of white matter structures has been shown to increase the relative contribution of PVE contaminated voxels due to an increase in surface area to volume ratio. This occurs in areas where white matter abuts the CSF spaces. This problem was addressed by Free water elimination method [228, 229]. This was done by modelling the effect of cerebrospinal fluid contamination on intra-voxel diffusion data directly by adopting a two compartment model and fitting two tensors to diffusion data, one anisotropic and one isotropic with diffusion characteristics of free water. The advantages of this technique is that it can be employed in data acquired by single b-value acquisition protocols. A by-product of this method is that it provides a voxel-wise map of tissue volume fraction(f), which might provide complementary information on tract structure attributable to atrophy at a microstructural scale [230].

The final stage in a standard Diffusion Tensor MRI pipeline is to derive parameters of interest from the diffusion tensor. Maps of the following microstructural measures were then created: Mean diffusivity, Axial Diffusivity and Fractional anisotropy and the principal diffusion orientation which can be used to create directionally encoded colour maps[185] or for fibre tracking analyses [195, 196, 231].

2.6.3 White matter Tractography and Tract specific measures

White matter tractography was carried out by on the assumption that previous positive studies in obesity, ageing ,insulin resistance and diabetes have shown changes in white matter microstructure and similar changes might be reflected in our cohort of patients with PCOS. Based on previous studies 3 major white matter tracts connecting frontal, temporal and parietal regions namely the Fornix, Uncinate Fasciculus and the

Parahippocampal Cingulum were selected [202, 232-234]. I did the white matter tractography initially under the guidance of Dr Claudia Metzler-Baddeley and Dr Michael O’Sullivan who trained me through the process of obtaining accurate and reproducible white matter tractography using the EXPLORE-DTI software and supervised me through the first six MRI images. I was blinded to the dataset containing the MRI images before I started the tractography.

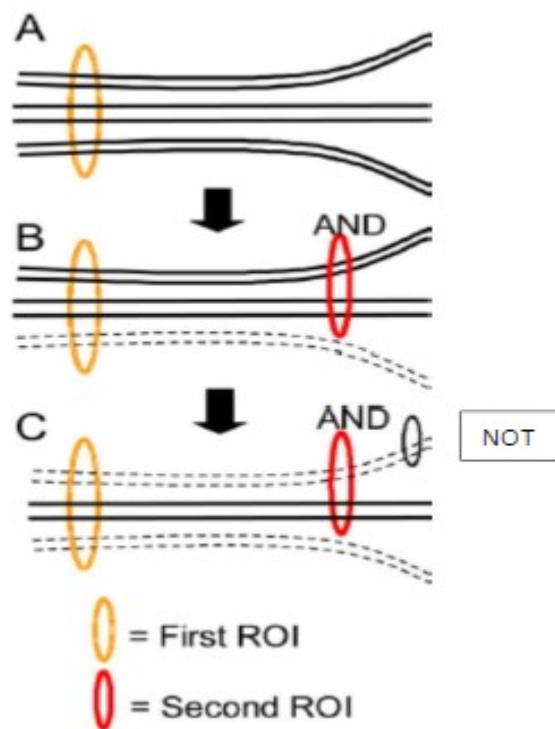


Fig 2.3 A schematic diagram of 2 types of Region of Interest (ROI) operations. When the first ROI (seedpoint) is drawn, all tracts that penetrate the ROI are retrieved (A). If the second ROI is applied as an “AND” operation, the fibres that penetrate both ROIs are retained (B). If a “NOT” operation is used, a subset of the fibres penetrating the NOT ROI is removed (C).

Fibre tracking was performed using a multi-ROI approach. This was used to reconstruct tracts of interest which exploits existing anatomical knowledge of tract trajectories. Tracking was performed from all pixels inside the brain and results penetrating the manually defined ROIs were assigned to the specific tracts associated with the ROIs. When multiple ROIs were used for a tract of interest, two types of operations were

employed namely ‘AND’ and ‘NOT’, the use of which would depend on the characteristic trajectory of each path.(Fig 2.3)

Fornix: The fornix is an integral white matter bundle which projects into the medial diencephalon and is part of the limbic system. It has been demonstrated as the link between the hippocampus, mammillary bodies, and the anterior thalamic nuclei [235, 236]. Recent Diffusion weighted imaging studies have found that changes in fornix microstructure in young people correlate selectively with recollective memory [237]. These studies closely support clinical studies of fornix pathology [238, 239] although the specificity of this association remains unclear.

Uncinate Fasciculus (UF): is a bidirectional pathway that links the anterior temporal lobe with the orbital and medial prefrontal cortex. It provides an afferent sensory route for prefrontal cognitive functions and is known to be associated with auditory-verbal memory and declarative memory [240, 241]. Variations in UF microstructure have been linked to aspects of memory in older adults [241].

Parahippocampal cingulum : include white matter fibres which link the hippocampal formation with the cingulate cortex and recent evidence suggests that it may be critical for strategic memory processes related to successful encoding/retrieval and meta memory.[242]

Tractography based on the diffusion tensor model has been shown to generate anatomically plausible and reproducible reconstructions of tracts within regions of coherently oriented fibres [196, 197]. Tractography was performed using Explore-DTI software package. The deterministic tracking algorithm estimated the principal diffusion orientation at each seed point and propagated in 0.5 mm steps along this direction. The fibre orientation(s) was/were then estimated at the new location and the

tracking moved a further 0.5 mm along the direction that subtended the smallest angle to the current trajectory. In this way, a pathway was traced through the data until either FA fell below an arbitrary threshold (in this case 0.15) or the direction of the pathway changed through an angle of 60°.

Whole-brain tractography was performed using every voxel as a seed point. Three-dimensional reconstructions of the three tracts (Fig. 2.4) were then extracted from whole-brain tractograms by applying multiple waypoint regions of interest (ROIs) masks. Representative ROIs for the three tracts are shown in Figure 4.3. All ROIs were manually drawn in native space on colour-coded fibre orientation maps for each individual dataset by myself using landmark techniques that have previously been shown to be highly reproducible. These are detailed for each tract below. The mean FA and MD were then calculated for all reconstructed pathways in Explore-DTI by averaging the values sampled at each 0.5 mm step along the pathways providing tract-specific means of FA and MD for the left and the right UF, left and right PHC, and the fornix. The precise neuropathological correlates of FA and MD are not known but these measures were adopted as they are most widely used and FA has been shown to have neurophysiological relevance.

Fornix - A seed point ROI (Fig. 2.4A, blue) was placed medially on a coronal slice around the fornix bundle at the level of the entry point of the anterior pillars into the body of the fornix, approximately below the sagittal midline of the corpus callosum. An AND ROI (Fig. 2.4A, green) was defined on an axial slice capturing the crus fornici in both hemispheres at the level of the inferior border of the splenium of the corpus callosum. NOT ROIs (Fig. 2.4A, red) were drawn on coronal slices rostral to the anterior fornix pillars and caudal to the crus fornici as well as on axial slices through

the corpus callosum and the upper pons to exclude streamlines from the corpus callosum and the corticospinal tract. After visual inspection, obvious anatomically implausible outlier streams, if present, were removed using additional NOT ROIs.

Uncinate fasciculus - A seed point ROI was drawn on a coronal slice around the region where the UF enters the frontal lobe immediately rostral to the genu of the corpus callosum (Fig. 2.4B). An AND ROI was placed on an axial slice capturing the UF bundle at the point where the bundle bends into the inferior temporal lobe region. This bend was visually identified on the midline sagittal plane with the axial slice being placed at a level immediately dorsal to the upper pons. A NOT ROI was drawn across the coronal slice level with the front of the pons to remove tracts of the internal frontal-occipital fasciculus. The tract was then visually inspected and any obvious outlier streamlines that were not consistent with the known UF anatomy were removed using additional NOT ROIs. This procedure was performed for both hemispheres.

Parahippocampal cingulum: A seed point ROI was placed on an axial slice level with the pons–midbrain junction around the cingulum fibre bundle that runs caudal and lateral to the pons (Fig 2.4C). A NOT ROI was drawn across the midline sagittal plane to remove inter-hemispheric projections. After visual inspection, further NOT ROIs were placed, when necessary, to remove projections to the occipital lobe and any outlier tracts that were not consistent with the known anatomy of the PHC. This procedure was performed separately for the left and the right PHC.

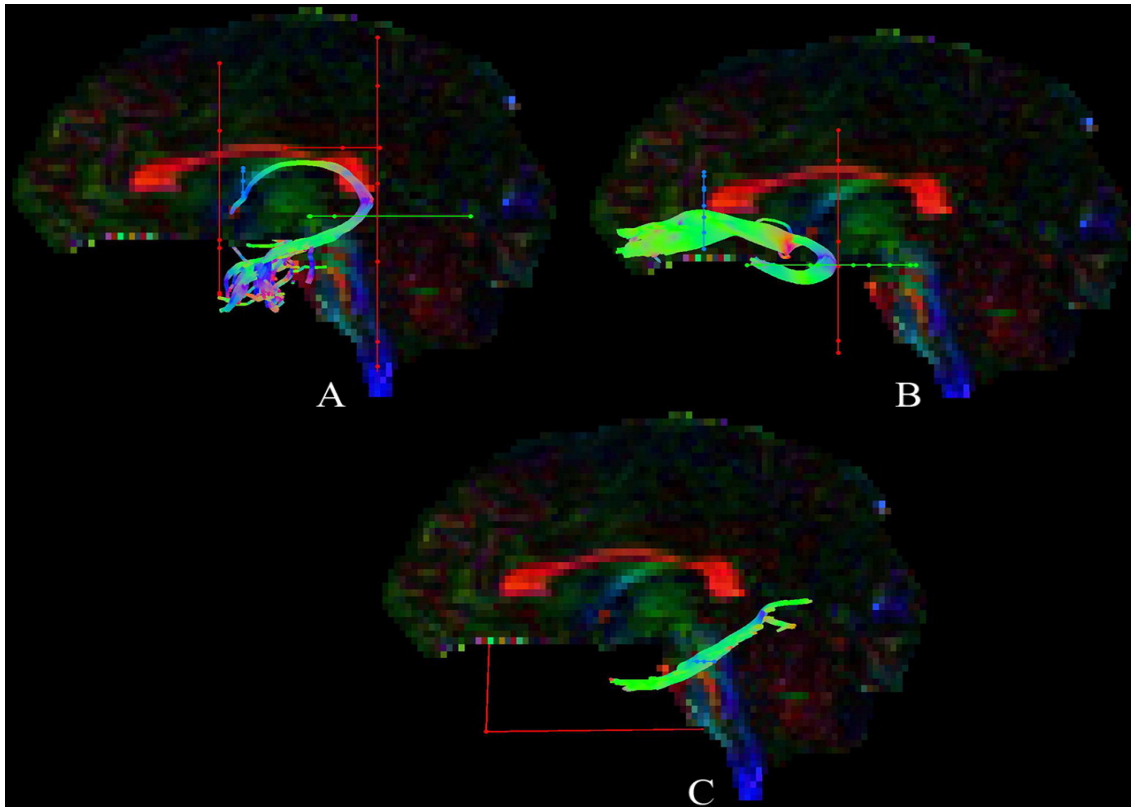


Fig 2.4 Tractography using region of interest (ROI waypoints) Reconstruction based on a standardized atlas of white matter tracts.

Fornix (A) - A seed point ROI (blue) drawn medially on a coronal slice around the fornix bundle at the level of the entry point of the anterior pillars into the body of the fornix and an AND ROI (green) defined on an axial slice capturing the crus fornici in both hemispheres at the level of the inferior border of the splenium of the corpus callosum.

Uncinate fasciculus (B) - A seed point ROI (blue) drawn on a coronal slice around the region where the UF enters the frontal lobe immediately rostral to the genu of the corpus callosum and an AND ROI (green) placed on an axial slice capturing the UF bundle at the point where the bundle bends into the inferior temporal lobe region.

Parahippocampal cingulum (C) - A seed point ROI (blue) placed on an axial slice level with the pons–midbrain junction around the cingulum fibre bundle that runs caudal and lateral to the pons.

2.6.4 Tract –based spatial statistics (TBSS)

This method is executed by the software FSL (FMRIB software Library). TBSS was performed by Dr Rok Berlot, a neuroscientist based at Kings College London. Data analysis and the results were provided by Dr Berlot.

The summary of TBSS is presented as follows.

- Identify a common registration target and align all subjects' FA images to this target place.
- After identifying the most typical subject as the target, a mean FA skeleton image from all aligned images by applying 'thinning' (non-maximum-suppression perpendicular to the local tract structure). Threshold this to remove areas of low FA values and areas with high inter-subject variability.
- Project each subjects' FA data onto the skeleton by filling the skeleton with FA values from the nearest relevant track centre. This is done by searching along all voxels in the local 'tract perpendicular direction', and the voxel with the highest FA is identified as the centre of the tract.
- Carry out voxel-wise statistics across subjects on the skeleton-space FA data.

The detail of each step is described in the section below.

Voxel-wise statistical analysis of diffusion data was carried out using TBSS (Tract-Based spatial Statistics), part of FSL (FMRIB Software Library <http://www.fmrib.ox.ac.uk/fsl/> Version 5.0)[205]. The recommended FMRIB58_FA standard-space image was used as the registration target. Each subject's aligned FA data were then projected to the mean FA skeleton. Voxel projections defined in this way were applied to project voxel values of MD, AD, RD and f to the white matter skeleton for each subject. Resulting data were used to generate voxel-wise statistical analyses. The details of this analysis was carried out as below.

Preprocessing

The first step in TBSS is preprocessing the FA image. It includes removing eddy current which is created by gradient coils of MRI and head motion during scanning. Head motion creates rigid body image motion while eddy current forms first order

linear image transformation .[243] Eddy current is removed by using built-in software eddy current correction in FSL. After preprocessing, diffusion tensors can be calculated with extraction of tensor eigenvalues measurement of FA. Finally, the BET brain extraction tool is used to exclude nondiffusion brain voxels from further consideration.[244]

Non-linear alignment

The next step for aligning multiple FA images to each other is using nonlinear alignment.(Fig 2.5) Here, the main anatomical features of the images will not change and keeping the general tract structure intact is important to prepare for the next stage (projection of data on tract skeleton). Non-linear registration was completed by registering FA images to FMRIB58_FA standard-space image, an averaged FA map included with the software package.[245]

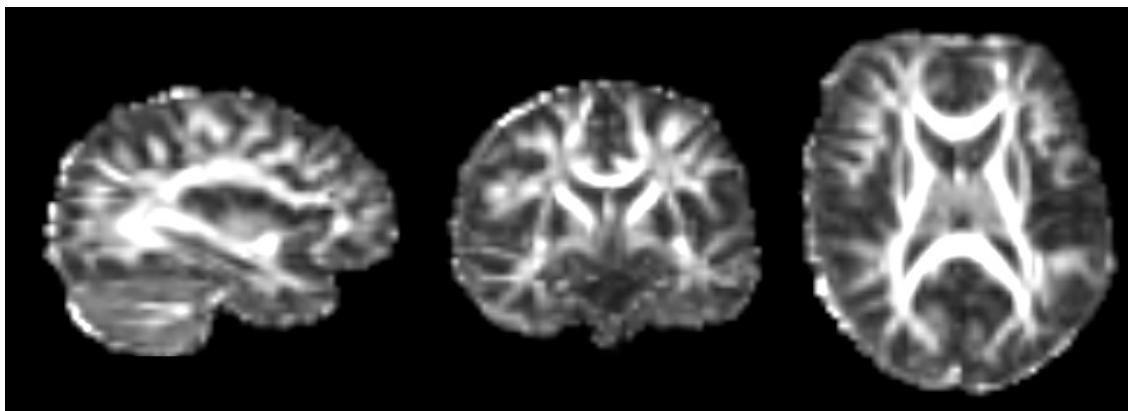


Fig 2.5 Tract Based Spatial Statistics Voxel-wise non-linear registration to prealign all subject's FA images which is done by registering all subjects FA images to a standard FMRIB58_FA standard space image (high-resolution averaged of 58 well-aligned good quality FA images from healthy male and female subjects aged between 20-50).

Identifying the target for alignment

Registration of a target is more successful if the target is a real FA image rather than an average FA image as a single subject will be sharper than an averaged image, giving

better information to drive the alignment. A single subject's FA image is identified to act as the target for all nonlinear registrations. This is done by registering every subject to every other subject, summarising each warp field by its mean displacement, and choosing the 'most representative' individual.

Creating mean FA image and skeleton:

After identifying the most typical subject as the target, all subjects' FA images are aligned to this. This target image is then aligned into MNI152 (Montreal Neurosciences Institute) standard space. MNI152 is a standard template derived by the averaging of 152 diffusion tensor images of the brain obtained from 152 different people. An 'average' brain is seen when visualising the MNI152 image. Registration of all study subjects' scan to this space enables easier statistical analysis of imaging data. Every image is transformed into 1x1x1mm MNI152 space by combining the nonlinear transform to the target FA image with the affine transform from that target to MNI152 space. All subsequent processing is carried out using this space and resolution. Affine and nonlinear registrations were combined in order to avoid resampling the images twice. The mean FA image is created by averaging the transformed images. This image is smooth due to averaging of FA images across subjects and resolution up sampling. It is then used to create the skeleton image which represents all the 'common' tracts of the aligned images.

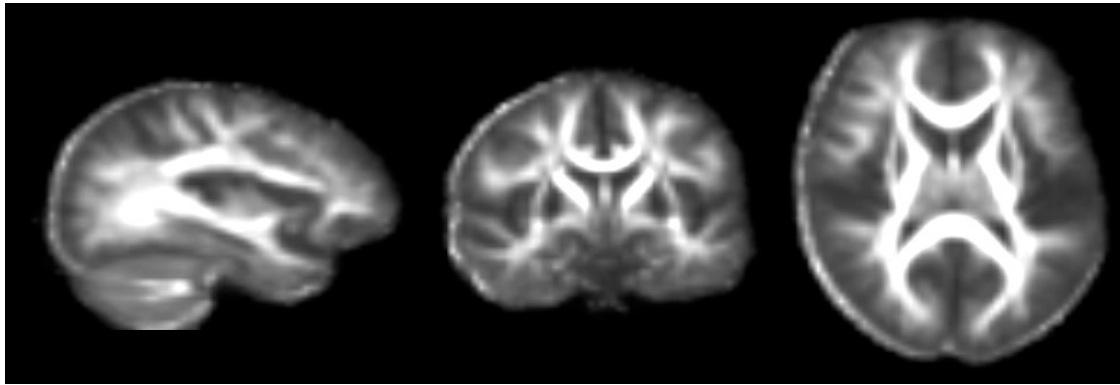


Fig 2.6. Tract based spatial statistics (TBSS) Mean fractional anisotropy (FA) image with no smoothing. Mean FA is fed into tract skeleton generation which aims to represent all tracts which are common to all subjects. This is highlighted in the figure above in white in the sagittal (left), coronal (middle) and axial (right) views.

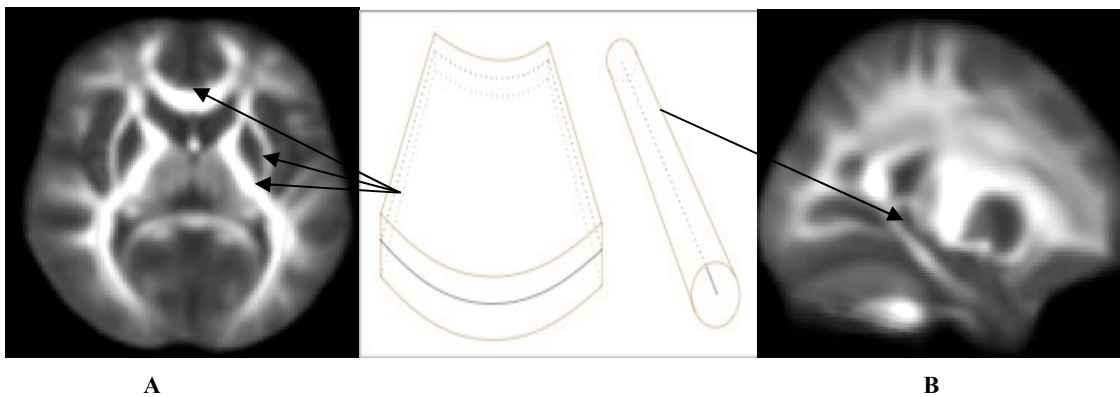


Fig 2.7. Examples of fibre bundles; a thick sheet with a thin surface as its skeleton (A) and a ‘tube’, with a line as its skeleton (B). Tract skeleton will represent each white matter tract as a single line or surface running down the centre of the tract. Contiguous sets of tracts appear as curved sheets as shown in figure A (eg the corpus callosum) or, less frequently, curved “tubes” (e.g., the cingulum bundle) as shown in figure B.

The next step involves making the skeleton image from the mean FA image. The first step is to estimate local surface perpendicular direction (at all voxels in the image) and search for all voxels in this direction (tract perpendicular direction), the one with the highest FA value is identified as the centre of the tract. If the voxel of interest is far from tract centre, the FA value will be higher in the neighbouring voxels on one side of the voxel than on the other side and the direction in which it is highest shows toward the centre of the tracts. This can be explained in Figure 2.8 below.

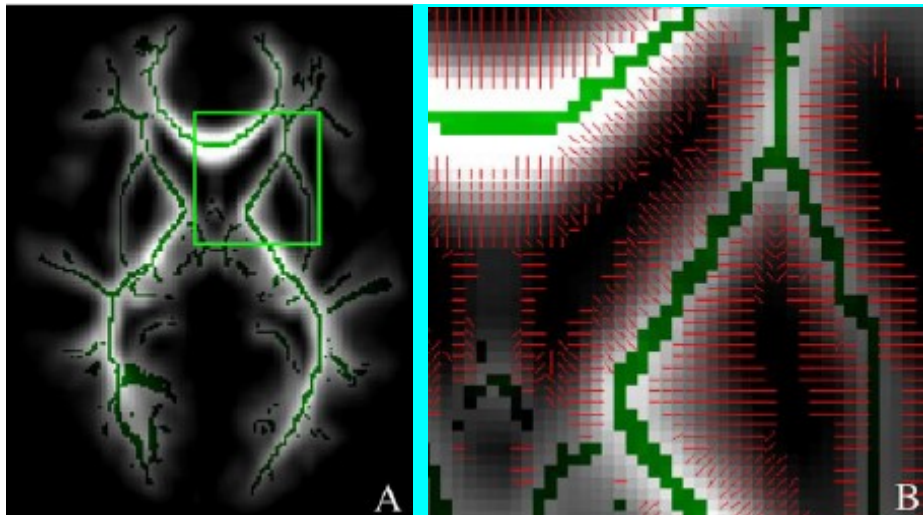


Fig 2.8. A. Original mean FA image with final skeleton and region of interest (ROI) used for sub-image. **B.** Skeletonisation, using local FA centre-of-gravity to find tract perpendiculars (search for the voxel with highest FA which is projected on to the skeleton). This results in a FA skeleton which is thresholded in order to remove areas with large inter subject variations .

The constructed skeleton FA value is thresholded in order to remove areas with large inter subject variations.

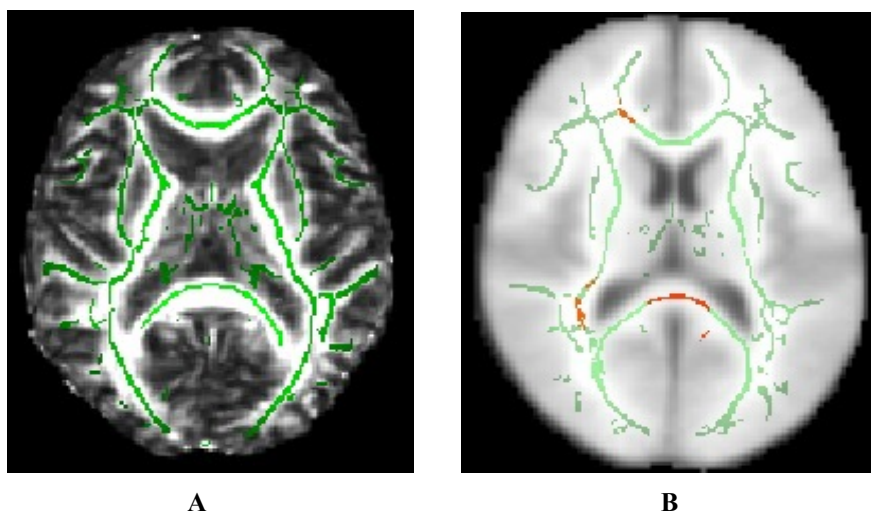


Fig 2.9 A) Example of white matter skeleton which is shown in green. This defines the set of voxels used in all subsequent processing. All FA image (containing all subjects' aligned FA data) and, for each "timepoint" (i.e., subject ID), is projected onto the mean FA skeleton. This results in a 4D image file containing the (projected) skeletonised FA data.

Fig 2.9 B) Voxel-wise statistics on skeletonised FA data (Comparison of data across groups)
 The final step involves projection of data using voxel-wise statistical analysis (measures of diffusion such as axial diffusivity (AD), mean diffusivity (MD), radial diffusivity (RD), f (tissue volume fraction) onto the skeleton which delineates for eg which FA skeleton voxels are significantly different between two groups of subjects

Projecting individual subjects FA onto skeleton

After the skeleton tract is ready, we now ‘project’ each subject FA image onto the mean FA skeleton. This projection from the tract centre to the mean skeleton is accurate providing a sort of “fix” for such misalignments in actual tracts. For each voxel in the skeleton tract, a maximum FA value in a perpendicular direction is searched from a subject’s FA image. The perpendicular directions of the skeleton are already prepared from the previous skeleton formation. This assignment is valid only in perpendicular direction as the change in FA value is greatly pronounced in this direction than the parallel direction. There are two limitations for the searching of maximum FA value to the skeleton tract. The first limitation is that search is limited to voxels closer to the starting section of the skeleton than that of the farther section of the skeleton. Space between two separate sections of skeleton are divided into two and each skeleton section can search voxels from its space. This is achieved by using distance map which shows the distance of each voxel from the nearest skeleton voxel. This constraint also ensures each voxel in the image is mapped only to a single point in the skeleton.

Statistics and thresholding

At this stage the data are ready to be fed into voxel-wise cross subject statistical analysis. Since each FA image of the subjects is aligned into a common space using constrained nonlinear registration, common tract skeleton has been formed, and each subject FA has been projected into the skeleton via perpendicular search for local tract centre. In order to find group differences between two groups, an unpaired t-test is used.

2.7 Statistical Analysis

In the absence of *a priori* information about the most sensitive cognitive tests in PCOS, I chose to generate a composite score from Principal Components Analysis (Appendix 1 Page 95). The principal component was derived from a combination of the following tests: Digit Span, Free and Cued Selective reminding test, Rey Osterrieth Complex figure test, Verbal Trails, Digit Symbol Substitution and the letter and semantic fluency test. General cognition score which accounted for 35% of the variance across all test scores, was used as a summary score and compared across the two groups using an unpaired t-test. A threshold of significance of 0.05 was used for this single comparison. Subsequent comparisons for individual test scores were performed as a means of exploring the pattern of any significant difference between groups: uncorrected p-values are presented but not interpreted in terms of significance for individual test scores.

For TBSS, two-sample unpaired t-tests for reduced and increased DTI measures in PCOS patients compared to controls were performed. Additionally, microstructural measures were correlated with the value of the general cognition score and hormonal levels in each group separately. Statistical inference was based on permutation: five thousand permutations were performed using randomise software [246]. Resulting statistical maps were thresholded for $p < 0.05$, correcting for multiple comparisons using threshold-free cluster enhancement (TFCE) [247].

2.8 Power Calculations

In the absence of any prior data in subjects with PCOS, sample size calculations were based on data from a previous study which examined the influence of BMI on corpus

callosum microstructure [207]. A BMI difference of 10kg/m^2 corresponded to a difference in FA of 0.05 (SD of FA measures 0.04). I calculated that a sample of 18 participants per group would provide at least 95% power to detect a between-group difference in FA of 0.05 at the 5% significance level.

CHAPTER 3 RESULTS

3.1 Introduction

There is increasing appreciation of the importance of mid life risk states and its association with late life cognitive decline. Risk states in middle age include behavioural factors such as smoking [44, 248], aspects of cardiovascular function such as hypertension [33, 249-251], cardiac structure and metabolic traits. Metabolic factors shown to confer risk in cohort studies include diabetes [202, 252-254] and prediabetes [255, 256]. Adiposity generally indexed by body mass index (BMI), has also been associated with subsequent dementia [19, 29, 257]. A negative association between visceral adiposity and performance in the domain of verbal learning and memory has been observed in recent studies in healthy young women aged between 20 – 45 years of age [29] . Insulin resistance is the main pathological condition underlying vascular disorders, such as diabetes, obesity and cardiovascular disease and has been implicated as a major risk factor for cognitive decline in recent studies [258-260] . We hypothesised that women with PCOS and hyperandrogenism along with insulin resistance would demonstrate worsening cognitive function in the context of working and episodic memory compared to healthy volunteers.

3.2 Aims

The aims of this Chapter are to:

1. Compare the demographic, anthropometric and metabolic characteristics between PCOS subjects and healthy volunteers.
2. Compare cognitive function between subjects with PCOS and healthy volunteers.

3.2.1 Study recruitment

From the departmental database and outpatient endocrine clinics at the University Hospital of Wales, 18 women with a diagnosis of PCOS were identified. From local advertisement, 22 women expressed an interest in being a healthy volunteer. Healthy volunteers (n=18, all Caucasian) were recruited as controls with 1 to 1 matching for age and BMI. For each individual patient, a control was identified matched for age (within 2 years) and BMI (within 2 kg/m²). Controls needed to have regular menstrual cycles (menses every 27–32 d). Control subjects with signs of hirsutism or with a personal history of diabetes or hypertension, or a family history of PCOS were excluded.

3.2.2 Demographic Data

The number of subjects in each group, their age, BMI, smoking status, ethnicity and medications taken are presented below.

Eighteen women with PCOS (n = 18, 16 Caucasian and 2 Afro – Caribbean) and eighteen healthy volunteers (n = 18) participated in the study. The mean age and standard deviation of the PCOS and HV groups were 31 ± 6 years and 31 ± 7 years respectively, which was evenly matched (p=0.9). Results are displayed in Table 3.2.

There were two current smokers in each group. Two subjects in each group were taking a combined oral contraceptive pill. No subjects were on antidepressants.

Participants in the PCOS group included all subphenotypes as described by the Rotterdam criteria and are shown below in Table 3.1.

Table 3.1 PCOS (subphenotypes as per Rotterdam Criteria)

PCOS (subphenotype)	No (%)
PCO Complete	8 (44)
Normo-androgenic	5 (28)
Non Polycystic Ovary	1 (6)
Ovulatory	4 (22)

PCO complete : Presence of oligo/anovulation (O) + polycystic ovaries (P) + hyperandrogenism (H)

Normo-androgenic : Presence of oligo/anovulation (O) + polycystic ovaries (P)

Non Polycystic ovary : Presence of oligo/anovulation (O) + hyperandrogenism (H)

Ovulatory : hyperandrogenism (H) + Polycystic ovary (P)

Table 3.2 General characteristics of the study population

	PCOS (n=18) Mean \pm SD	Controls (n=18) Mean \pm SD	<i>p-value</i>
Age	31 \pm 6	31 \pm 7	0.9
Estimated Premorbid Intelligence	122 \pm 4	121 \pm 8	0.35
Weight (kg)	78 \pm 21	76 \pm 15	0.68
BMI (kg/m ²)	30 \pm 6	29 \pm 6	0.61
Systolic BP (mmHg)	119 \pm 8	120 \pm 11	0.96
Diastolic BP (mmHg)	66 \pm 8	69 \pm 10	0.36
Waist (cm)	91 \pm 15	86 \pm 13	0.31
Hip (cm)	111 \pm 16	106 \pm 12	0.24
Visceral fat area (cm ²)	31 \pm 23	26 \pm 14	0.46
Subcutaneous fat area (cm ²)	287 \pm 119	298 \pm 114	0.78
Total fat area (cm ²)	318 \pm 133	324 \pm 124	0.89

BMI: body mass index; Estimation of premorbid intelligence was based on the National Adult Reading -Revised.

3.3 Biochemical Characteristics of the Study Population

There was a significant increase in the testosterone, androstenedione and Insulin AUC in subjects with PCOS compared to controls. Biochemical parameters are shown in Table 3.3.

3.3.1 Glucose Tolerance Status

5 subjects in the PCOS group and 2 controls had prediabetes as per the World Health Organisation (WHO) criteria which is described in Table 3.4.

Table 3.3 Biochemical characteristics of the study population

	PCOS (n=18) Mean ± SD	HV(n=18) Mean ± SD	<i>p-value</i>
Testosterone (nmol/l)	1.6±0.6	0.9 ±0.6	0.01
Androstenedione (nmol/l)	13.4 ± 7.3	6.8± 2.5	0.001
hsCRP (mg/l)	1.2 (0.2 -21.8)	0.9 (0.1 -16.7)	0.73
Total cholesterol (mmol/l)	4.6 ±1.3	4.8 ±1.1	0.67
Triglycerides (mmol/l)	1.2 ±1.4	1.0 ±0.5	0.52
LDL cholesterol (mmol/l)	2.4 ±1.4	2.5 ±1.3	0.79
HDL cholesterol (mmol/l)	1.2 ±0.5	1.3 ±0.6	0.65
Insulin AUC (pmol min/litre)	93151 ± 42694	61933 ± 29614	0.04
HOMA-IR	2.6164 ± 0.95	2.005 ± 1.43	0.32
Glucose AUC (mmol min/l)	764 ± 217	692 ± 133	0.24

hsCRP: high sensitivity c-reactive protein; LDL: low density lipoprotein; HDL: high density lipoprotein; Insulin AUC: Insulin area under curve (during oral glucose tolerance test); HOMA-IR: Homeostatic model assessment for insulin resistance. Serum Testosterone, Androstenedione and Insulin area under curve (Insulin AUC) are significantly raised in the PCOS group compared to controls

Table 3.4 Outcome of screening tests for diabetes and dysglycaemia in PCOS and healthy volunteers

Subject No	Status	Diagnosis	HbA1c mmol/mol	FPG mmol/l	2 hour glucose mmol/mol	BMI kg/m ²	Age years
1	PCOS	IGT	40	4.6	8.0	32.5	37
2	PCOS	IGT	30	4.9	8.4	29	31
3	PCOS	IGT	43	4.3	9.1	36.5	33
4	PCOS	IGT	37	5.8	8.3	44	24
5	PCOS	IGT	33	4.7	7.8	30.1	33
6	HV	IGT	36	5.2	8.4	33	36
7	HV	IGT	38	5.4	8.6	32	34

PCOS: Polycystic Ovary Syndrome; HV:Healthy Volunteer; FPG: fasting plasma glucose; BMI: body mass index; IGT: impaired glucose tolerance

Diabetes: WHO/ADA HbA1c ≥ 48 mmol/mol or FPG ≥ 7.0 mmol/l or 2 hour glucose OGTT ≥ 11.1 mmol/l

Impaired glucose tolerance: WHO/ADA FPG < 7.0 mmol/l and 2 hour glucose OGTT ≥ 7.8 mmol/l

Impaired fasting glycaemia: WHO FPG ≥ 6.1 mmol/l and < 7.0 mmol/l, ADA FPG ≥ 5.6 mmol/l and < 7.0 mmol/l

High risk of diabetes: WHO HbA1c 42-47mmol/mol, ADA 39mmol/mol-47mmol/mol

Results displayed in red are abnormal as per WHO criteria

Results displayed in blue are abnormal according to ADA criteria; this is also the cut off for an oral glucose tolerance test according to NICE

3.4 Cognitive Function Tests

There are very few studies which have looked at the effects of PCOS on cognitive function and have focussed predominantly on the effects of androgens and estrogen. Furthermore these studies have been limited by the lack of adequately matched controls [177] or sample size [208]. Cognitive function was assessed in our study cohort as previously explained where they performed a battery of neuropsychological tests and the results were compared across the PCOS group and controls.

3.4.1 Results

No individual in either group had evidence of depression based on Beck depression inventory score (scores all < 15). The groups were well matched for premorbid intelligence as assessed by the National Adult Reading Test. Both groups showed similar high levels of general intelligence with scores of 122.4 in the PCOS group and 120.5 in controls ($p=0.35$).

Cognitive performance was degraded in patients with PCOS compared to controls. For the summary score, the between group difference was significant: $t = 2.88$, $P = .007$. (Appendix 2 Page 97) Subjects with PCOS performed less well compared to controls in tests of short term and verbal working memory as measured by the Digit Span Task. Current IQ was lower in the PCOS cohort as well which was evaluated using the Wechsler Abbreviated Scale of Intelligence (WASI) although it must be emphasised that only raw scores were calculated for this measure of intelligence. Controls showed a better level of functioning across the domains of episodic memory, attention and executive function. Table 3.5 summarises performance on underlying individual cognitive measures.

Metabolic status and cognition in PCOS

No correlation was observed between cognitive performance and testosterone or Insulin AUC in subjects with PCOS (testosterone : $r = -0.12$, $P = 0.64$; insulin AUC : $r = 0.01$, $P = 0.98$).

Table 3.5 Performance on individual cognitive tests

Cognitive Function Tests	Population(n=36, mean ± SD)	PCOS(n=18, mean±SD)	Controls(n=18 mean±SD)	<i>p-value</i>
Intelligence and Executive Function				
National Adult Reading Test	121.4 ± 6.1	122.4 ± 3.6	120.5 ± 7.9	0.35
Digit span forward	12.8 ± 2.2	12 ± 1.9	13.6 ± 2.2	0.02
Digit span backward	8.2 ± 2.5	7.4 ± 2.5	9.1 ± 2.3	0.04
Digit Symbol	86.5 ± 14.5	83 ± 15.8	90.1 ± 12.5	0.14
Verbal Trails (switching cost)	39.5 ± 17.4	44.5 ± 21.2	33.4 ± 9.8	0.03
Verbal Trails (errors)	0.8 ± 1.3	1.1 ± 1.5	.55 ± 1.1	0.23
Letter Fluency	38.6 ± 10.8	38.1 ± 11	39.1 ± 11	0.79
Category Fluency	41.8 ± 7.2	39.6 ± 7.5	44 ± 6.3	0.06
Stroop Colour Word Test (duration)	112.3 ± 22.2	118.3 ± 22.7	106.4 ± 20.5	0.11
WASI (vocabulary)	66.9 ± 8	64 ± 9.2	69.88 ± 5.5	0.02
WASI (block design)	52.6 ± 12	49.1 ± 13.7	56.2 ± 8.9	0.07
WASI (similarities)	41.5 ± 4.4	39.5 ± 4.8	43.61 ± 2.8	0.04
WASI (matrix reasoning)	27.5 ± 5.1	27.1 ± 6.6	27.8 ± 3.2	0.7
Episodic memory				
FCSRT Immediate recall	14.6 ± 2.3	13.7 ± 1.9	15.4 ± 2.4	0.03
FCSRT Free recall	38.4 ± 8.8	35.7 ± 8.9	41.1 ± 8.1	0.06
FCSRT Total recall	43.2 ± 7	41.7 ± 7.7	44.7 ± 6.1	0.20
FCSRT Delayed free recall	14 ± 2	13.2 ± 2.4	14.9 ± 1.2	0.01
FCSRT Delayed total recall	15.9 ± 0.3	15.8 ± 0.4	15.9 ± 0.2	0.65
Rey-Osterrieth Complex figure	28.6 ± 5.9	26.7 ± 6.9	30.6 ± 4	0.05

NART: National Adult Reading test, a score of premorbid intelligence, General Population mean ± S.D: 107.4 ± 17.1 [261] higher score indicates better performance

Verbal Trails (switching cost and errors)/ Stroop Test: higher readings indicate poor performance

Digit span forward / Digit span backward: no normative data: higher score indicates better performance

Digit Symbol Test: Population mean ± S.D: 80.26 ± 14.76 [262]: higher score indicates better performance

Letter Fluency mean ± S.D: 43.1 ± 12.2 : higher score indicates better performance.

WASI: Wechsler Abbreviated Scale Of Intelligence, all scores indicated are raw scores for vocabulary, block design, similarities and matrix reasoning, no normative data for raw scores recorded.

Rey-Osterrieth Complex Figure Test: Immediate Recall General Population mean ± S.D: 20.75 ± 5.75: higher score indicates better performance [263]

FCSRT: Free and Cued Selective Reminding test: higher score indicates better performance. No normative data available in the 18-45 year age group for the english version of this test [264].

3.5 Discussion

The subphenotypes identified under the PCOS group showed a predominance of the PCO complete group who comprised 44% of the PCOS cohort. The two groups were well matched with reference to age and body mass index. No significant differences in anthropometric indices were observed between the 2 groups.

The prevalence of newly established impaired glucose tolerance was higher in the PCOS group (27%) compared to the healthy volunteers (11%). This is not surprising as women with PCOS are at increased risk of developing glucose intolerance and diabetes [127, 265]. The prevalence rates of diabetes and impaired glucose tolerance in PCOS are between 2 to 10% [116, 141, 266] and 10 to 35% respectively [42-44]. In this study 5(27%) subjects in the PCOS group had IGT.

Subjects with PCOS showed a significantly higher levels of testosterone and androstenedione compared to controls. This was anticipated since hyperandrogenism is common in women with PCOS, although the presence of biochemical hyperandrogenism is not absolutely necessary to establish a diagnosis of PCOS according to the Rotterdam criteria.

Markers of insulin resistance (Insulin AUC) were significantly higher in the PCOS group. This is consistent with other studies. Previous authors have also shown increased basal and glucose- stimulated insulin levels in women with PCOS compared to weight-matched controls [65], and IR is present in PCOS independently of obesity [148] . However although the HOMA-IR was raised in the PCOS group this did not reach statistical significance. This is a major limitation of HOMA as many young PCOS women display stimulated but not fasting metabolic abnormalities [267]. In fact, HOMA in young PCOS patients may miss as much as 50% of IR as compared to OGTT with insulin-AUC calculations[268]. Hence measuring insulin AUC may be a

better measure than other tests to assess insulin resistance in non-obese PCOS patients [267].

Subjects with PCOS showed subtle decrements across a broad range of cognitive tests as shown by principal component analysis despite similar education and premorbid intelligence. This was an interesting finding as this could not be attributed to BMI and age. However looking at the individual test scores there does not appear to be a clear selective pattern of impairment, it is more a general degradation across several domains. The Beck depression inventory was also applied which did not find any evidence of depression with all scores less than 15. This contrasts with studies in PCOS which showed an increased prevalence of depression [168, 169, 171]. This may be related to the small cohort of patients used in this study who did not show any signs of depression the presence of which may have impacted on cognitive function test scores as seen in previous studies [269, 270]. Subjects in both groups had a similar level of general intelligence. Barnard *et al* carried out an internet based computerised study which compared neuropsychological functioning in women with PCOS. They hypothesised that women with PCOS would display enhanced cognitive performance on sexually dimorphic tasks. However no difference in performance was observed on mental rotation and spatial location tasks. Despite presumed hyper-oestrogenism women with PCOS demonstrated impaired performance in terms of speed and accuracy on reaction time and word recognition tasks. The subjects in this study were stratified according to the use of anti-androgen medication and level of depression. This study did not evaluate the biochemical and anthropometric data of the subjects involved and failed to account for the cognitive impairments on the basis of raised testosterone levels [177]. Furthermore another study by Schattmann *et al.* [208] tried to study the possible influence of testosterone on cognitive function in women with PCOS. This

study compared 29 women with PCOS with raised testosterone levels with 22 age and education matched women with normal testosterone levels. Women with PCOS exhibited significantly worse performance on tests of verbal fluency, verbal memory, manual dexterity and visuo-spatial working memory. Another study by the same group investigated cognitive functioning (visuospatial abilities, verbal abilities, and perceptual speed) in women with PCOS after manipulation of testosterone. Hormonal treatment to suppress the level of free Testosterone with cyproterone acetate plus oestrogen did not result in changes in most of the cognitive functions, except for verbal fluency, which appeared to improve. It must be remembered that the earlier studies were limited by poor case-control matching. A recent study by Barry *et al.* found evidence of better visuo-spatial task performance in women with PCOS compared with subfertile controls, but this difference was no longer significant when age and BMI were controlled for in the analysis [271]. Another study evaluating effects of PCOS on cognitive function showed poor performance in the PCOS group on tests of spatial ability and manual dexterity with both reproductive and metabolic features such as menstrual cycle length, number of follicles, triglycerides, Free Androgen Index (FAI), androstenedione and HbA1c emerging as independent predictors [272]. There was no information on anthropometric or biochemical indices provided in this study.

A study by Soleman *et al.* evaluated working memory in women with PCOS with the help of functional MRI [179]. This was a case control study with working memory being evaluated before and after treatment of subjects with PCOS with anti-androgen therapy. The incidence of anxiety and depression was found to be significantly higher in the PCOS group before hormonal manipulation but no differences were seen after treatment. General level of premorbid intelligence as measured by the NART test showed no differences between the 2 groups which was similar to the findings in my

study. The groups were evenly matched for age and BMI. Differences in biochemical parameters were observed in the 2 groups with significant differences between the 2 groups relating to testosterone, oestradiol, LH levels and Free Androgen Index (FAI). Measures of insulin resistance were not evaluated as in our study which was significantly raised in the PCOS group. There was no difference found in reaction time in executing a working memory task before and after treatment with anti-androgens although women with PCOS made fewer errors while completing the task after hormonal manipulation. This may suggest that women with PCOS may need recruitment of additional neural resources during a working memory task suggesting less efficient executive functioning.

The advantages of this study was that the subjects in each group were closely matched for age and BMI which are major confounding factors. Subtle decrements in cognitive function were observed in the PCOS group but I did not find any correlation between cognitive performance and testosterone or insulin AUC in PCOS. Although there is some evidence to suggest that manipulation of testosterone may improve cognitive outcomes these are far from conclusive. I did not look into the effects of specific subphenotypes of PCOS and the effects on cognition. There are indications that menstrual pattern dependent oestradiol levels relate to working memory although this was not investigated in our study cohort [273, 274].

CHAPTER 4 . WHITE MATTER TRACTOGRAPHY AND TRACT BASED SPATIAL STATISTICS

4.1 Introduction

Some early evidence suggests that metabolic risk states may have an influence on brain structure . Diffusion tensor MRI is a non invasive technique that is sensitive to subtle alterations in white matter pathology in the brain. It provides an unprecedented insight into the organisation of white fibres and tracts. Furthermore it provides quantitative indices of white matter fibres and tracts. Damage to white matter matter fibres such as demyelination and axonal changes may lead to changes in the diffusion of water molecules and therefore to a change in DTI parameters. Both Type 1 and Type 2 Diabetes are associated with altered microstructural measures derived from diffusion tensor MRI[206, 215, 275]. Several studies have now shown associations between BMI and white matter microstructure [203, 207, 276]. Furthermore in Type 2 diabetes ,alterations in tract microstructure have been found to correlate with cognitive function. As PCOS is characterised by metabolic risk factors such as obesity and insulin resistance I chose to investigate brain structure in women in early adulthood with a diagnosis of PCOS.

4.2 Aims

The aims of this chapter are to present

1. The results of the diffusion parameters of reconstructed individual white matter tracts in the study group with a view to exploring any changes in white matter microstructure in the prespecified tracts of interest.
2. An analysis of diffusion MRI images to look for changes in white matter microstructure with the application of TBSS to compare between PCOS and controls.

4.3 WHITE MATTER TRACTOGRAPHY

Introduction

Tractography based on diffusion MRI was performed using ExploreDTI [226] software package. 4 white matter tracts were reconstructed as they are known to link components of memory networks. These tracts link frontotemporal regions and have an important role in episodic memory. Diffusion parameters that were used to quantify microstructural white matter abnormalities: Fractional anisotropy (FA), Mean Diffusivity (MD) and Axial Diffusivity (AD) were obtained for each tract.

1. Fornix (Fig 4.1)
2. Right and Left Parahippocampal cingulum (Fig 4.2)
3. Uncinate fasciculus (Fig 4.3)

FORNIX

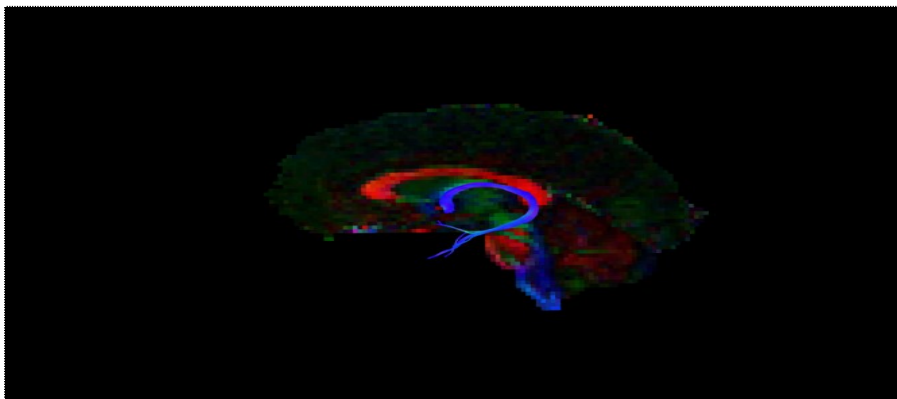


Fig 4.1 Example of reconstruction of the Fornix registered on native space of one participant obtained using EXPLORE-DTI software

UNCINATE FASCICULUS

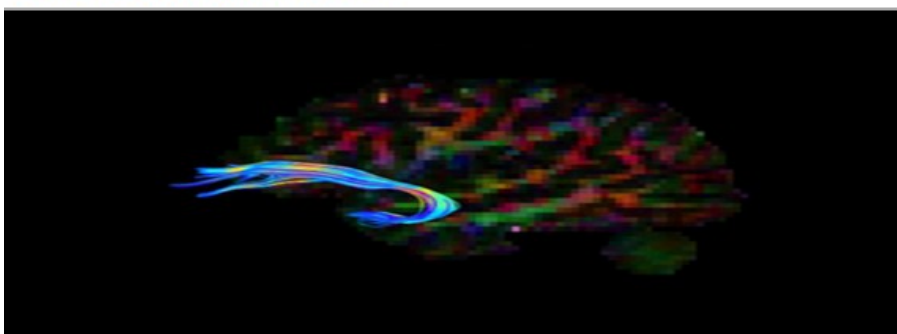


Fig 4.2 Example of reconstruction of the Uncinate Fasciculus registered on native space of one participant using EXPLORE-DTI software

PARAHIPPOCAMPAL CINGULUM

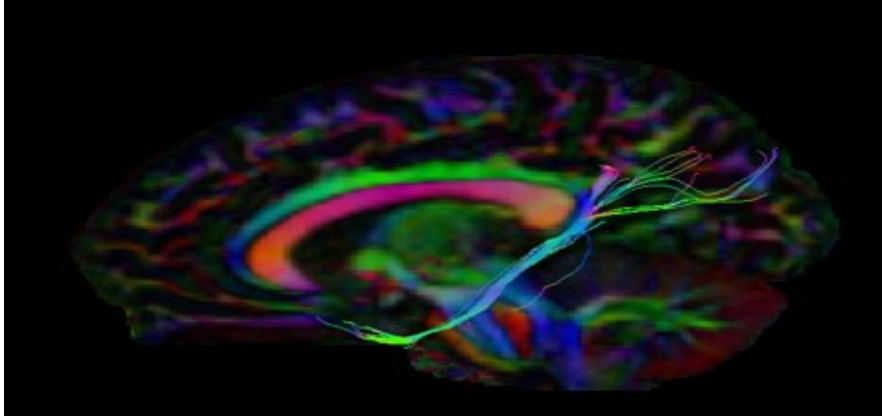


Fig 4.3 Example of reconstruction of the Parahippocampal cingulum registered on native space of one participant using EXPLORE-DTI software

Table 4.1 Group differences in fractional anisotropy (FA), mean diffusivity (MD) and axial diffusivity (AD)

	Controls	PCOS	<i>p</i> value
Fornix			
FA	0.37 ± 0.03	0.36 ± 0.03	0.264
MD	1.22 ± 0.03	1.25 ± 0.04	0.561
AD	1.76 ± 0.10	1.78 ± 0.12	0.752
Uncinate Fasciculus (UF)			
FA	0.43 ± 0.01	0.43 ± 0.02	0.795
MD	0.83 ± 0.12	0.82 ± 0.17	0.773
AD	1.26 ± 0.16	1.25 ± 0.10	0.509
Parahippocampal Cingulum (PHC)			
FA Left	0.38 ± 0.04	0.38 ± 0.06	0.593
MD Left	0.80 ± 0.12	0.78 ± 0.18	0.118
AD Left	1.15 ± 0.13	1.14 ± 0.19	0.301
FA Right	0.39 ± 0.05	0.40 ± 0.04	0.140
MD Right	0.80 ± 0.06	0.78 ± 0.09	0.190
AD Right	1.17 ± 0.11	1.15 ± 0.16	0.124

FA : dimensionless; MD : $10^{-3}\text{mm}^2/\text{s}$; AD : $10^{-3}\text{mm}^2/\text{s}$

Comparative data showing no differences in measures of diffusion (FA, MD and AD) across PCOS and controls obtained through specific white matter tractography of Fornix, Uncinate Fasciculus and Parahippocampal Cingulum

The above tabulated data (Table 4.1) presents the measures of diffusion in the three white matter tracts in the PCOS group and healthy volunteers. No significant differences were observed between the two groups.

4.4 Tract Based Spatial Statistics (TBSS)

No changes were observed in specifically reconstructed white matter tracts in Diffusion weighted tractography. This is a limitation of white matter tractography as a presumed region of interest is studied based on previous data which looked at the involvement of similar tracts connecting frontotemporal regions in conditions such as obesity and diabetes.

After attaining diffusion measurements in each voxel in the brain, the images were all mapped to a single template in order to compare measurements across the PCOS and control groups. This allows measures to be compared voxel by voxel (also described as ‘voxel-based analysis’) with the problem of comparisons across many voxels being addressed one of a number of statistical approaches that are widely accepted in neuroimaging research. The advantage of this approach is that it is free of *a priori* bias about the likely location of structural alteration in the brain. In this study I applied Tract-based spatial statistics which is a widely accepted approach for statistical analysis of diffusion data .

For TBSS, two-sampled unpaired t-tests for reduced and increased diffusion measures in PCOS patients compared to controls were performed. Additionally microstructural measures were correlated with the value of the first Principal Component and hormonal levels in each group separately.

This section aims to present the results and highlight the group differences based on TBSS with respect to:

1. Differences in white matter microstructure between PCOS and controls.
2. Correlation between insulin resistance measured by insulin area under the curve (insulin AUC) and white matter microstructure.
3. Correlation between androgens (testosterone) and white matter microstructure.
4. Correlation between metabolic status , white matter microstructure and cognition in PCOS.

4.4.1 Results

4.4.1.1 Diffusion metrics and white matter microstructure

Analysis of diffusion MRI images revealed differences in white matter microstructure between PCOS and control groups. Areas of decreased AD in PCOS were found throughout the mean white matter skeleton. This is illustrated in Figure 4.4 in blue. In addition, tissue volume fraction was increased in the anterior part of main body of the corpus callosum and parts of anterior white matter which is illustrated in red in Figure 4.4 . No significant differences in voxel-wise values of FA, MD or RD were found between the PCOS group and controls.

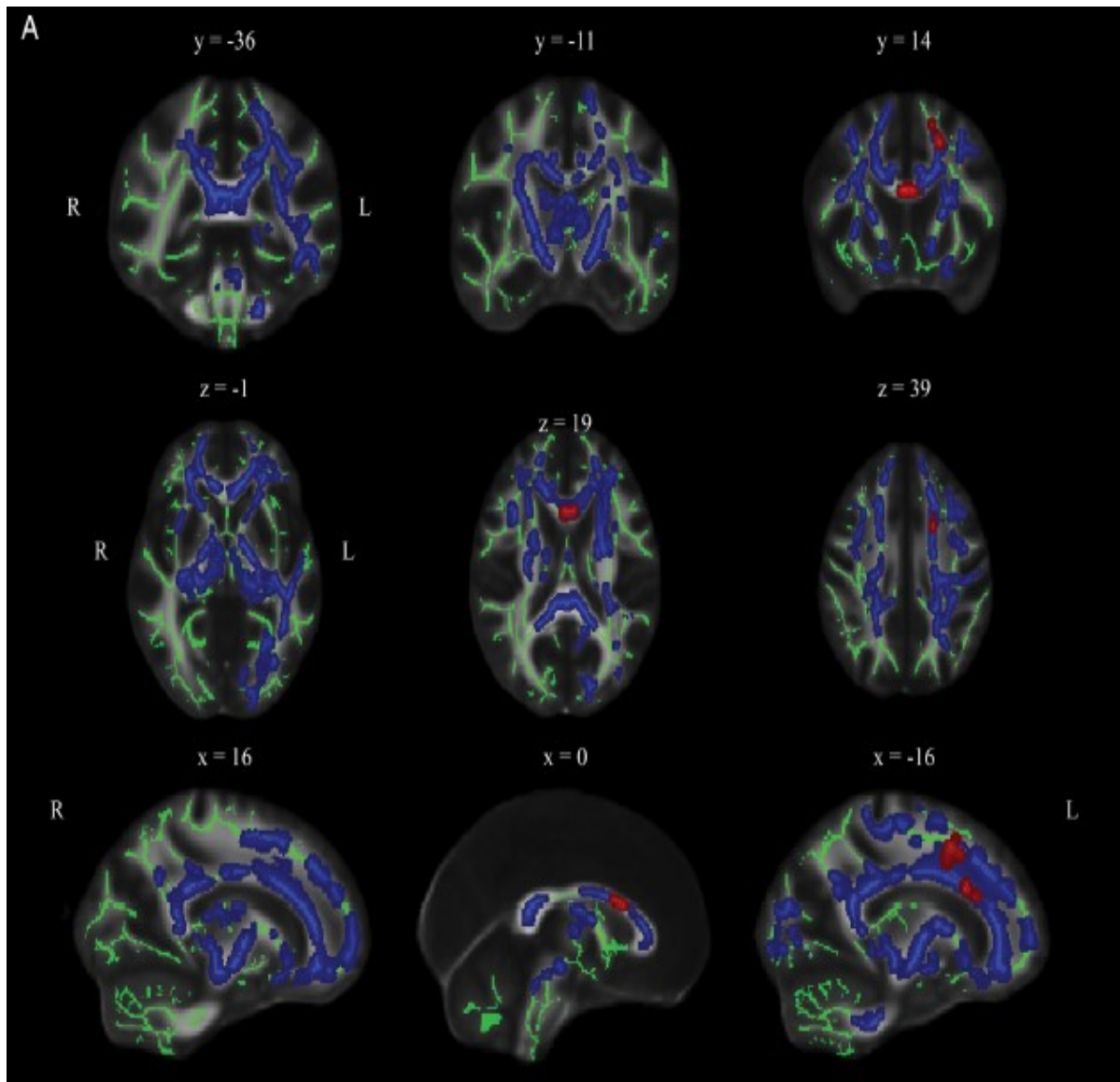


Fig 4.4A. Tract Based Spatial Statistics using voxelwise statistical analyses comparing axial diffusivity (AD) and tissue volume fraction (f) across PCOS and control groups. Mean AD and f in PCOS group are depicted in blue and red respectively.

Mean white matter skeleton voxels showing significantly lower value of AD (blue) throughout the white matter skeleton and higher value tissue volume fraction in the PCOS group (red) compared with healthy volunteers. Results are shown in different cross-sections in coronal (top), axial (middle) and sagittal view (bottom). Letters x, y and z represent the location of the cross-sections according to standard coordinates. Displayed results are corrected for family-wise error and thresholded for $P < 0.05$. The white matter skeleton is shown in green and is generated from projection of mean fractional anisotropy (FA) data obtained from all subjects. Individual voxel values of each participants' AD, mean diffusivity (MD), radial diffusivity (RD) and f are projected to the white matter skeleton with resulting data used to generate voxelwise statistical analyses across the PCOS and control groups. No differences were noted in FA, MD or RD.

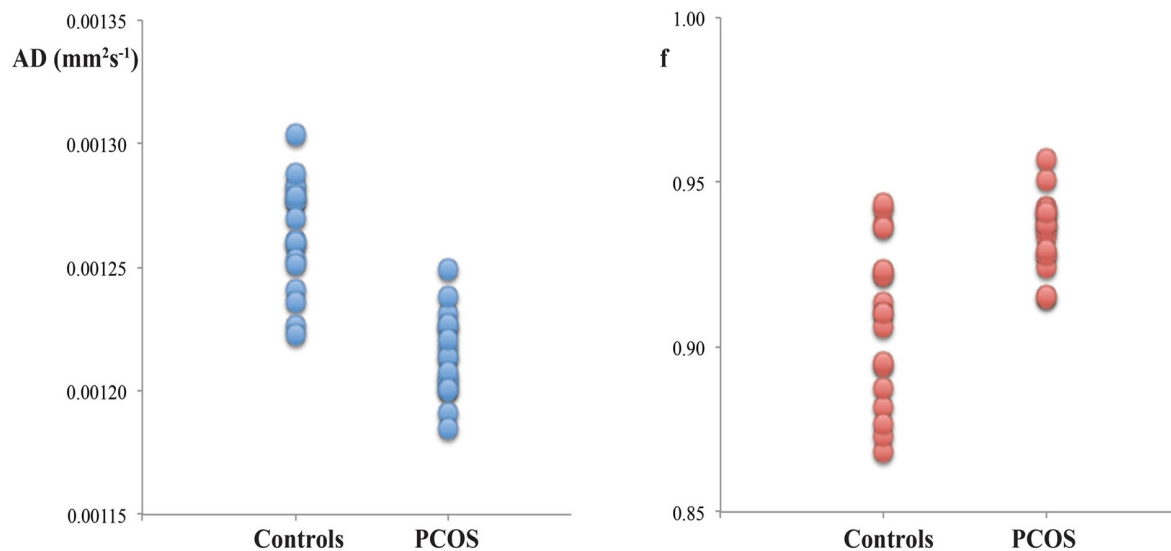


Figure 4.4 B Group differences based on Tract based Spatial statistics in Axial diffusivity (AD) and tissue volume fraction(*f*)

Mean values of AD (depicted on the left side in blue) and tissue volume fraction *f* (red) across parts of the skeleton showing a significant group difference for each participant. AD in PCOS is significantly decreased compared to controls whereas the converse picture is seen with *f* which is raised in PCOS compared to controls.

4.4.1.2 Insulin resistance and white matter microstructure

No significant differences were observed between the PCOS and control groups in voxel-wise correlations between insulin AUC and AD. However there was a significant group by insulin AUC interaction. This is shown in Figure 4.5 A. This suggests that the relationship between insulin resistance and white matter microstructure differed in PCOS and control groups.

To explore this further, mean values of AD were extracted from this region and plotted against insulin AUC. This is illustrated in figure 4.5 B. Increasing insulin resistance was associated with reduction of AD in controls (Pearson's $r = -0.75$) but with increasing AD in those with PCOS (Pearson's $r = 0.73$), a reversal of the relationship found in controls. The reduction in AD found, on average, in patients with PCOS compared with controls was evident in those with relatively normal insulin

AUC < 100000 pmol/min/l) but AD was increased in a subset of PCOS subjects with marked insulin resistance.

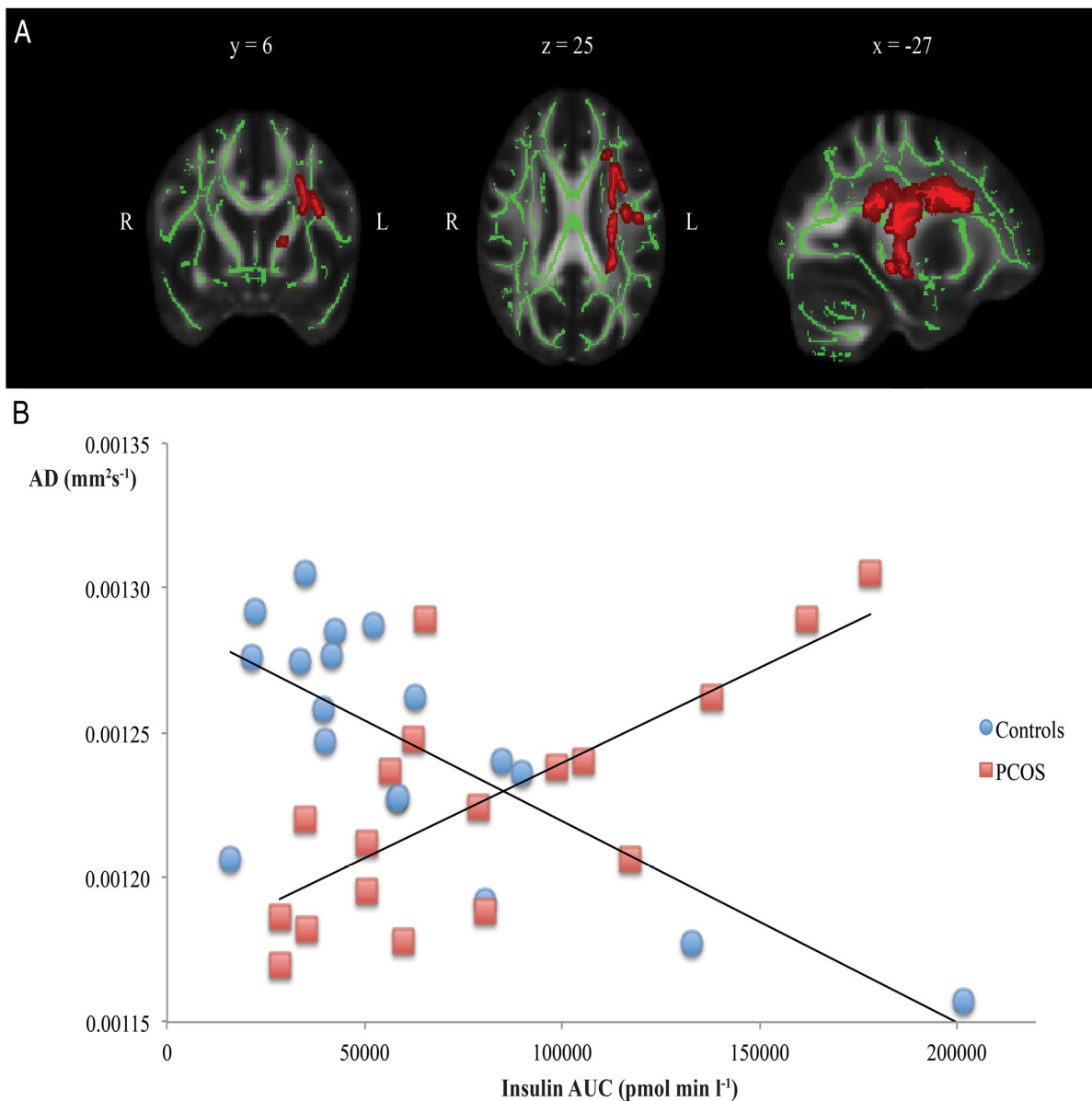


Figure 4.5 Contrasting associations between white matter microstructure and insulin resistance in PCOS and healthy volunteers.

A, White matter skeleton voxels exhibiting a significant group by insulin AUC interaction are shown in red ($P < .05$ corrected for familywise error). Results are shown in different cross-sections in coronal (left), axial (middle) and sagittal view (right).

B, Graphical description of Mean Axial Diffusivity (AD) values extracted from the region of significant interaction for each participant and plotted against insulin Area under Curve (Insulin AUC). Although AD was reduced in the PCOS group as a whole the direction of association is positive in PCOS and negative in controls.

4.4.1.3 Androgens and white matter microstructure

Serum testosterone correlated positively with both AD and FA in the PCOS group (Figure 4.6). No association was observed in control participants. The direction of effect was consistent with that found between insulin AUC and diffusion metrics, ie, increasing values of AD were associated with both increases in testosterone and insulin AUC (Figure 4.6) in patients with PCOS.

4.4.1.4 Metabolic status and white matter microstructure

No correlation was observed between cognitive performance and testosterone or insulin AUC in PCOS (testosterone: $r = 0.12$, $P = .64$; insulin AUC: $r = 0.01$, $P = .98$). No significant correlations were observed between microstructural measures and cognition. Similarly, no significant associations with cognitive performance were found in the control group.

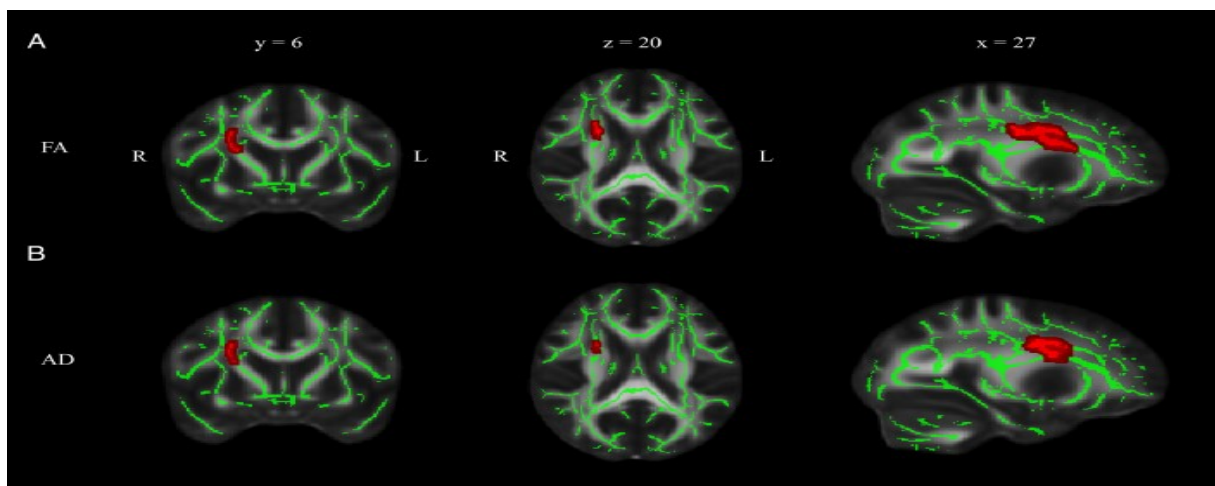


Figure 4.6. Correlation of testosterone level with microstructural measures in PCOS.

Top panel A) White matter skeleton voxels exhibiting a positive correlation with fractional anisotropy (FA) shown in red.

Bottom panel B) White matter skeleton voxels exhibiting a positive correlation with axial diffusivity (AD) shown in red. Displayed results are corrected for family-wise error and thresholded for $P < .05$. Results are shown in different cross-sections in coronal (left), axial (middle) and sagittal view (right). This illustrates a similar pattern of interaction as with Insulin AUC with increasing values of AD being associated with increase in testosterone level.

4.5 Discussion

This was the first study to look at the effects of PCOS on white matter microstructure. The current study did not demonstrate microstructural abnormalities in the major white matter tracts of interest in subjects with PCOS. These specific tracts were reconstructed with the hypothesis that changes in white matter microstructure may be observed in the PCOS group as it is a heterogeneous disorder which encompasses risk factors of obesity and insulin resistance which have been associated with white matter abnormalities associated with cognitive dysfunction. Although these tracts can be affected in disorders of metabolic dysfunction such as diabetes[202] and obesity[277], as seen in previous studies, these may have not been elicited as the study was carried out in a relatively young cohort of patients between the ages of 18 and 45 when these changes are not likely to be apparent. Moreover the Rotterdam criteria was used for diagnosis which may have picked up subtle cases of PCOS which would contrast with the more severe phenotypes that would be diagnosed by other criteria such as NIH [278]. As I did not find any changes in white matter microstructure in the pre-specified regions of interest I proceeded to apply TBSS which is free of *a priori* bias about the likely location of structural alteration in the brain and is a widely accepted approach for statistical analysis of diffusion data.

Although there were no significant differences in voxel-wise values of FA, MD or RD between the groups, PCOS was associated with a reduction in axial diffusivity in a large portion of the white matter skeleton and tissue volume fraction was increased in the anterior corpus callosum. Similar findings have been reported in studies on sexual dimorphism. Kumar *et al.*[279] attempted to describe age-related axonal and myelin changes in various sites in the brain and sex-related differences in those areas in healthy

adults using DTI measures such as axial and radial diffusivity. There was widespread reduction of axial and radial diffusivity in the bilateral amygdala, anterior and mid thalamus, hypothalamus and superior pons, right inferior cerebellar peduncle and putamen in males. Axial diffusivity was significantly decreased in the mid corpus callosum compared to females. Another study combined DTI and diffusion tractography with myelin -water fraction (MWF) imaging to investigate sex differences in microstructural measures in the corpus callosum [280]. This study illustrated increased myelin density in males for the rostral body and the posterior mid-body of the corpus callosum. No significant sex differences existed for axial or radial diffusivity. The changes in myelin density are possibly concordant with my findings of increased f in the anterior part of the corpus callosum reflecting atrophy at a microstructural scale even though these studies address structural characteristics that are not necessarily closely correlated. This might suggest that an influence of androgens on brain structure produces alterations in PCOS that parallel the characteristics of the male brain.

A positive association was seen between serum testosterone levels and axial diffusivity and fractional anisotropy. This was contrary to the evidence that white matter axial diffusivity is reduced in PCOS. Raised testosterone levels and insulin resistance in the PCOS group were associated with increasing axial diffusivity and this was despite a mean reduction in the PCOS group as a whole. These findings may be explained by a reversal of the normal relationship between microstructure and metabolic status in patients with PCOS, reflected in a significant group by insulin AUC interaction. These findings raise the possibility that the brain responds differently to the effect of androgens in PCOS and perhaps appear to correlate with the findings of another study by Soleman *et al* which used functional MRI to evaluate working memory function. Group differences in brain activity were seen in the superior, inferior parietal lobe and

the superior temporal lobe in PCOS versus controls with no difference in performance during a working memory task. Although hormonal levels were not significantly correlated with brain activation it is still likely that androgen levels play a role in the differences between the two groups. It was thought that there are already differences in brain function and structure in women with PCOS independent of current hormonal levels. Although no specific data exists to support this in human studies animal studies by Abbott *et al.*[281] reported that excessive androgen exposure prenatally may result in remarkable phenotypical similarities to women with PCOS, suggesting a foetal origin for this syndrome which may also have effects on organisation of the brain.

These data clearly suggest that changes in white matter microstructure occur relatively early in our cohort of PCOS aged between 18 and 45 years of age and this was reflected by the decrease in axial diffusivity and an increase in tissue volume fraction in the anterior corpus callosum. Although no correlation was seen between cognitive function and white matter microstructure, risk factors such as insulin resistance and hyperandrogenaemia may play a role in these changes. This was an observational case control study and a therapeutic trial of intervention in the form of anti-androgenic therapy or insulin sensitising agents would help in assessing the role of these risk factors further.

CHAPTER 5

Discussion

Polycystic ovary syndrome (PCOS) was associated with both subtle decrements of cognitive function and alterations in microstructure of brain white matter. These differences were not attributable to BMI, which was closely matched between groups as was general intelligence. PCOS is one of the most common metabolic syndromes, affecting up to 10% of women of reproductive age [163]. Many body systems are affected in PCOS resulting in several health complications including menstrual dysfunction, infertility, hirsutism, acne, obesity, and metabolic syndrome. The public health importance of PCOS is amplified by the association with the risk of developing type 2 diabetes mellitus and possibly cardiovascular disease [127].

Traditional approaches to treatment of PCOS has focussed on the management of infertility and reducing cardiovascular risk. The results of my study suggest that the potential consequences of PCOS are wider, and the possibility that PCOS represents a midlife risk state for cognitive decline in old age should be explored. The case control design effectively isolated two features of PCOS – insulin resistance and hyperandrogenaemia – as possible causes of the alterations in white matter structure and cognition that were observed. Attention to these specific factors would help to define such a risk state and potential treatments more precisely.

The current findings suggest a subtle but widespread erosion of cognitive performance. In an internet-based computerised study, Barnard *et al* hypothesised that women with PCOS would display enhanced cognitive performance on sexually dimorphic tasks [177]. However, no difference was found in performance of mental rotation or spatial

location tasks. Contrary to expectation, women with PCOS showed impaired performance on reaction time and word recognition tasks. Schattmann and Sherwin similarly found no differences on tests of mental rotation, spatial visualisation, or spatial perception in PCOS [208]. However, subjects with PCOS performed less well on tests of verbal fluency, verbal memory, manual dexterity, and visuospatial working memory. Previous studies have often been limited by poor case-control matching. For example, Barry et al found evidence of better visuospatial task performance in women with PCOS compared with subfertile controls, but this difference was no longer significant when age and BMI were controlled for in the analysis [271].

In parallel with metabolic and cognitive differences, microstructural alterations in cerebral white matter were observed in the PCOS group. AD was reduced in a large portion of the white matter skeleton in PCOS and tissue volume fraction was increased in the anterior corpus callosum. Intriguingly, similar findings have been reported in studies on sexual dimorphism. For example, Kumar *et al* [279] found widespread reductions of axial and RD values in the male brain. The corpus callosum is generally larger in males. Further, a study with myelin-water fraction imaging has illustrated increased myelin density in males in the rostral body and posterior midbody of the corpus callosum [280], possibly concordant with our findings of increased f in the anterior part of the corpus callosum even though these studies address structural characteristics that are not necessarily closely correlated. One interpretation of the findings in the present study, therefore, is that an influence of androgens on brain structure produces alterations in PCOS that parallel the characteristics of the male brain.

The finding of a positive association between androgens and AD within the PCOS group was a surprise, given evidence that white matter AD is reduced in PCOS. Hyperandrogenemia and insulin resistance in the PCOS group were associated with increasing AD, despite a mean reduction in the PCOS group as a whole. The likely explanation was a reversal of the normal relationship between microstructure and metabolic status in patients with PCOS, reflected in a significant group by insulin AUC interaction. These findings raise the possibility that the brain responds differently to the effect of androgens in PCOS.

A more recent study by Soleman *et al.*[179] on the effects of PCOS on cognition sought to explore working memory before and after anti androgenic treatment using functional MRI. Women with PCOS differed in brain activation in the inferior and superior parietal lobe and in the superior temporal lobe than control women but not in performance (number of errors and reaction time) during a working memory task. Similar significant differences in biochemical parameters (testosterone/ free androgen index and androstenedione) were noted in the PCOS group although this did not correlate with brain activity in the regions of interest. Following anti-androgenic treatment, the between-group differences in brain activation were no longer apparent. Although this study did not look at indices of insulin resistance, it was considered likely that the differences between the two groups were possibly related to the level of androgens. It may be possible that there are already differences in brain functions and structure in women with PCOS independent of current hormonal levels [281].

Alternatively, there may be significant heterogeneity among individuals that is currently not captured by the coarse diagnostic categories in current use. For example, there may be distinct subtypes of PCOS with and without insulin resistance that differ in a variety of ways that are not yet fully understood; similarly, the presence of

increased insulin resistance in some BMI-matched controls suggests heterogeneity in the healthy population.

Previous studies have reported differences in diffusion metrics in both type 2 diabetes [202] and obesity. Type 2 diabetes is associated with increases in AD in a number of specific tracts. Studies in obesity are less consistent, with at least 1 study reporting effects that vary by anatomical location in the brain and include both increases and decreases of AD in different regions [203, 282, 283]. These reports illustrate that there is no simple relationship between diffusion measures and better or worse white matter “integrity”[284]. The histological basis of alterations in disease states remains unclear and further work is required to aid the interpretation of direction as well as the magnitude of effects.

Previous epidemiological studies suggest a complex relationship between BMI and dementia risk. Both high and low body mass states have been associated with future dementia risk, with evidence that the relationship might differ in mid and later life [285]. One recent report highlighted this complexity by showing a relationship between low body weight in midlife and dementia [286], contradicting previously held views about midlife obesity [285, 287] . The average age of individuals at entry to this recent retrospective study was 55; even less is known about the risk implications of BMI in the twenties and thirties, the age range relevant to the current study.

Study Limitations

There were some limitations to the experimental approach. Firstly, PCOS subjects were selected by the Rotterdam criteria, which embrace a less severe metabolic phenotype than other definitions of the syndrome. However, if anything this might be expected to underestimate the extent of white matter alteration in PCOS subjects with more severe

hyperandrogenism and insulin resistance. The Rotterdam criteria also encompass a heterogeneous group, hence future studies should compare distinct PCOS phenotypes, including lean subjects alone, in order to establish whether cognitive function and white matter microstructure are altered in all PCOS patients or only in some. Secondly, I did not capture information on physical activity levels in my study; future studies should look to record this in view of the possible relationship between sedentary behaviour and cognitive decline. Thirdly although cognitive function tests showed subtle differences in cognitive function across different domains, no clear correlation was found between cognition and white matter structure of relevant regions or connections. This related partly to power. Another factor was the unexpected interaction between group and metabolic factors in their influence on white matter structure. The National Adult Reading test although used as a widely accepted research tool in the assessment of premorbid intelligence may not be an entirely reliable tool in a cohort of patients not known to show any evidence of cognitive impairment as seen in this study.

White matter tractography has several limitations. Although it is the only means of non invasive imaging of white matter tracts the issues identified relate to accurate identification of anatomical landmarks which can vary between different operators although customised tract based algorithms using region of interest approaches have been published [201, 288] which has helped to make this a reliable and reproducible imaging technique. The limitations of the diffusion tensor in areas of complex white matter architecture, where fibre tracts intersect, branch, or are otherwise partial volume averaged within a voxel, affect the ability of DTI fibre tractography to fully delineate an axonal pathway and may also lead to the generation of spurious tracks.

Functional MRI is an emerging and useful tool in addition to diffusion tensor imaging to investigate and explore areas of activation and whether the differences in cognitive

function are significant. It would be interesting to see the effects of hormonal manipulation in the form of anti-androgen therapy and insulin sensitising agents on measures of diffusion and on functional MRI.

Conclusion

A key question that follows from these observations is whether alterations in brain structure and function can be reversed, reducing the risk of future cognitive decline. Interestingly, one study in PCOS suggested improvement in a single cognitive measure (verbal fluency), after combined treatment with an antiandrogen plus oestrogen [178]. Based on the current results, both insulin resistance and hyperandrogenism are potential targets, and advanced MRI has a potential role as a biomarker of treatment effect.

APPENDIX 1

Total Variance Explained

Component	Initial Eigenvalues			Extraction Sums of Squared Loadings		
	Total	% of Variance	Cumulative %	Total	% of Variance	Cumulative %
1	4.978	35.555	35.555	4.978	35.555	35.555
2	1.740	12.429	47.984	1.740	12.429	47.984
3	1.526	10.899	58.883	1.526	10.899	58.883
4	1.299	9.277	68.160	1.299	9.277	68.160
5	.959	6.852	75.012			
6	.803	5.736	80.749			
7	.637	4.550	85.298			
8	.605	4.321	89.619			
9	.463	3.309	92.929			
10	.408	2.911	95.840			
11	.257	1.835	97.675			
12	.164	1.169	98.844			
13	.128	.912	99.756			
14	.034	.244	100.000			

Extraction Method (SPSS): Principal Component Analysis (PCA). First Principal Component accounts for 35% of the variance across all cognitive test scores and was used as the summary score (General Cognition score)

General Cognition Score (First Principal Component) was based on all of the cognitive tests that are appropriate (excluding tests of premorbid IQ, IQ (WASI) and Stroop which is known to be tricky in terms of covariance and PCA. The tests included in Principal component Analysis was derived from a combination of the following tests: Digit Span, Free and Cued Selective Reminding Test, Roy Osterrieth Complex Figure Test, Verbal Trails, Digit Symbol Substitution and the letter and semantic fluency test.

APPENDIX 2

Group difference between PCOS and control in terms of summary score obtained through Principal Component analysis

Independent Samples Test					
		F	Sig (2-tailed)	t	Mean Difference
REGR factor score 1 for analysis	Equal variance assumed	5.218	0.007	2.878	0.8727
	Equal variances not assumed		0.008	2.878	0.8727

References

1. Alonso, A., et al., *Risk of dementia hospitalisation associated with cardiovascular risk factors in midlife and older age: the Atherosclerosis Risk in Communities (ARIC) study*. J Neurol Neurosurg Psychiatry, 2009. **80**(11): p. 1194-201.
2. Solomon, A., et al., *Serum cholesterol changes after midlife and late-life cognition: twenty-one-year follow-up study*. Neurology, 2007. **68**(10): p. 751-6.
3. Shepardson, N.E., G.M. Shankar, and D.J. Selkoe, *Cholesterol level and statin use in Alzheimer disease: I. Review of epidemiological and preclinical studies*. Arch Neurol, 2011. **68**(10): p. 1239-44.
4. Moroney, J.T., et al., *Low-density lipoprotein cholesterol and the risk of dementia with stroke*. JAMA, 1999. **282**(3): p. 254-60.
5. Dufouil, C., et al., *APOE genotype, cholesterol level, lipid-lowering treatment, and dementia: the Three-City Study*. Neurology, 2005. **64**(9): p. 1531-8.
6. Whitmer, R.A., et al., *Midlife cardiovascular risk factors and risk of dementia in late life*. Neurology, 2005. **64**(2): p. 277-81.
7. Tan, Z.S., et al., *Plasma total cholesterol level as a risk factor for Alzheimer disease: the Framingham Study*. Arch Intern Med, 2003. **163**(9): p. 1053-7.
8. Mielke, M.M., et al., *High total cholesterol levels in late life associated with a reduced risk of dementia*. Neurology, 2005. **64**(10): p. 1689-95.
9. Tan, Z.S., et al., *Association of metabolic dysregulation with volumetric brain magnetic resonance imaging and cognitive markers of subclinical brain aging in middle-aged adults: the Framingham Offspring Study*. Diabetes Care, 2011. **34**(8): p. 1766-70.
10. Rawlings, A.M., et al., *Diabetes in midlife and cognitive change over 20 years: a cohort study*. Ann Intern Med, 2014. **161**(11): p. 785-93.

11. Schnaider Beerli, M., et al., *Diabetes mellitus in midlife and the risk of dementia three decades later*. *Neurology*, 2004. **63**(10): p. 1902-7.
12. Biessels, G.J., et al., *Risk of dementia in diabetes mellitus: a systematic review*. *Lancet Neurol*, 2006. **5**(1): p. 64-74.
13. Arvanitakis, Z., et al., *Diabetes is related to cerebral infarction but not to AD pathology in older persons*. *Neurology*, 2006. **67**(11): p. 1960-5.
14. Sonnen, J.A., et al., *Different patterns of cerebral injury in dementia with or without diabetes*. *Arch Neurol*, 2009. **66**(3): p. 315-22.
15. Cherbuin, N., P. Sachdev, and K.J. Anstey, *Higher normal fasting plasma glucose is associated with hippocampal atrophy: The PATH Study*. *Neurology*, 2012. **79**(10): p. 1019-26.
16. Crane, P.K., R. Walker, and E.B. Larson, *Glucose levels and risk of dementia*. *N Engl J Med*, 2013. **369**(19): p. 1863-4.
17. Kerti, L., et al., *Higher glucose levels associated with lower memory and reduced hippocampal microstructure*. *Neurology*, 2013. **81**(20): p. 1746-52.
18. Avadhani, R., et al., *Glycemia and cognitive function in metabolic syndrome and coronary heart disease*. *Am J Med*, 2015. **128**(1): p. 46-55.
19. Schuur, M., et al., *Insulin-resistance and metabolic syndrome are related to executive function in women in a large family-based study*. *Eur J Epidemiol*, 2010. **25**(8): p. 561-8.
20. Segura, B., et al., *Mental slowness and executive dysfunctions in patients with metabolic syndrome*. *Neurosci Lett*, 2009. **462**(1): p. 49-53.
21. Whitmer, R.A., et al., *Obesity in middle age and future risk of dementia: a 27 year longitudinal population based study*. *BMJ*, 2005. **330**(7504): p. 1360.
22. Cournot, M., et al., *Relation between body mass index and cognitive function in healthy middle-aged men and women*. *Neurology*, 2006. **67**(7): p. 1208-14.

23. Gunstad, J., et al., *Longitudinal examination of obesity and cognitive function: results from the Baltimore longitudinal study of aging*. *Neuroepidemiology*, 2010. **34**(4): p. 222-9.
24. Brooks, S.J., et al., *Late-life obesity is associated with smaller global and regional gray matter volumes: a voxel-based morphometric study*. *Int J Obes (Lond)*, 2013. **37**(2): p. 230-6.
25. Cholerton, B., L.D. Baker, and S. Craft, *Insulin resistance and pathological brain ageing*. *Diabet Med*, 2011. **28**(12): p. 1463-75.
26. Crichton, G.E., et al., *Metabolic syndrome, cognitive performance, and dementia*. *J Alzheimers Dis*, 2012. **30 Suppl 2**: p. S77-87.
27. Benedict, C., et al., *Impaired insulin sensitivity as indexed by the HOMA score is associated with deficits in verbal fluency and temporal lobe gray matter volume in the elderly*. *Diabetes Care*, 2012. **35**(3): p. 488-94.
28. Gonzales, M.M., et al., *Insulin sensitivity as a mediator of the relationship between BMI and working memory-related brain activation*. *Obesity (Silver Spring)*, 2010. **18**(11): p. 2131-7.
29. Bove, R.M., et al., *Metabolic and endocrine correlates of cognitive function in healthy young women*. *Obesity (Silver Spring)*, 2013. **21**(7): p. 1343-9.
30. Porter, D.W., et al., *Prolonged GIP receptor activation improves cognitive function, hippocampal synaptic plasticity and glucose homeostasis in high-fat fed mice*. *Eur J Pharmacol*, 2011. **650**(2-3): p. 688-93.
31. Frisardi, V., et al., *Is insulin resistant brain state a central feature of the metabolic-cognitive syndrome?* *J Alzheimers Dis*, 2010. **21**(1): p. 57-63.
32. Sakata, A., et al., *Female exhibited severe cognitive impairment in type 2 diabetes mellitus mice*. *Life Sci*, 2010. **86**(17-18): p. 638-45.
33. Elias, M.F., et al., *Untreated blood pressure level is inversely related to cognitive functioning: the Framingham Study*. *Am J Epidemiol*, 1993. **138**(6): p. 353-64.

34. Launer, L.J., et al., *The association between midlife blood pressure levels and late-life cognitive function. The Honolulu-Asia Aging Study.* JAMA, 1995. **274**(23): p. 1846-51.
35. Elias, P.K., et al., *Blood pressure-related cognitive decline: does age make a difference?* Hypertension, 2004. **44**(5): p. 631-6.
36. Wang, L.Y., et al., *Blood pressure and brain injury in older adults: findings from a community-based autopsy study.* J Am Geriatr Soc, 2009. **57**(11): p. 1975-81.
37. Strassburger, T.L., et al., *Interactive effects of age and hypertension on volumes of brain structures.* Stroke, 1997. **28**(7): p. 1410-7.
38. Beason-Held, L.L., et al., *Longitudinal changes in cerebral blood flow in the older hypertensive brain.* Stroke, 2007. **38**(6): p. 1766-73.
39. Forette, F., et al., *The prevention of dementia with antihypertensive treatment: new evidence from the Systolic Hypertension in Europe (Syst-Eur) study.* Arch Intern Med, 2002. **162**(18): p. 2046-52.
40. Tzourio, C., et al., *Effects of blood pressure lowering with perindopril and indapamide therapy on dementia and cognitive decline in patients with cerebrovascular disease.* Arch Intern Med, 2003. **163**(9): p. 1069-75.
41. Lithell, H., et al., *The Study on Cognition and Prognosis in the Elderly (SCOPE): principal results of a randomized double-blind intervention trial.* J Hypertens, 2003. **21**(5): p. 875-86.
42. Herbert, L.E., et al., *Relation of smoking and low-to-moderate alcohol consumption to change in cognitive function: a longitudinal study in a defined community of older persons.* Am J Epidemiol, 1993. **137**(8): p. 881-91.
43. Almeida, O.P., et al., *Smoking as a risk factor for Alzheimer's disease: contrasting evidence from a systematic review of case-control and cohort studies.* Addiction, 2002. **97**(1): p. 15-28.
44. Anstey, K.J., et al., *Smoking as a risk factor for dementia and cognitive decline: a meta-analysis of prospective studies.* Am J Epidemiol, 2007. **166**(4): p. 367-78.

45. Sonnen, J.A., et al., *Free radical damage to cerebral cortex in Alzheimer's disease, microvascular brain injury, and smoking*. *Ann Neurol*, 2009. **65**(2): p. 226-9.
46. Azziz, R., D.A. Dumesic, and M.O. Goodarzi, *Polycystic ovary syndrome: an ancient disorder?* *Fertil Steril*, 2011. **95**(5): p. 1544-8.
47. Zawadzki JK, D.A.B.B.S.P.p., *Diagnostic criteria for polycystic ovary syndrome: towards a rational approach*. In: *Dunaif A, Givens JR, Haseltine FP, Merriam GR, editors. Polycystic Ovary Syndrome*. Blackwell Scientific Publications, 1992: p. 377-384.
48. Legro, R.S., et al., *Diagnosis and treatment of polycystic ovary syndrome: an Endocrine Society clinical practice guideline*. *J Clin Endocrinol Metab*, 2013. **98**(12): p. 4565-92.
49. Rotterdam, E.A.-S.P.c.w.g., *Revised 2003 consensus on diagnostic criteria and long-term health risks related to polycystic ovary syndrome (PCOS)*. *Hum Reprod*, 2004. **19**(1): p. 41-7.
50. Azziz, R., et al., *Positions statement: criteria for defining polycystic ovary syndrome as a predominantly hyperandrogenic syndrome: an Androgen Excess Society guideline*. *J Clin Endocrinol Metab*, 2006. **91**(11): p. 4237-45.
51. Rosner, W., et al., *Position statement: Utility, limitations, and pitfalls in measuring testosterone: an Endocrine Society position statement*. *J Clin Endocrinol Metab*, 2007. **92**(2): p. 405-13.
52. Balen, A.H., et al., *Ultrasound assessment of the polycystic ovary: international consensus definitions*. *Hum Reprod Update*, 2003. **9**(6): p. 505-14.
53. Mortensen, M., et al., *Asymptomatic volunteers with a polycystic ovary are a functionally distinct but heterogeneous population*. *J Clin Endocrinol Metab*, 2009. **94**(5): p. 1579-86.
54. Taylor, A.E., et al., *Determinants of abnormal gonadotropin secretion in clinically defined women with polycystic ovary syndrome*. *J Clin Endocrinol Metab*, 1997. **82**(7): p. 2248-56.
55. Rosenfield, R.L., *Ovarian and adrenal function in polycystic ovary syndrome*. *Endocrinol Metab Clin North Am*, 1999. **28**(2): p. 265-93.

56. Ehrmann, D.A., R.B. Barnes, and R.L. Rosenfield, *Polycystic ovary syndrome as a form of functional ovarian hyperandrogenism due to dysregulation of androgen secretion*. *Endocr Rev*, 1995. **16**(3): p. 322-53.
57. Rosenfield, R.L. and B. Bordini, *Evidence that obesity and androgens have independent and opposing effects on gonadotropin production from puberty to maturity*. *Brain Res*, 2010. **1364**: p. 186-97.
58. Kumar, A., et al., *Prevalence of adrenal androgen excess in patients with the polycystic ovary syndrome (PCOS)*. *Clin Endocrinol (Oxf)*, 2005. **62**(6): p. 644-9.
59. Longcope, C., *Adrenal and gonadal androgen secretion in normal females*. *Clin Endocrinol Metab*, 1986. **15**(2): p. 213-28.
60. Rosencrantz, M.A., et al., *Clinical evidence for predominance of delta-5 steroid production in women with polycystic ovary syndrome*. *J Clin Endocrinol Metab*, 2011. **96**(4): p. 1106-13.
61. Ehrmann, D.A., et al., *Insulin secretory defects in polycystic ovary syndrome. Relationship to insulin sensitivity and family history of non-insulin-dependent diabetes mellitus*. *J Clin Invest*, 1995. **96**(1): p. 520-7.
62. Rosenfield, R.L., *Polycystic ovary syndrome and insulin-resistant hyperinsulinemia*. *J Am Acad Dermatol*, 2001. **45**(3 Suppl): p. S95-104.
63. Diamanti-Kandarakis, E. and A. Dunaif, *Insulin resistance and the polycystic ovary syndrome revisited: an update on mechanisms and implications*. *Endocr Rev*, 2012. **33**(6): p. 981-1030.
64. Ciaraldi, T.P., et al., *Polycystic ovary syndrome is associated with tissue-specific differences in insulin resistance*. *J Clin Endocrinol Metab*, 2009. **94**(1): p. 157-63.
65. Burghen, G.A., J.R. Givens, and A.E. Kitabchi, *Correlation of hyperandrogenism with hyperinsulinism in polycystic ovarian disease*. *J Clin Endocrinol Metab*, 1980. **50**(1): p. 113-6.

66. Barbieri, R.L., A. Makris, and K.J. Ryan, *Insulin stimulates androgen accumulation in incubations of human ovarian stroma and theca*. *Obstet Gynecol*, 1984. **64**(3 Suppl): p. 73S-80S.
67. Nestler, J.E., *Metformin and the polycystic ovary syndrome*. *J Clin Endocrinol Metab*, 2001. **86**(3): p. 1430.
68. Damon, S.E., et al., *Overexpression of an inhibitory insulin-like growth factor binding protein (IGFBP), IGFBP-4, delays onset of prostate tumor formation*. *Endocrinology*, 1998. **139**(8): p. 3456-64.
69. Munir, I., et al., *Insulin augmentation of 17alpha-hydroxylase activity is mediated by phosphatidyl inositol 3-kinase but not extracellular signal-regulated kinase-1/2 in human ovarian theca cells*. *Endocrinology*, 2004. **145**(1): p. 175-83.
70. Chen, Y.H., et al., *miRNA-93 inhibits GLUT4 and is overexpressed in adipose tissue of polycystic ovary syndrome patients and women with insulin resistance*. *Diabetes*, 2013. **62**(7): p. 2278-86.
71. Abbott, D.H., D.A. Dumesic, and S. Franks, *Developmental origin of polycystic ovary syndrome - a hypothesis*. *J Endocrinol*, 2002. **174**(1): p. 1-5.
72. Dumesic, D.A., D.H. Abbott, and V. Padmanabhan, *Polycystic ovary syndrome and its developmental origins*. *Rev Endocr Metab Disord*, 2007. **8**(2): p. 127-41.
73. Hickey, M., et al., *The relationship between maternal and umbilical cord androgen levels and polycystic ovary syndrome in adolescence: a prospective cohort study*. *J Clin Endocrinol Metab*, 2009. **94**(10): p. 3714-20.
74. de Zegher, F. and L. Ibanez, *Early Origins of polycystic ovary syndrome: hypotheses may change without notice*. *J Clin Endocrinol Metab*, 2009. **94**(10): p. 3682-5.
75. Prentice, A.M., P. Rayco-Solon, and S.E. Moore, *Insights from the developing world: thrifty genotypes and thrifty phenotypes*. *Proc Nutr Soc*, 2005. **64**(2): p. 153-61.

76. Ibanez, L., F. de Zegher, and N. Potau, *Premature pubarche, ovarian hyperandrogenism, hyperinsulinism and the polycystic ovary syndrome: from a complex constellation to a simple sequence of prenatal onset*. J Endocrinol Invest, 1998. **21**(9): p. 558-66.
77. Ibanez, L., et al., *Early metformin therapy (age 8-12 years) in girls with precocious pubarche to reduce hirsutism, androgen excess, and oligomenorrhea in adolescence*. J Clin Endocrinol Metab, 2011. **96**(8): p. E1262-7.
78. Azziz, R. and M.D. Kashar-Miller, *Family history as a risk factor for the polycystic ovary syndrome*. J Pediatr Endocrinol Metab, 2000. **13 Suppl 5**: p. 1303-6.
79. Khasar-Miller, M.D., et al., *Prevalence of polycystic ovary syndrome (PCOS) in first-degree relatives of patients with PCOS*. Fertil Steril, 2001. **75**(1): p. 53-8.
80. Vink, J.M., et al., *Heritability of polycystic ovary syndrome in a Dutch twin-family study*. J Clin Endocrinol Metab, 2006. **91**(6): p. 2100-4.
81. Goodarzi, M.O., et al., *Replication of association of DENND1A and THADA variants with polycystic ovary syndrome in European cohorts*. J Med Genet, 2012. **49**(2): p. 90-5.
82. Zeggini, E., et al., *Meta-analysis of genome-wide association data and large-scale replication identifies additional susceptibility loci for type 2 diabetes*. Nat Genet, 2008. **40**(5): p. 638-45.
83. Barber, T.M., et al., *Association of variants in the fat mass and obesity associated (FTO) gene with polycystic ovary syndrome*. Diabetologia, 2008. **51**(7): p. 1153-8.
84. Wojciechowski, P., et al., *Impact of FTO genotypes on BMI and weight in polycystic ovary syndrome: a systematic review and meta-analysis*. Diabetologia, 2012. **55**(10): p. 2636-45.
85. Li, T., et al., *Common variant rs9939609 in gene FTO confers risk to polycystic ovary syndrome*. PLoS One, 2013. **8**(7): p. e66250.
86. March, W.A., et al., *The prevalence of polycystic ovary syndrome in a community sample assessed under contrasting diagnostic criteria*. Hum Reprod, 2010. **25**(2): p. 544-51.

87. Diamanti-Kandarakis, E., et al., *A survey of the polycystic ovary syndrome in the Greek island of Lesbos: hormonal and metabolic profile*. J Clin Endocrinol Metab, 1999. **84**(11): p. 4006-11.
88. Michelmores, K.F., et al., *Polycystic ovaries and associated clinical and biochemical features in young women*. Clin Endocrinol (Oxf), 1999. **51**(6): p. 779-86.
89. Asuncion, M., et al., *A prospective study of the prevalence of the polycystic ovary syndrome in unselected Caucasian women from Spain*. J Clin Endocrinol Metab, 2000. **85**(7): p. 2434-8.
90. Tehrani, F.R., H. Rashidi, and F. Azizi, *The prevalence of idiopathic hirsutism and polycystic ovary syndrome in the Tehran Lipid and Glucose Study*. Reprod Biol Endocrinol, 2011. **9**: p. 144.
91. Broekmans, F.J., et al., *PCOS according to the Rotterdam consensus criteria: Change in prevalence among WHO-II anovulation and association with metabolic factors*. BJOG, 2006. **113**(10): p. 1210-7.
92. Hartz, A.J., et al., *The association of obesity with infertility and related menstrual abnormalities in women*. Int J Obes, 1979. **3**(1): p. 57-73.
93. Yildiz, B.O., E.S. Knochenhauer, and R. Azziz, *Impact of obesity on the risk for polycystic ovary syndrome*. J Clin Endocrinol Metab, 2008. **93**(1): p. 162-8.
94. Codner, E., et al., *Diagnostic criteria for polycystic ovary syndrome and ovarian morphology in women with type 1 diabetes mellitus*. J Clin Endocrinol Metab, 2006. **91**(6): p. 2250-6.
95. Conn, J.J., H.S. Jacobs, and G.S. Conway, *The prevalence of polycystic ovaries in women with type 2 diabetes mellitus*. Clin Endocrinol (Oxf), 2000. **52**(1): p. 81-6.
96. Holte, J., et al., *High prevalence of polycystic ovaries and associated clinical, endocrine, and metabolic features in women with previous gestational diabetes mellitus*. J Clin Endocrinol Metab, 1998. **83**(4): p. 1143-50.

97. Ibanez, L., et al., *Premature adrenarche--normal variant or forerunner of adult disease?* *Endocr Rev*, 2000. **21**(6): p. 671-96.
98. Legro, R.S., et al., *Evidence for a genetic basis for hyperandrogenemia in polycystic ovary syndrome.* *Proc Natl Acad Sci U S A*, 1998. **95**(25): p. 14956-60.
99. Hull, M.G., *Epidemiology of infertility and polycystic ovarian disease: endocrinological and demographic studies.* *Gynecol Endocrinol*, 1987. **1**(3): p. 235-45.
100. Imani, B., et al., *Predictors of patients remaining anovulatory during clomiphene citrate induction of ovulation in normogonadotropic oligomenorrheic infertility.* *J Clin Endocrinol Metab*, 1998. **83**(7): p. 2361-5.
101. Kjerulff, L.E., L. Sanchez-Ramos, and D. Duffy, *Pregnancy outcomes in women with polycystic ovary syndrome: a metaanalysis.* *Am J Obstet Gynecol*, 2011. **204**(6): p. 558 e1-6.
102. Bolumar, F., et al., *Body mass index and delayed conception: a European Multicenter Study on Infertility and Subfecundity.* *Am J Epidemiol*, 2000. **151**(11): p. 1072-9.
103. Azziz, R., et al., *Androgen excess in women: experience with over 1000 consecutive patients.* *J Clin Endocrinol Metab*, 2004. **89**(2): p. 453-62.
104. Lowenstein, E.J., *Diagnosis and management of the dermatologic manifestations of the polycystic ovary syndrome.* *Dermatol Ther*, 2006. **19**(4): p. 210-23.
105. Arias-Santiago, S., et al., *Androgenetic alopecia and cardiovascular risk factors in men and women: a comparative study.* *J Am Acad Dermatol*, 2010. **63**(3): p. 420-9.
106. Matilainen, V., et al., *Hair loss, insulin resistance, and heredity in middle-aged women. A population-based study.* *J Cardiovasc Risk*, 2003. **10**(3): p. 227-31.
107. Ekmekci, T.R., et al., *The presence of insulin resistance and comparison of various insulin sensitivity indices in women with androgenetic alopecia.* *Eur J Dermatol*, 2007. **17**(1): p. 21-5.
108. Ehrmann, D.A., *Polycystic ovary syndrome.* *N Engl J Med*, 2005. **352**(12): p. 1223-36.

109. Apridonidze, T., et al., *Prevalence and characteristics of the metabolic syndrome in women with polycystic ovary syndrome*. J Clin Endocrinol Metab, 2005. **90**(4): p. 1929-35.
110. Dokras, A., et al., *Screening women with polycystic ovary syndrome for metabolic syndrome*. Obstet Gynecol, 2005. **106**(1): p. 131-7.
111. Conway, G.S., et al., *Risk factors for coronary artery disease in lean and obese women with the polycystic ovary syndrome*. Clin Endocrinol (Oxf), 1992. **37**(2): p. 119-25.
112. Lo, J.C., et al., *Epidemiology and adverse cardiovascular risk profile of diagnosed polycystic ovary syndrome*. J Clin Endocrinol Metab, 2006. **91**(4): p. 1357-63.
113. Talbott, E., et al., *Adverse lipid and coronary heart disease risk profiles in young women with polycystic ovary syndrome: results of a case-control study*. J Clin Epidemiol, 1998. **51**(5): p. 415-22.
114. Berneis, K., et al., *Atherogenic lipoprotein phenotype and low-density lipoproteins size and subclasses in women with polycystic ovary syndrome*. J Clin Endocrinol Metab, 2007. **92**(1): p. 186-9.
115. Phelan, N., et al., *Lipoprotein subclass patterns in women with polycystic ovary syndrome (PCOS) compared with equally insulin-resistant women without PCOS*. J Clin Endocrinol Metab, 2010. **95**(8): p. 3933-9.
116. Ehrmann, D.A., et al., *Prevalence of impaired glucose tolerance and diabetes in women with polycystic ovary syndrome*. Diabetes Care, 1999. **22**(1): p. 141-6.
117. Colilla, S., N.J. Cox, and D.A. Ehrmann, *Heritability of insulin secretion and insulin action in women with polycystic ovary syndrome and their first degree relatives*. J Clin Endocrinol Metab, 2001. **86**(5): p. 2027-31.
118. Vgontzas, A.N., et al., *Polycystic ovary syndrome is associated with obstructive sleep apnea and daytime sleepiness: role of insulin resistance*. J Clin Endocrinol Metab, 2001. **86**(2): p. 517-20.

119. Vassilatou, E., *Nonalcoholic fatty liver disease and polycystic ovary syndrome*. World J Gastroenterol, 2014. **20**(26): p. 8351-63.
120. Schwimmer, J.B., et al., *Abnormal aminotransferase activity in women with polycystic ovary syndrome*. Fertil Steril, 2005. **83**(2): p. 494-7.
121. Setji, T.L., et al., *Nonalcoholic steatohepatitis and nonalcoholic Fatty liver disease in young women with polycystic ovary syndrome*. J Clin Endocrinol Metab, 2006. **91**(5): p. 1741-7.
122. Cerda, C., et al., *Nonalcoholic fatty liver disease in women with polycystic ovary syndrome*. J Hepatol, 2007. **47**(3): p. 412-7.
123. Schmidt, J., et al., *Cardiovascular disease and risk factors in PCOS women of postmenopausal age: a 21-year controlled follow-up study*. J Clin Endocrinol Metab, 2011. **96**(12): p. 3794-803.
124. Solomon, C.G., et al., *Menstrual cycle irregularity and risk for future cardiovascular disease*. J Clin Endocrinol Metab, 2002. **87**(5): p. 2013-7.
125. Rexrode, K.M., et al., *Sex hormone levels and risk of cardiovascular events in postmenopausal women*. Circulation, 2003. **108**(14): p. 1688-93.
126. Shaw, L.J., et al., *Postmenopausal women with a history of irregular menses and elevated androgen measurements at high risk for worsening cardiovascular event-free survival: results from the National Institutes of Health--National Heart, Lung, and Blood Institute sponsored Women's Ischemia Syndrome Evaluation*. J Clin Endocrinol Metab, 2008. **93**(4): p. 1276-84.
127. Morgan, C.L., et al., *Evaluation of adverse outcome in young women with polycystic ovary syndrome versus matched, reference controls: a retrospective, observational study*. J Clin Endocrinol Metab, 2012. **97**(9): p. 3251-60.
128. Talbott, E.O., et al., *The relationship between C-reactive protein and carotid intima-media wall thickness in middle-aged women with polycystic ovary syndrome*. J Clin Endocrinol Metab, 2004. **89**(12): p. 6061-7.

129. Talbott, E.O., et al., *Evidence for an association between metabolic cardiovascular syndrome and coronary and aortic calcification among women with polycystic ovary syndrome*. J Clin Endocrinol Metab, 2004. **89**(11): p. 5454-61.
130. Christian, R.C., et al., *Prevalence and predictors of coronary artery calcification in women with polycystic ovary syndrome*. J Clin Endocrinol Metab, 2003. **88**(6): p. 2562-8.
131. Orio, F., Jr., et al., *The cardiovascular risk of young women with polycystic ovary syndrome: an observational, analytical, prospective case-control study*. J Clin Endocrinol Metab, 2004. **89**(8): p. 3696-701.
132. Yarali, H., et al., *Diastolic dysfunction and increased serum homocysteine concentrations may contribute to increased cardiovascular risk in patients with polycystic ovary syndrome*. Fertil Steril, 2001. **76**(3): p. 511-6.
133. Meyer, C., B.P. McGrath, and H.J. Teede, *Overweight women with polycystic ovary syndrome have evidence of subclinical cardiovascular disease*. J Clin Endocrinol Metab, 2005. **90**(10): p. 5711-6.
134. Carmina, E., et al., *Endothelial dysfunction in PCOS: role of obesity and adipose hormones*. Am J Med, 2006. **119**(4): p. 356 e1-6.
135. Kravariti, M., et al., *Predictors of endothelial dysfunction in young women with polycystic ovary syndrome*. J Clin Endocrinol Metab, 2005. **90**(9): p. 5088-95.
136. Rees, E., et al., *Central arterial stiffness and diastolic dysfunction are associated with insulin resistance and abdominal obesity in young women but polycystic ovary syndrome does not confer additional risk*. Hum Reprod, 2014. **29**(9): p. 2041-9.
137. Orio, F., Jr., et al., *Improvement in endothelial structure and function after metformin treatment in young normal-weight women with polycystic ovary syndrome: results of a 6-month study*. J Clin Endocrinol Metab, 2005. **90**(11): p. 6072-6.

138. Diamanti-Kandarakis, E., et al., *Metformin administration improves endothelial function in women with polycystic ovary syndrome*. Eur J Endocrinol, 2005. **152**(5): p. 749-56.
139. Agarwal, N., et al., *Metformin reduces arterial stiffness and improves endothelial function in young women with polycystic ovary syndrome: a randomized, placebo-controlled, crossover trial*. J Clin Endocrinol Metab, 2010. **95**(2): p. 722-30.
140. Legro, R.S., et al., *Prevalence and predictors of risk for type 2 diabetes mellitus and impaired glucose tolerance in polycystic ovary syndrome: a prospective, controlled study in 254 affected women*. J Clin Endocrinol Metab, 1999. **84**(1): p. 165-9.
141. Palmert, M.R., et al., *Screening for abnormal glucose tolerance in adolescents with polycystic ovary syndrome*. J Clin Endocrinol Metab, 2002. **87**(3): p. 1017-23.
142. Vrbikova, J. and B. Bendlova, [*Polycystic ovary syndrome in 2006*]. Cas Lek Cesk, 2007. **146**(3): p. 218-22.
143. Boudreaux, M.Y., et al., *Risk of T2DM and impaired fasting glucose among PCOS subjects: results of an 8-year follow-up*. Curr Diab Rep, 2006. **6**(1): p. 77-83.
144. Barr EL, M.D., Zimmet PZ, et al., *AusDiab 2005: the Australian diabetes, obesity and lifestyle study. Melbourne (Australia): International Diabetes Institute;2006*

Melbourne (Australia): International Diabetes Institute

2006.

145. Alberti, K.G., P. Zimmet, and J. Shaw, *International Diabetes Federation: a consensus on Type 2 diabetes prevention*. Diabet Med, 2007. **24**(5): p. 451-63.
146. Dunaif, A., et al., *Characterization of groups of hyperandrogenic women with acanthosis nigricans, impaired glucose tolerance, and/or hyperinsulinemia*. J Clin Endocrinol Metab, 1987. **65**(3): p. 499-507.
147. Poretsky, L., *Commentary: Polycystic ovary syndrome--increased or preserved ovarian sensitivity to insulin?* J Clin Endocrinol Metab, 2006. **91**(8): p. 2859-60.

148. Dunaif, A., et al., *Profound peripheral insulin resistance, independent of obesity, in polycystic ovary syndrome*. *Diabetes*, 1989. **38**(9): p. 1165-74.
149. Robinson, S., et al., *The relationship of insulin insensitivity to menstrual pattern in women with hyperandrogenism and polycystic ovaries*. *Clin Endocrinol (Oxf)*, 1993. **39**(3): p. 351-5.
150. Dunaif, A., *Insulin resistance and the polycystic ovary syndrome: mechanism and implications for pathogenesis*. *Endocr Rev*, 1997. **18**(6): p. 774-800.
151. Pierpoint, T., et al., *Mortality of women with polycystic ovary syndrome at long-term follow-up*. *J Clin Epidemiol*, 1998. **51**(7): p. 581-6.
152. Younossi, Z.M., et al., *Nonalcoholic fatty liver disease: assessment of variability in pathologic interpretations*. *Mod Pathol*, 1998. **11**(6): p. 560-5.
153. Matteoni, C.A., et al., *Nonalcoholic fatty liver disease: a spectrum of clinical and pathological severity*. *Gastroenterology*, 1999. **116**(6): p. 1413-9.
154. Baranova, A., et al., *Molecular signature of adipose tissue in patients with both non-alcoholic fatty liver disease (NAFLD) and polycystic ovarian syndrome (PCOS)*. *J Transl Med*, 2013. **11**: p. 133.
155. Brown, A.J., et al., *Polycystic ovary syndrome and severe nonalcoholic steatohepatitis: beneficial effect of modest weight loss and exercise on liver biopsy findings*. *Endocr Pract*, 2005. **11**(5): p. 319-24.
156. Gambarin-Gelwan, M., et al., *Prevalence of nonalcoholic fatty liver disease in women with polycystic ovary syndrome*. *Clin Gastroenterol Hepatol*, 2007. **5**(4): p. 496-501.
157. Baranova, A., et al., *Systematic review: association of polycystic ovary syndrome with metabolic syndrome and non-alcoholic fatty liver disease*. *Aliment Pharmacol Ther*, 2011. **33**(7): p. 801-14.
158. Karoli, R., et al., *Prevalence of hepatic steatosis in women with polycystic ovary syndrome*. *J Hum Reprod Sci*, 2013. **6**(1): p. 9-14.

159. de Ledinghen, V., et al., *Diagnostic and predictive factors of significant liver fibrosis and minimal lesions in patients with persistent unexplained elevated transaminases. A prospective multicenter study.* J Hepatol, 2006. **45**(4): p. 592-9.
160. Legro, R.S., *The genetics of obesity. Lessons for polycystic ovary syndrome.* Ann N Y Acad Sci, 2000. **900**: p. 193-202.
161. Balen, A.H., et al., *Polycystic ovary syndrome: the spectrum of the disorder in 1741 patients.* Hum Reprod, 1995. **10**(8): p. 2107-11.
162. Rosenzweig, J.L., et al., *Primary prevention of cardiovascular disease and type 2 diabetes in patients at metabolic risk: an endocrine society clinical practice guideline.* J Clin Endocrinol Metab, 2008. **93**(10): p. 3671-89.
163. Azziz, R., et al., *The prevalence and features of the polycystic ovary syndrome in an unselected population.* J Clin Endocrinol Metab, 2004. **89**(6): p. 2745-9.
164. Pasquali, R., A. Gambineri, and U. Pagotto, *The impact of obesity on reproduction in women with polycystic ovary syndrome.* BJOG, 2006. **113**(10): p. 1148-59.
165. Pasquali, R., *Obesity and androgens: facts and perspectives.* Fertil Steril, 2006. **85**(5): p. 1319-40.
166. Rausch, M.E., et al., *Predictors of pregnancy in women with polycystic ovary syndrome.* J Clin Endocrinol Metab, 2009. **94**(9): p. 3458-66.
167. Venkatesan, A.M., A. Dunaif, and A. Corbould, *Insulin resistance in polycystic ovary syndrome: progress and paradoxes.* Recent Prog Horm Res, 2001. **56**: p. 295-308.
168. Weiner, C.L., M. Primeau, and D.A. Ehrmann, *Androgens and mood dysfunction in women: comparison of women with polycystic ovarian syndrome to healthy controls.* Psychosom Med, 2004. **66**(3): p. 356-62.
169. Bhattacharya, S.M. and A. Jha, *Prevalence and risk of depressive disorders in women with polycystic ovary syndrome (PCOS).* Fertil Steril, 2010. **94**(1): p. 357-9.

170. Mansson, M., et al., *Women with polycystic ovary syndrome are often depressed or anxious-- a case control study*. Psychoneuroendocrinology, 2008. **33**(8): p. 1132-8.
171. Hollinrake, E., et al., *Increased risk of depressive disorders in women with polycystic ovary syndrome*. Fertil Steril, 2007. **87**(6): p. 1369-76.
172. Weber, B., et al., *Testosterone, androstenedione and dihydrotestosterone concentrations are elevated in female patients with major depression*. Psychoneuroendocrinology, 2000. **25**(8): p. 765-71.
173. Rasgon, N.L., et al., *Depression in women with polycystic ovary syndrome: clinical and biochemical correlates*. J Affect Disord, 2003. **74**(3): p. 299-304.
174. Gopal, M., et al., *The role of obesity in the increased prevalence of obstructive sleep apnea syndrome in patients with polycystic ovarian syndrome*. Sleep Med, 2002. **3**(5): p. 401-4.
175. Vgontzas, A.N., et al., *Sleep apnea and daytime sleepiness and fatigue: relation to visceral obesity, insulin resistance, and hypercytokinemia*. J Clin Endocrinol Metab, 2000. **85**(3): p. 1151-8.
176. Vamvakopoulos, N.C. and G.P. Chrousos, *Hormonal regulation of human corticotropin-releasing hormone gene expression: implications for the stress response and immune/inflammatory reaction*. Endocr Rev, 1994. **15**(4): p. 409-20.
177. Barnard, L., et al., *Cognitive functioning in polycystic ovary syndrome*. Psychoneuroendocrinology, 2007. **32**(8-10): p. 906-14.
178. Schattmann, L. and B.B. Sherwin, *Effects of the pharmacologic manipulation of testosterone on cognitive functioning in women with polycystic ovary syndrome: a randomized, placebo-controlled treatment study*. Horm Behav, 2007. **51**(5): p. 579-86.
179. Soleman, R.S., et al., *Does polycystic ovary syndrome affect cognition? A functional magnetic resonance imaging study exploring working memory*. Fertil Steril, 2016. **105**(5): p. 1314-1321 e1.

180. Mansfield, P. and A.A. Maudsley, *Medical imaging by NMR*. Br J Radiol, 1977. **50**(591): p. 188-94.
181. Moseley, M.E., et al., *Diffusion-weighted MR imaging of anisotropic water diffusion in cat central nervous system*. Radiology, 1990. **176**(2): p. 439-45.
182. Pierpaoli, C., et al., *Diffusion tensor MR imaging of the human brain*. Radiology, 1996. **201**(3): p. 637-48.
183. Chenevert, T.L., J.A. Brunberg, and J.G. Pipe, *Anisotropic diffusion in human white matter: demonstration with MR techniques in vivo*. Radiology, 1990. **177**(2): p. 401-5.
184. Makris, N., et al., *Morphometry of in vivo human white matter association pathways with diffusion-weighted magnetic resonance imaging*. Ann Neurol, 1997. **42**(6): p. 951-62.
185. Pajevic, S. and C. Pierpaoli, *Color schemes to represent the orientation of anisotropic tissues from diffusion tensor data: application to white matter fiber tract mapping in the human brain*. Magn Reson Med, 1999. **42**(3): p. 526-40.
186. Witwer, B.P., et al., *Diffusion-tensor imaging of white matter tracts in patients with cerebral neoplasm*. J Neurosurg, 2002. **97**(3): p. 568-75.
187. Le Bihan, D., et al., *Diffusion tensor imaging: concepts and applications*. J Magn Reson Imaging, 2001. **13**(4): p. 534-46.
188. Alexander, A.L., et al., *Diffusion tensor imaging of the brain*. Neurotherapeutics, 2007. **4**(3): p. 316-29.
189. Shragar, R.I. and P.J. Basser, *Anisotropically weighted MRI*. Magn Reson Med, 1998. **40**(1): p. 160-5.
190. Papadakis, N.G., et al., *A comparative study of acquisition schemes for diffusion tensor imaging using MRI*. J Magn Reson, 1999. **137**(1): p. 67-82.
191. Basser, P.J. and C. Pierpaoli, *Microstructural and physiological features of tissues elucidated by quantitative-diffusion-tensor MRI*. J Magn Reson B, 1996. **111**(3): p. 209-19.

192. Song, S.K., et al., *Dysmyelination revealed through MRI as increased radial (but unchanged axial) diffusion of water*. Neuroimage, 2002. **17**(3): p. 1429-36.
193. Mukherjee, P., et al., *Diffusion tensor MR imaging and fiber tractography: theoretic underpinnings*. AJNR Am J Neuroradiol, 2008. **29**(4): p. 632-41.
194. Conturo, T.E., et al., *Tracking neuronal fiber pathways in the living human brain*. Proc Natl Acad Sci U S A, 1999. **96**(18): p. 10422-7.
195. Mori, S., et al., *Three-dimensional tracking of axonal projections in the brain by magnetic resonance imaging*. Ann Neurol, 1999. **45**(2): p. 265-9.
196. Basser, P.J., et al., *In vivo fiber tractography using DT-MRI data*. Magn Reson Med, 2000. **44**(4): p. 625-32.
197. Catani, M., et al., *Virtual in vivo interactive dissection of white matter fasciculi in the human brain*. Neuroimage, 2002. **17**(1): p. 77-94.
198. Pierpaoli, C., et al., *Water diffusion changes in Wallerian degeneration and their dependence on white matter architecture*. Neuroimage, 2001. **13**(6 Pt 1): p. 1174-85.
199. Wiegell, M.R., H.B. Larsson, and V.J. Wedeen, *Fiber crossing in human brain depicted with diffusion tensor MR imaging*. Radiology, 2000. **217**(3): p. 897-903.
200. Mori, S., et al., *Imaging cortical association tracts in the human brain using diffusion-tensor-based axonal tracking*. Magn Reson Med, 2002. **47**(2): p. 215-23.
201. Wakana, S., et al., *Fiber tract-based atlas of human white matter anatomy*. Radiology, 2004. **230**(1): p. 77-87.
202. Reijmer, Y.D., et al., *Microstructural white matter abnormalities and cognitive functioning in type 2 diabetes: a diffusion tensor imaging study*. Diabetes Care, 2013. **36**(1): p. 137-44.
203. Xu, J., et al., *Body mass index correlates negatively with white matter integrity in the fornix and corpus callosum: a diffusion tensor imaging study*. Hum Brain Mapp, 2013. **34**(5): p. 1044-52.

204. O'Sullivan, M., et al., *Evidence for cortical "disconnection" as a mechanism of age-related cognitive decline*. *Neurology*, 2001. **57**(4): p. 632-8.
205. Smith, S.M., et al., *Tract-based spatial statistics: voxelwise analysis of multi-subject diffusion data*. *Neuroimage*, 2006. **31**(4): p. 1487-505.
206. Aye, T., et al., *White matter structural differences in young children with type 1 diabetes: a diffusion tensor imaging study*. *Diabetes Care*, 2012. **35**(11): p. 2167-73.
207. Metzler-Baddeley, C., et al., *Individual differences in fornix microstructure and body mass index*. *PLoS One*, 2013. **8**(3): p. e59849.
208. Schattmann, L. and B.B. Sherwin, *Testosterone levels and cognitive functioning in women with polycystic ovary syndrome and in healthy young women*. *Horm Behav*, 2007. **51**(5): p. 587-96.
209. DeFronzo, R.A., J.D. Tobin, and R. Andres, *Glucose clamp technique: a method for quantifying insulin secretion and resistance*. *Am J Physiol*, 1979. **237**(3): p. E214-23.
210. Matthews, D.R., et al., *Homeostasis model assessment: insulin resistance and beta-cell function from fasting plasma glucose and insulin concentrations in man*. *Diabetologia*, 1985. **28**(7): p. 412-9.
211. Katz, A., et al., *Quantitative insulin sensitivity check index: a simple, accurate method for assessing insulin sensitivity in humans*. *J Clin Endocrinol Metab*, 2000. **85**(7): p. 2402-10.
212. Pyorala, M., et al., *Plasma insulin and all-cause, cardiovascular, and noncardiovascular mortality: the 22-year follow-up results of the Helsinki Policemen Study*. *Diabetes Care*, 2000. **23**(8): p. 1097-102.
213. Ribeiro-Filho, F.F., et al., *Two-hour insulin determination improves the ability of abdominal fat measurement to identify risk for the metabolic syndrome*. *Diabetes Care*, 2003. **26**(6): p. 1725-30.

214. Watson, S., et al., *Can abdominal bioelectrical impedance refine the determination of visceral fat from waist circumference?* *Physiol Meas*, 2009. **30**(7): p. N53-8.
215. Reijmer, Y.D., et al., *Cognitive dysfunction in patients with type 2 diabetes*. *Diabetes Metab Res Rev*, 2010. **26**(7): p. 507-19.
216. Coltheart, M., *Varieties of developmental dyslexia: a comment on Bryant and Impey*. *Cognition*, 1987. **27**(1): p. 97-101.
217. Baddeley, A. and S. Della Sala, *Working memory and executive control*. *Philos Trans R Soc Lond B Biol Sci*, 1996. **351**(1346): p. 1397-403; discussion 1403-4.
218. Baddeley, A., et al., *Random generation and the executive control of working memory*. *Q J Exp Psychol A*, 1998. **51**(4): p. 819-52.
219. Shao, Z., et al., *What do verbal fluency tasks measure? Predictors of verbal fluency performance in older adults*. *Front Psychol*, 2014. **5**: p. 772.
220. Jensen, A.R. and W.D. Rohwer, Jr., *The Stroop color-word test: a review*. *Acta Psychol (Amst)*, 1966. **25**(1): p. 36-93.
221. Grober, E., et al., *Screening for dementia by memory testing*. *Neurology*, 1988. **38**(6): p. 900-3.
222. Shin, M.S., et al., *Clinical and empirical applications of the Rey-Osterrieth Complex Figure Test*. *Nat Protoc*, 2006. **1**(2): p. 892-9.
223. Himelein, M.J. and S.S. Thatcher, *Depression and body image among women with polycystic ovary syndrome*. *J Health Psychol*, 2006. **11**(4): p. 613-25.
224. Reese, T.G., et al., *Reduction of eddy-current-induced distortion in diffusion MRI using a twice-refocused spin echo*. *Magn Reson Med*, 2003. **49**(1): p. 177-82.
225. Bakshi, R., et al., *Fluid-attenuated inversion recovery magnetic resonance imaging detects cortical and juxtacortical multiple sclerosis lesions*. *Arch Neurol*, 2001. **58**(5): p. 742-8.

226. Leemans, A. and D.K. Jones, *The B-matrix must be rotated when correcting for subject motion in DTI data*. Magn Reson Med, 2009. **61**(6): p. 1336-49.
227. Leemans A, J.B., Sijbers J, Jones DK, *ExploreDTI: a graphical toolbox for processing, analyzing, and visualizing diffusion MR data*. Proceedings of the ISMRM 17th Annual Meeting, Honolulu, HI. 2009: p. 3536.
228. Pasternak, O., et al., *Free water elimination and mapping from diffusion MRI*. Magn Reson Med, 2009. **62**(3): p. 717-30.
229. Berlot, R., et al., *CSF contamination contributes to apparent microstructural alterations in mild cognitive impairment*. Neuroimage, 2014. **92**: p. 27-35.
230. Metzler-Baddeley, C., et al., *Temporal association tracts and the breakdown of episodic memory in mild cognitive impairment*. Neurology, 2012. **79**(23): p. 2233-40.
231. Jones, D.K., et al., *Non-invasive assessment of axonal fiber connectivity in the human brain via diffusion tensor MRI*. Magn Reson Med, 1999. **42**(1): p. 37-41.
232. Kantarci, K., *Fractional anisotropy of the fornix and hippocampal atrophy in Alzheimer's disease*. Front Aging Neurosci, 2014. **6**: p. 316.
233. Fletcher, E., et al., *Loss of fornix white matter volume as a predictor of cognitive impairment in cognitively normal elderly individuals*. JAMA Neurol, 2013. **70**(11): p. 1389-95.
234. Metzler-Baddeley, C., et al., *Cingulum microstructure predicts cognitive control in older age and mild cognitive impairment*. J Neurosci, 2012. **32**(49): p. 17612-9.
235. Aggleton, J.P. and M.W. Brown, *Episodic memory, amnesia, and the hippocampal-anterior thalamic axis*. Behav Brain Sci, 1999. **22**(3): p. 425-44; discussion 444-89.
236. Levy, J.A. and G.J. Chelune, *Cognitive-behavioral profiles of neurodegenerative dementias: beyond Alzheimer's disease*. J Geriatr Psychiatry Neurol, 2007. **20**(4): p. 227-38.
237. Rudebeck, S.R., et al., *Fornix microstructure correlates with recollection but not familiarity memory*. J Neurosci, 2009. **29**(47): p. 14987-92.

238. Aggleton, J.P., et al., *Differential cognitive effects of colloid cysts in the third ventricle that spare or compromise the fornix*. Brain, 2000. **123 (Pt 4)**: p. 800-15.
239. Tsivilis, D., et al., *A disproportionate role for the fornix and mammillary bodies in recall versus recognition memory*. Nat Neurosci, 2008. **11(7)**: p. 834-42.
240. Mabbott, D.J., et al., *The relations between white matter and declarative memory in older children and adolescents*. Brain Res, 2009. **1294**: p. 80-90.
241. Sasson, E., et al., *Structural correlates of memory performance with diffusion tensor imaging*. Neuroimage, 2010. **50(3)**: p. 1231-42.
242. Daselaar, S.M., et al., *Posterior midline and ventral parietal activity is associated with retrieval success and encoding failure*. Front Hum Neurosci, 2009. **3**: p. 13.
243. Horsfield, M.A., *Mapping eddy current induced fields for the correction of diffusion-weighted echo planar images*. Magn Reson Imaging, 1999. **17(9)**: p. 1335-45.
244. Smith, S.M., *Fast robust automated brain extraction*. Hum Brain Mapp, 2002. **17(3)**: p. 143-55.
245. Rueckert, D., et al., *Nonrigid registration using free-form deformations: application to breast MR images*. IEEE Trans Med Imaging, 1999. **18(8)**: p. 712-21.
246. Winkler, A.M., et al., *Permutation inference for the general linear model*. Neuroimage, 2014. **92**: p. 381-97.
247. Smith, S.M. and T.E. Nichols, *Threshold-free cluster enhancement: addressing problems of smoothing, threshold dependence and localisation in cluster inference*. Neuroimage, 2009. **44(1)**: p. 83-98.
248. Richards, M., et al., *Cigarette smoking and cognitive decline in midlife: evidence from a prospective birth cohort study*. Am J Public Health, 2003. **93(6)**: p. 994-8.
249. Vicario, A., et al., *Hypertension and cognitive decline: impact on executive function*. J Clin Hypertens (Greenwich), 2005. **7(10)**: p. 598-604.

250. Harrington, F., et al., *Cognitive performance in hypertensive and normotensive older subjects*. Hypertension, 2000. **36**(6): p. 1079-82.
251. Tzourio, C., et al., *Cognitive decline in individuals with high blood pressure: a longitudinal study in the elderly*. EVA Study Group. *Epidemiology of Vascular Aging*. Neurology, 1999. **53**(9): p. 1948-52.
252. Christman, A.L., et al., *Cranial volume, mild cognitive deficits, and functional limitations associated with diabetes in a community sample*. Arch Clin Neuropsychol, 2010. **25**(1): p. 49-59.
253. Allen, K.V., B.M. Frier, and M.W. Strachan, *The relationship between type 2 diabetes and cognitive dysfunction: longitudinal studies and their methodological limitations*. Eur J Pharmacol, 2004. **490**(1-3): p. 169-75.
254. Cukierman, T., H.C. Gerstein, and J.D. Williamson, *Cognitive decline and dementia in diabetes--systematic overview of prospective observational studies*. Diabetologia, 2005. **48**(12): p. 2460-9.
255. Luchsinger, J.A., et al., *Hyperinsulinemia and risk of Alzheimer disease*. Neurology, 2004. **63**(7): p. 1187-92.
256. Yaffe, K., et al., *Diabetes, impaired fasting glucose, and development of cognitive impairment in older women*. Neurology, 2004. **63**(4): p. 658-63.
257. Segura, B. and M.A. Jurado, *[Metabolic syndrome and ageing: cognitive impairment and structural alterations of the central nervous system]*. Rev Neurol, 2009. **49**(8): p. 417-24.
258. Ekblad, L.L., et al., *Insulin resistance is associated with poorer verbal fluency performance in women*. Diabetologia, 2015. **58**(11): p. 2545-53.
259. Geroldi, C., et al., *Insulin resistance in cognitive impairment: the InCHIANTI study*. Arch Neurol, 2005. **62**(7): p. 1067-72.

260. Wisse, L.E., et al., *Hippocampal disconnection in early Alzheimer's disease: a 7 tesla MRI study*. J Alzheimers Dis, 2015. **45**(4): p. 1247-56.
261. Nelson, H.E.W., J, *The National Adult Reading Test (NART)*. 1991: p. 1-26.
262. Joy, S., E. Kaplan, and D. Fein, *Speed and memory in the WAIS-III Digit Symbol--Coding subtest across the adult lifespan*. Arch Clin Neuropsychol, 2004. **19**(6): p. 759-67.
263. Gallagher, C. and T. Burke, *Age, gender and IQ effects on the Rey-Osterrieth Complex Figure Test*. Br J Clin Psychol, 2007. **46**(Pt 1): p. 35-45.
264. Ivnik, R.J., et al., *Free and cued selective reminding test: MOANS norms*. J Clin Exp Neuropsychol, 1997. **19**(5): p. 676-91.
265. Moran, L.J., et al., *Impaired glucose tolerance, type 2 diabetes and metabolic syndrome in polycystic ovary syndrome: a systematic review and meta-analysis*. Hum Reprod Update, 2010. **16**(4): p. 347-63.
266. Vrbikova, J., et al., *Prevalence of insulin resistance and prediction of glucose intolerance and type 2 diabetes mellitus in women with polycystic ovary syndrome*. Clin Chem Lab Med, 2007. **45**(5): p. 639-44.
267. Takeuchi, T., O. Tsutsumi, and Y. Taketani, *Abnormal response of insulin to glucose loading and assessment of insulin resistance in non-obese patients with polycystic ovary syndrome*. Gynecol Endocrinol, 2008. **24**(7): p. 385-91.
268. Fulghesu, A.M., et al., *Failure of the homeostatic model assessment calculation score for detecting metabolic deterioration in young patients with polycystic ovary syndrome*. Fertil Steril, 2006. **86**(2): p. 398-404.
269. Grossman, I., et al., *Neurocognitive abilities for a clinically depressed sample versus a matched control group of normal individuals*. Psychiatry Res, 1994. **51**(3): p. 231-44.
270. Burt, D.B., M.J. Zembar, and G. Niederehe, *Depression and memory impairment: a meta-analysis of the association, its pattern, and specificity*. Psychol Bull, 1995. **117**(2): p. 285-305.

271. Barry, J.A., H.S. Parekh, and P.J. Hardiman, *Visual-spatial cognition in women with polycystic ovarian syndrome: the role of androgens*. Hum Reprod, 2013. **28**(10): p. 2832-7.
272. Lujan ME, M.R. *Cognitive function in women with Polycystic Ovary syndrome (PCOS): Impact OF Reproductive and Metabolic factors*. Fertility and Sterility, 2015. P-68.
273. Joseph, J.E., et al., *Influence of estradiol on functional brain organization for working memory*. Neuroimage, 2012. **59**(3): p. 2923-31.
274. Grigorova, M., B.B. Sherwin, and T. Tulandi, *Effects of treatment with leuprolide acetate depot on working memory and executive functions in young premenopausal women*. Psychoneuroendocrinology, 2006. **31**(8): p. 935-47.
275. Yau, P.L., et al., *Preliminary evidence for brain complications in obese adolescents with type 2 diabetes mellitus*. Diabetologia, 2010. **53**(11): p. 2298-306.
276. Stanek, K.M., et al., *Body mass index and neurocognitive functioning across the adult lifespan*. Neuropsychology, 2013. **27**(2): p. 141-51.
277. Shimoji, K., et al., *White matter alteration in metabolic syndrome: diffusion tensor analysis*. Diabetes Care, 2013. **36**(3): p. 696-700.
278. Zawadski JK, D.A., *Diagnostic criteria for polycystic ovary syndrome: towards a rational approach*. . In: Dunaif A, Givens JR, Haseltine FP, Merriam GR, eds. Polycystic ovary syndrome 1992, Boston: Blackwell Scientific.
279. Kumar, R., et al., *Brain axial and radial diffusivity changes with age and gender in healthy adults*. Brain Res, 2013. **1512**: p. 22-36.
280. Liu, F., et al., *Sex differences in the human corpus callosum microstructure: a combined T2 myelin-water and diffusion tensor magnetic resonance imaging study*. Brain Res, 2010. **1343**: p. 37-45.
281. Abbott, D.H., V. Padmanabhan, and D.A. Dumesic, *Contributions of androgen and estrogen to fetal programming of ovarian dysfunction*. Reprod Biol Endocrinol, 2006. **4**: p. 17.

282. Mueller, K., et al., *Obesity Associated Cerebral Gray and White Matter Alterations Are Interrelated in the Female Brain*. PLoS One, 2014. **9**(12): p. e114206.
283. Mueller, K., et al., *Sex-dependent influences of obesity on cerebral white matter investigated by diffusion-tensor imaging*. PLoS One, 2011. **6**(4): p. e18544.
284. Jones, D.K., T.R. Knosche, and R. Turner, *White matter integrity, fiber count, and other fallacies: the do's and don'ts of diffusion MRI*. Neuroimage, 2013. **73**: p. 239-54.
285. Tolppanen, A.M., et al., *Midlife and late-life body mass index and late-life dementia: results from a prospective population-based cohort*. J Alzheimers Dis, 2014. **38**(1): p. 201-9.
286. Qizilbash, N., et al., *BMI and risk of dementia in two million people over two decades: a retrospective cohort study*. Lancet Diabetes Endocrinol, 2015. **3**(6): p. 431-6.
287. Xu, W.L., et al., *Midlife overweight and obesity increase late-life dementia risk: a population-based twin study*. Neurology, 2011. **76**(18): p. 1568-74.
288. Catani, M. and M. Thiebaut de Schotten, *A diffusion tensor imaging tractography atlas for virtual in vivo dissections*. Cortex, 2008. **44**(8): p. 1105-32.

